AMRL-TR-68-174

AN EXPERIMENTAL INVESTIGATION AND SYSTEM DESIGN FOR HUMIDITY AND CARBON DIOXIDE LEVEL CONTROL USING THERMAL RADIATION

JOHN S. MAULBETSCH

FOREWORD

This report has been prepared by the Dynatech R/D Company, a division of Dynatech Corporation, Cambridge, Massachusetts, under Air Force Contract No. F33615-67-C-1587, and in support of Project 6373, "Equipment for Life Support in Aerospace," and Task 637302, "Respiratory Support Equipment." The work was directed by the Air Force Aerospace Medical Research Laboratories, Wright-Patterson Air Force Base, Ohio, with Mr. Konrad Weiswurm, Biotechnology Branch, Life Support Division, Biomedical Laboratory,* as contract monitor.

This work was carried out over the period March 1, 1967 to October 1, 1968.

The author acknowledges the assistance of Messrs. J. P. Roos and N. F. Todtenkopf in the performance of this study.

This technical report has been reviewed and is approved.

C. H. KRATOCHVIL, Colonel, USAF, MC
Commander
Aerospace Medical Research Laboratory

---

* In December 1968, the Biotechnology Branch, Life Support Division and the Biomedical Laboratory were abolished, and the Laboratories were redesignated Aerospace Medical Research Laboratory.

ABSTRACT

An experimental investigation was carried out to verify the feasibility of controlling carbon dioxide levels in space cabin atmospheres by freeze-out techniques using thermal radiation as the only mode of heat rejection. A one-tenth scale system was constructed with the primary aim of gaining understanding of the CO_2 precipitation mechanism and determining the operating characteristics of a precipitator plate. Both quantitative measurements and visual observation of the frost formation were made. The geometric characteristics of the precipitator channel were found to be not critical. Uniform frost layer formation could be obtained and premature channel plugging was not a problem. Typical precipitator plate effectivenesses

$$\left(\text{defined as} \quad \epsilon_p = \frac{C_{in} - C_{out}}{C_{in} - C_p}\right)$$

of 0.75 - 0.85 were easily obtainable. Simultaneous CO_2 sublimation was achievable at a controllable rate. System stability was easily achieved. Solid CO_2 carryover in both the precipitating and sublimating streams is a real possiblity and preventive measures must be taken in the final design of the system. Based on these results, a complete test system was designed to handle the water vapor and carbon dioxide loads in a one-man, manned space enclosure. The design point is specified as follows:

Water Vapor Generation Rate: 45 gm/hr
Carbon Dioxide Generation Rate: 45 gm/hr
Relative Humidity: 50%
CO_2 Concentration: 0.5% (p_{CO_2} = 3.8 mm Hg)

The system, with a total weight of 51.2 lb, is a two-loop configuration where one loop maintains humidity control and the other removes the generated carbon dioxide and returns all of the accompanying water vapor to the cabin. The system will operate indefinitely with no operator intervention, is operable in zero-gravity, and is of low weight, volume, and power.

TABLE OF CONTENTS

TABLE OF CONTENTS (continued)

TABLE OF CONTENTS (continued)

LIST OF FIGURES

LIST OF FIGURES (Continued)

NOMENCLATURE

Symbol			Units
C	-	concentration by volume	%
c_p	-	specific heat	cal/gm- K
D	-	channel hydraulic diameter	cm, m
~~D~~	-	mass diffusivity	cm/sec
f	-	friction factor	---
G	-	mass velocity	kg/m^2-hr
h	-	heat transfer coefficient	watts/cm^2- K
h_{sg}	-	latent heat of precipitation	cal/kg
j_D	-	$(\equiv h_D/V\ (Sc)^{2/3})$	---
j_H	-	$(\equiv h/G c_p\ Pr^{2/3})$	---
k	-	thermal conductivity	watts/cm- K
L	-	channel length	cm, m
Le	-	Lewis No. $(\alpha/\mathcal{D})$	---
p	-	pressure	kg/m^2
Pr	-	Prandtl No. $(\mu c_p/k)$	---
(q/A)	-	heat flux	watts/cm^2
Q	-	heat transfer rate	watts
~~Q~~	-	volume flow	m^3/hr, cm^3/sec
T	-	temperature	°K
U	-	overall heat transfer coefficient	watts/cm^2- K
~~V~~	-	velocity	cm/sec
W	-	mass flow rate	kg/hr
x	-	distance from inlet	cm,m

Symbol			Units
		Greek	
α	-	thermal diffusivity ($\equiv k/\rho c_p$)	m^2/hr
δ	-	frost layer thickness	cm
ϵ	-	effectiveness	---
μ	-	dynamic viscosity	kg/cm-sec
		Subscripts	
CO_2	-	carbon dioxide component	
D (h_D)	-	denotes mass transfer coefficient	
H (ϵ_H)	-	heat transfer	
i	-	conditions at interface	
ℓ	-	layer	
M (ϵ_M)	-	mass transfer	
P	-	plate conditions	
1	-	channel inlet	
2	-	channel exit	

Additional notation used in design calculations and specifications is defined as used in Sections VI and VII.

SECTION I

INTRODUCTION

The presence of a live astronaut in a space-craft cabin requires the removal and control of the human output of water vapor and carbon dioxide. The absolute concentrations of the constituents must be maintained at such a low level for human comfort and survival that the removal task is relatively difficult. In particular, as mission length increases, presently existing schemes, utilizing nonregenerable absorbents and failing to provide for water recovery, impose increasingly severe weight and volume penalties on the total system.

From the thermodynamic standpoint, an obvious approach is one which takes advantage of the fact that these two gas species, carbon dioxide and water vapor, have condensation temperatures which are higher than that of the primary cabin atmosphere. Hence, these vapors will condense (precipitate) on surfaces which are maintained below their respective dew points. Previous attempts to devise atmospheric control systems operating on this principle have led to the conclusion that the high sensible heat loads, which result from cooling the total cabin atmosphere down to these temperatures, coupled with the low emissive power of the space radiator, which must operate below the carbon dioxide dew point, led to excessively large radiator sizes and an over-cooling of the cabin.

However, an arrangement proposed by Bonneville (ref 1) made use of state-of-the-art regenerative techniques to reduce the ultimate heat rejection load to a small fraction of what was previously assumed. Further improvement was shown to be possible through the simultaneous sublimation of accumulated carbon dioxide frost to absorb the heat of precipitation from the fresh stream. This work was described in AMRL-TR-66-118.

The present effort represents an extension of that study and was carried out in two phases. The first phase consisted of an experimental program to investigate the controlling mechanisms of carbon dioxide precipitation and sublimation and to determine a suitable configuration for precipitator-sublimator-radiator (PSR).

The second phase resulted in the design of a full scale test system utilizing these principles, which may be tested in space-simulation chambers on the ground.

BACKGROUND INVESTIGATION

This effort is intended as an experimental verification of the theoretical results obtained in an earlier study and reported in "A Study of Water and Carbon Dioxide Precipitation Techniques Using Thermal Radiation Principles " (ref 1). The conclusions of that study were the following:

- Effective control of humidity and carbon dioxide levels in spacecraft could be maintained through freeze-out techniques utilizing only radiation to space as the mode of ultimate heat rejection.
- Through the proper use of state-of-the-art regenerative techniques, the ultimate heat rejection rates and hence the radiator sizes could be kept within reasonable bounds.
- Simultaneous sublimation and precipitation of water vapor and carbon dioxide were recommended as a means of removing the heat of solidification from the ultimate heat rejection requirements and further reducing radiator sizes.
- One system out of many (a two-loop system with one loop used only for humidity control and the other only for CO_2 elimination) was selected as being the most promising and was recommended for further investigation.

GOALS OF PRESENT PROGRAM

At the conclusion of the initial study the most crucial item in fabricating a working freeze-out system was thought to be (would be) the proper design of the CO_2 precipitator. This was seen to require a thorough understanding of the precipitation

mechanism, the frost layer formation, and the physical and thermal properties of the frost layer. Therefore, the ultimate aim of this experimental program was to carry out actual CO_2 freeze-out under simulated spacecraft conditions, to determine the operating characteristics of a precipitator plate, and to obtain sufficient understanding of the precipitation process to permit the designing of an optimum configuration.

TYPE OF TESTS AND RESULTS

To design a functional CO_2 precipitator of the optimum configuration, two types of results are required from this test program. These may be categorized as qualitative behavior of the frost formation and quantitative performance characteristics. An understanding of the qualitative behavior, obtained largely through visual observation of the frost formation, forms the basis of choice for the general precipitator configuration. The quantitative results then enable the designer to size the precipitator to meet the design loads.

QUALITATIVE RESULTS

The important qualitative results concern the following questions:

1. Does the inception of frost nucleation present a problem? (i.e., does it require considerable supercooling or does it occur at the dew point?)

2. Is channel surface roughness an important consideration?

3. Does the frost form as a solid sheet or as a snowy layer?

4. Does the layer spread out over the channel with essentially uniform thickness or does it grow unstably leading to localized plugging of the channel?

5. What is the effect of channel geometry on frost layer build-up?

6. What are the effects of inlet and exit transitions, bends, sharp corners, or other channel discontinuities on frost distribution?

QUANTITATIVE PERFORMANCE CHARACTERISTICS

The performance of a particular precipitator configuration can be described or predicted through the correlation of the appropriate transfer coefficients. These are obtained by the measurement of CO_2 precipitation rates or precipitator exit stream concentrations as functions of inlet CO_2 concentration, flow rate, inlet temperature, plate temperature, and geometric variables.

Additional quantitative measurements include CO_2 sublimation rates as a function of subliming channel pressure, pressure drops in the precipitator, and temperature distributions in the plate and channels.

SECTION II

DESCRIPTION OF EXPERIMENTAL TEST SYSTEM - PHASE I

To the end of obtaining experimental verification of the feasibility of the carbon dioxide and humidity control system proposed in ref 1, a simulated system was constructed. This apparatus was intended to approximate the design point of a one-tenth scale model of a one-man space capsule with a sea-level cabin atmosphere. The system was sufficiently flexible to investigate off-design conditions. Provision was made for visual and photographic observations of frost formation to obtain a qualitative understanding of the precipitation mechanism as well as extensive instrumentation to provide a detailed quantitative description of the system behavior. The regenerative heat transfer and water vapor control aspects of the proposed system were not included in the apparatus.

The complete test system can best be described by considering five basic subsystems:

1. Space Simulation System
2. Cabin System
3. Primary Circulation System
4. Precooling System
5. Precipitator-Sublimator-Radiator (P-S-R)

The complete test system is integrated in a basic functional schematic shown in Figure 1.

SPACE SIMULATION SYSTEM

This system provides the simulated space environment of high vacuum and low temperature. It consists of a vacuum chamber with cryogenic walls, feedthroughs, and instrumentation. It is capable of maintaining a vacuum of approximately 10^{-5} mm Hg and a shroud temperature of 77 K (LN_2 boiling point).

THE CABIN SYSTEM

A one-tenth scale space cabin volume is provided in which the metabolic CO_2 production is simulated by injection of CO_2 gas at a controlled rate. Air lost by leakage

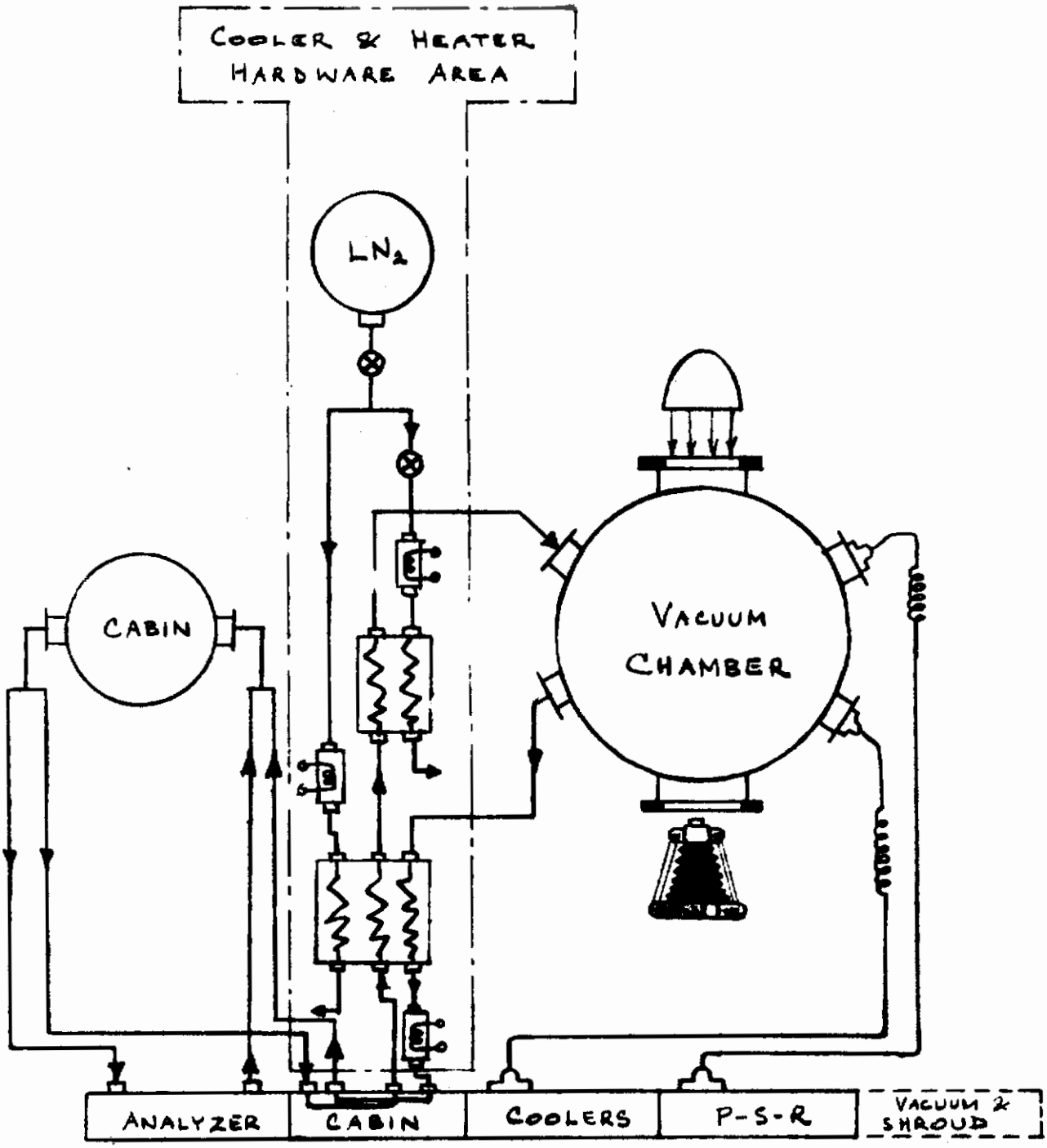

Figure 1

Schematic - WRI-18 Test Section

throughout the test system loops is replaced by make-up air. The cabin is provided with suitable instruments to monitor internal pressure, temperature and CO_2 concentration. A dryout loop is considered part of the cabin system. It allows the air to pass through an air dryer prior to circulating in the main loop. The dryer maintains a dew point of 170 K, which for all practical purposes is completely dry air.

PRIMARY CIRCULATION SYSTEM

This system pumps cabin air through a series of coolers into the vacuum system where it passes through the precipitator. From there the air leaves the vacuum system through reheaters and returns to the cabin at a low CO_2 concentration. The dump line branches off from the circulation loop. The sublimate of the CO_2 frost is passed through it to an auxiliary vacuum pump for disposal. This function simulates dumping of CO_2 sublimate overboard in an actual spacecraft.

PRECOOLING SYSTEM

This system consists of two convective heat exchangers, two cryogenic vapor generators and suitable controls provided for precooling the circulating air prior to entering the P-S-R system. This system simulates the function of the regenerative heat exchangers in the real system.

THE P-S-R SYSTEM

The P-S-R system consists of a two-channel P-S-R plate and suitable switching valves operated remotely. Each channel serves alternately as a precipitator and as a sublimator. During the precipitation phase, the CO_2 frost sublimate is released to vacuum. Heat rejection from the precipitator plate is accomplished by radiation to the cryogenic walls. The directional valves attached to the P-S-R are electrically operated, three-way solenoid valves.

DETAILED SUBSYSTEM DESCRIPTION

All five systems are described below in greater detail. Further details of the system are depicted in the so-called "Assembly Schematic", fig 2. This schematic served as the basis for design, fabrication and assembly of the actual loops and of the control and instrument panels in the laboratory.

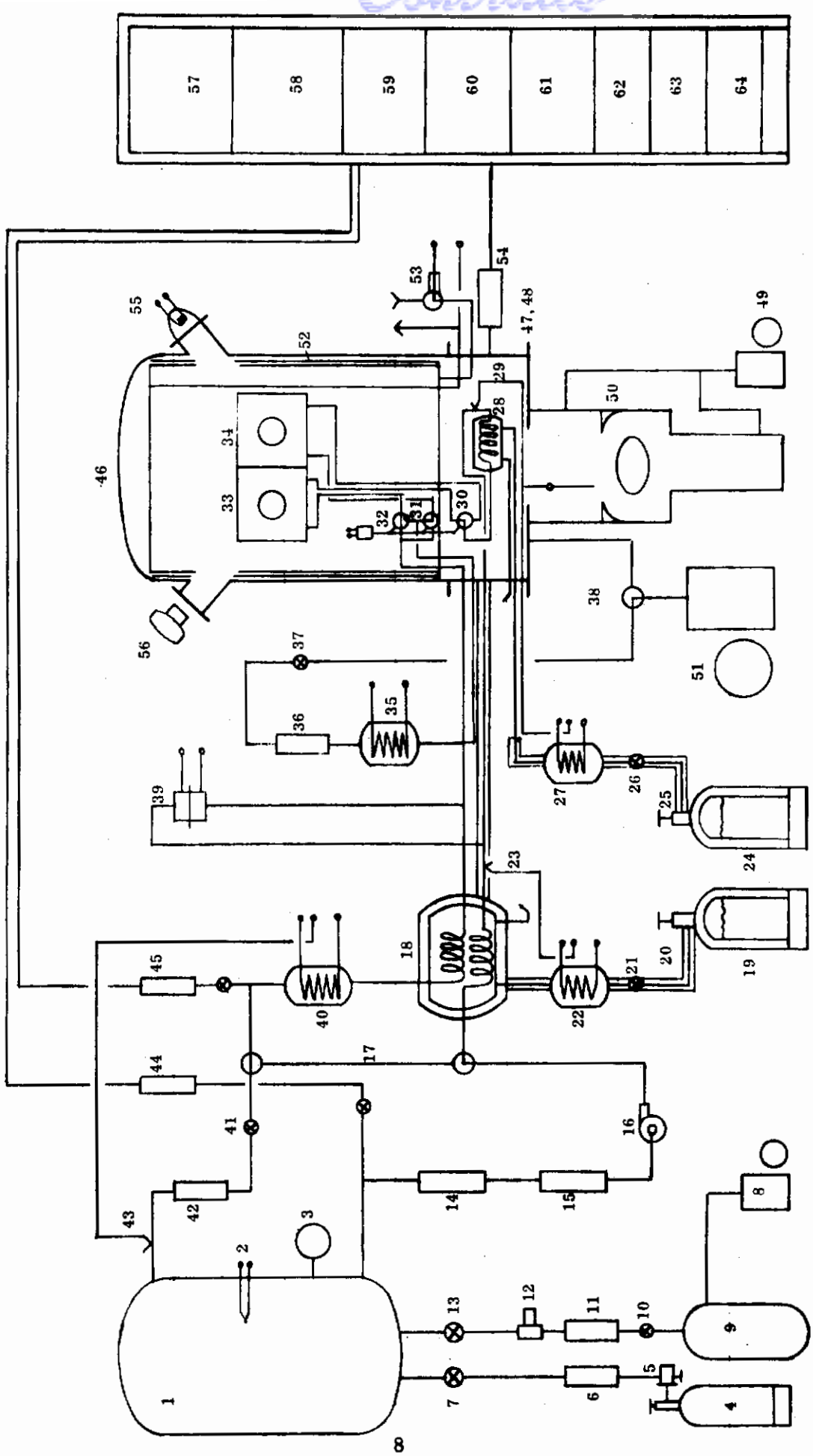

Figure 2

Assembly Schematic

Space Simulation System (See figure 3.)

The environment simulation system consists of a vacuum system and of a cryogenic wall system.

The vacuum system is composed of a bell jar (46) and a vacuum feedthrough collar (47), separating the bell jar from an elevated base plate (48). The collar has 8 small accessory ports (67) provided with four fluid-line feedthroughs and with four electrical feedthroughs. It also has two large observation ports with flange-sealed windows (65) and (66), diametrically opposed and mutually inclined in such a fashion as to permit illumination (55) and observation (56) of the test article located inside the bell jar. The vacuum pumping system consists of two mechanical positive displacement vacuum pumps (49) and (51) for roughing and an oil diffusion pump with accessories (10) for higher vacuum. The pumps can pull a vacuum of 10^{-4} millimeters of Hg in about 1 hour.

The cryogenic wall (52) is composed of three segments: a cylindrical sidewall shroud, a circular lid on top and a circular shield at the bottom. The sidewall and the top cover are controlled automatically by liquid-level controllers (15) while the bottom shield is maintained at a low temperature by manual adjustment of LN_2 supply and by a vapor vent. The wall is maintained at the LN_2 boiling point of 77 K.

Cabin System (See figure 4.)

The system consists of the cabin tank (1) of 0.32 cu. meter capacity and instrumented with a precision pressure/vacuum gauge (3) and two temperature gauges (2). The cabin is also equipped with a pressure relief valve (74).

The pressurized CO_2 storage bottle (4) of 0.566 cu. meter capacity is provided with an accurate pressure reducer (5). The CO_2 admission rate is metered by a precision rotameter (6) and controlled by a micrometric flow control valve (7).

The make-up air is piped from the shop compressed-air tank (9) through a shutoff valve (10), measured by a precision flow meter (11) at a reduced pressure maintained by a precision pressure regulator (12). The desired flow rate is regulated by a needle valve (13) at the entrance to the cabin.

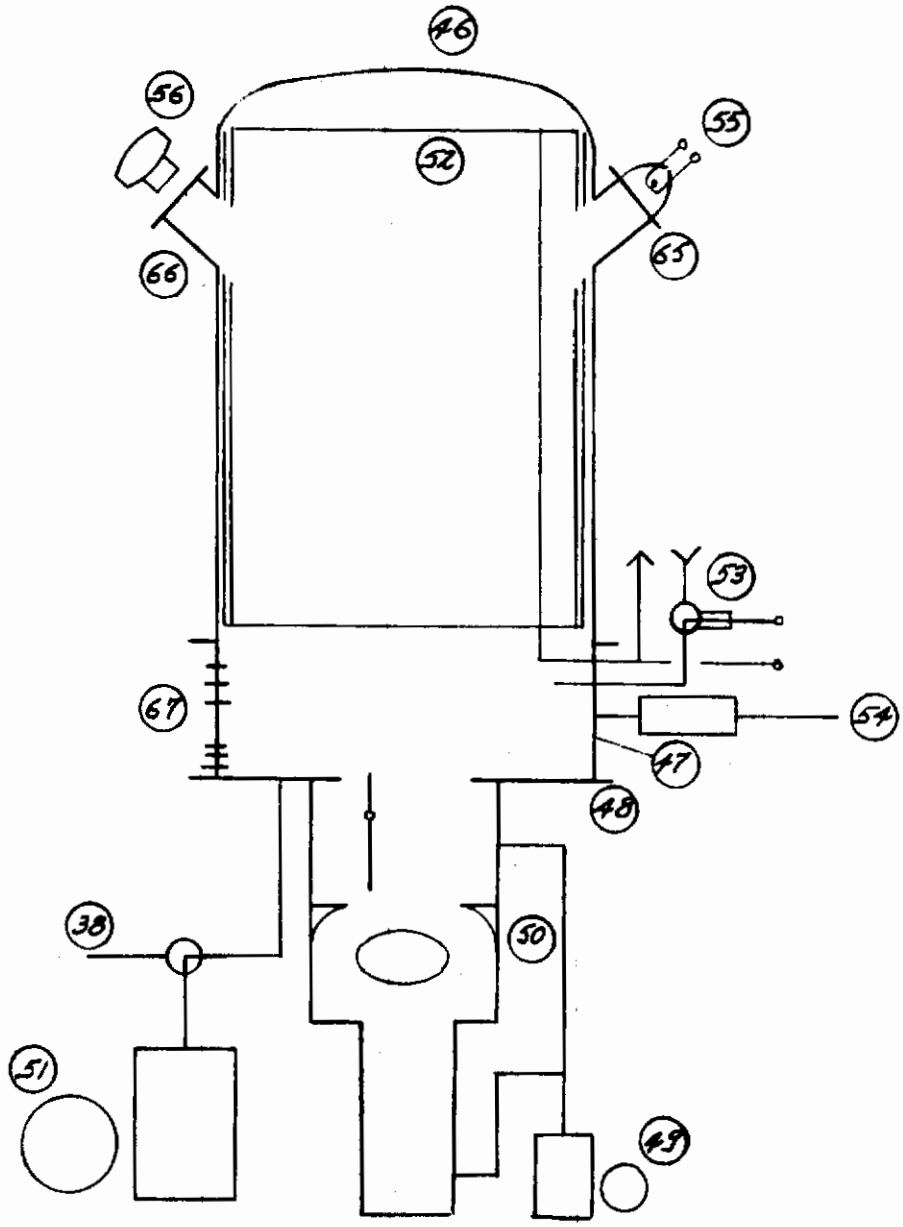

Figure 3

The Environment Simulation System

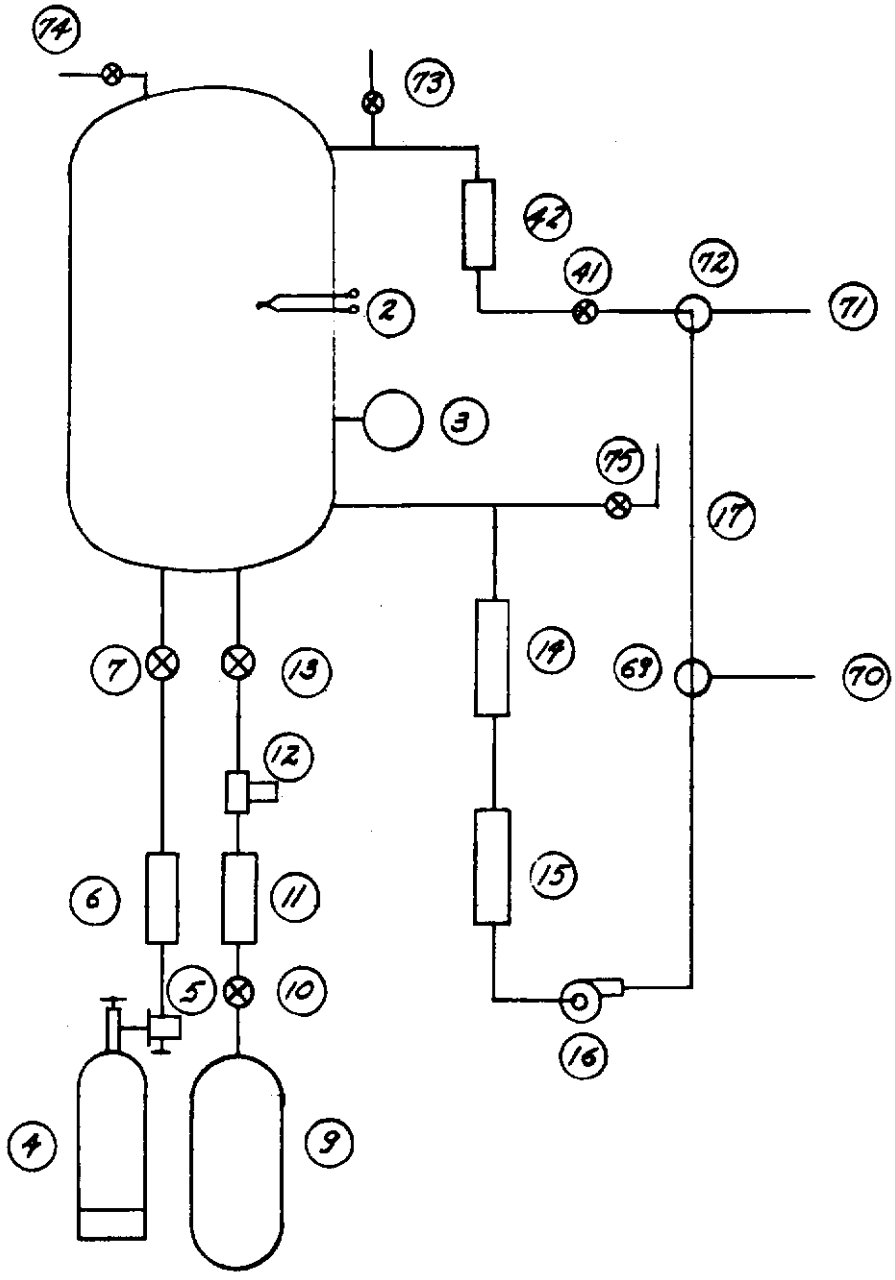

Figure 4

Cabin System

The dry-out bypass loop consists of a suction connection and suction line (75a), an air meter (14), the air drier (15) and a circulation blower (16). The circulation proceeds normally through directional valves (69) and (72) via the bypass 1 line (17). (If actuated, the valves divert the flow to the main loop intake line (70) and bring it back to the return line at station (71). The return flow is controlled by a meter valve (41) measured by an air meter (42) and returned to the cabin where it provides stirring action.

Take-off points with valves (73) and (75) are the CO_2 analyzer sampling and return lines.

Main Circulation System (See figure 5.)

This system provides the air circulation between the cabin and the vacuum-enclosed P-S-R. Air is ducted from the cabin (1) through the circulation flow meter (14) and the air drier (15). The flow resistance is overcome by a two stage air pump of the diaphragm type (16). If the bypass-1 switches are actuated, the air is precooled in the precooler (18), passes through the vacuum feedthrough collar wall (47) into the final cooler (28) located in the vacuum system, from which, at a desired temperature it is directed to one channel of the P-S-R by the admission valve (30). It passes through channel 1 (33) and returns (less CO_2) through the return valve (32) into the return system. In the meantime, the second channel of the P-S-R plate (34) is vented via the dump valve (31) into the dump system. If actuated by the solenoid actuator (79) all three valves (30), (31), and (32) reverse their functions and also reciprocate the functions of the two P-S-R channels. The P-S-R plate is provided with sealed observation windows (78). Both the return and dump lines pass out of the vacuum system via vacuum feedthroughs (67). The return line guides the return air through the regenerator-coil of the precooler (18), where it warms up. Further reheating is accomplished by the electric in-line heater (40). The actuated bypass return valve (72) directs the return air through a metering valve (41) and the return air meter (42) and returns this air back into the cabin (1).

Alternate sampling lines are provided for the circulated air at (75) and the return air at (76). The sample is pumped to the CO_2-analyzer console and returned to connection (73) where it is mixed with the return air.

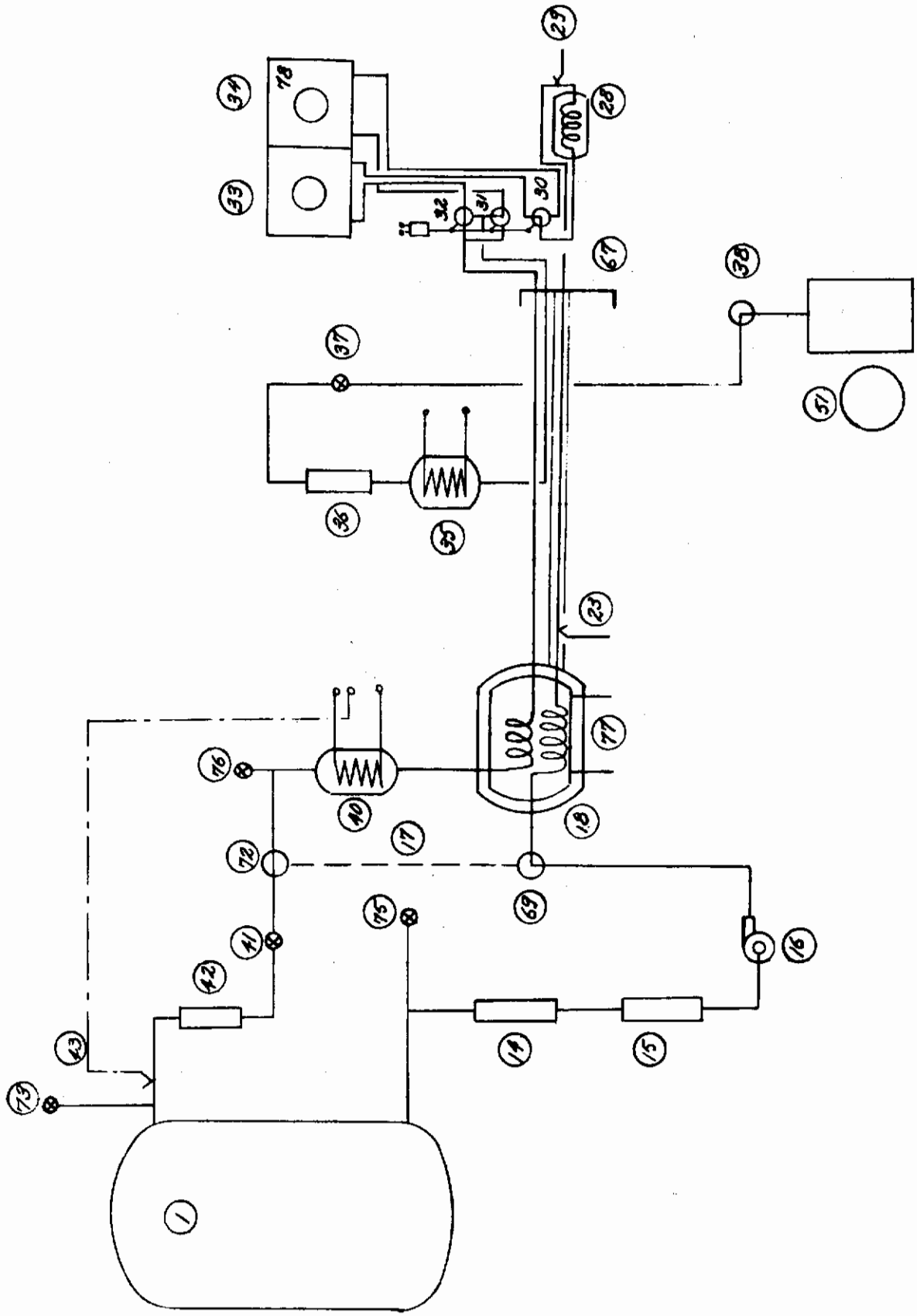

Figure 5

Main Circulation System with Dump Line

The dump line receives the CO_2 sublimate and heats it by an electric heater (35). The sublimate is metered by a flow meter (36) while the rate of sublimation is regulated by a flow restrictor (37). The dump valve (38) provides connection with a mechanical vacuum pump (51).

During a normal main-loop operation (bypass valves (69) and (72) activated), the bypass (17) is inactive.

The control of stream temperatures is accomplished as follows. Precooler (18) outlet temperature is sensed at point (23) and monitored. Adjustment of coolant flow through connections (77) of the precooler provides the control action. Similarly, the temperature sensor (29) provides a feedback signal for the fine cooler coolant flow and temperature. A thermocouple (43) provides feedback signal to the reheater (40) control.

Precooling System (See figure 6.)

Two parallel cooling systems are serving the precooler and the final cooler. Their functions are nearly the same.

The precooler cooling system, particularly necessary to start the regenerator functions, consists of an LN_2-vapor generator from which cold nitrogen gas is passed by an insulated flex-line and metered by a valve into a nitrogen-vapor heater where it is warmed up to a suitable temperature before entering the cooling pass of the 3-coil heat exchanger (18) from which it is vented. Thermocouple (23) provides feedback to the heater power control (80).

The final cooler cooling system has another LN_2 vapor generator (24), an insulated line, a metering valve (26), a nitrogen heater (27) and a constant temperature controller (80). The cool nitrogen gas enters (and leaves) the vacuum system in a feedthrough (82) and passes through the cold-side coil of the final cooler (28) before being vented to the atmosphere. A thermocouple (29) monitors the circulation air temperature just before entering P-S-R and provides feedback to the constant temperature controller.

P-S-R System

The P-S-R system described here consists of the prototype P-S-R plate assembly and of the selector valves attached to it. The whole P-S-R system is mounted

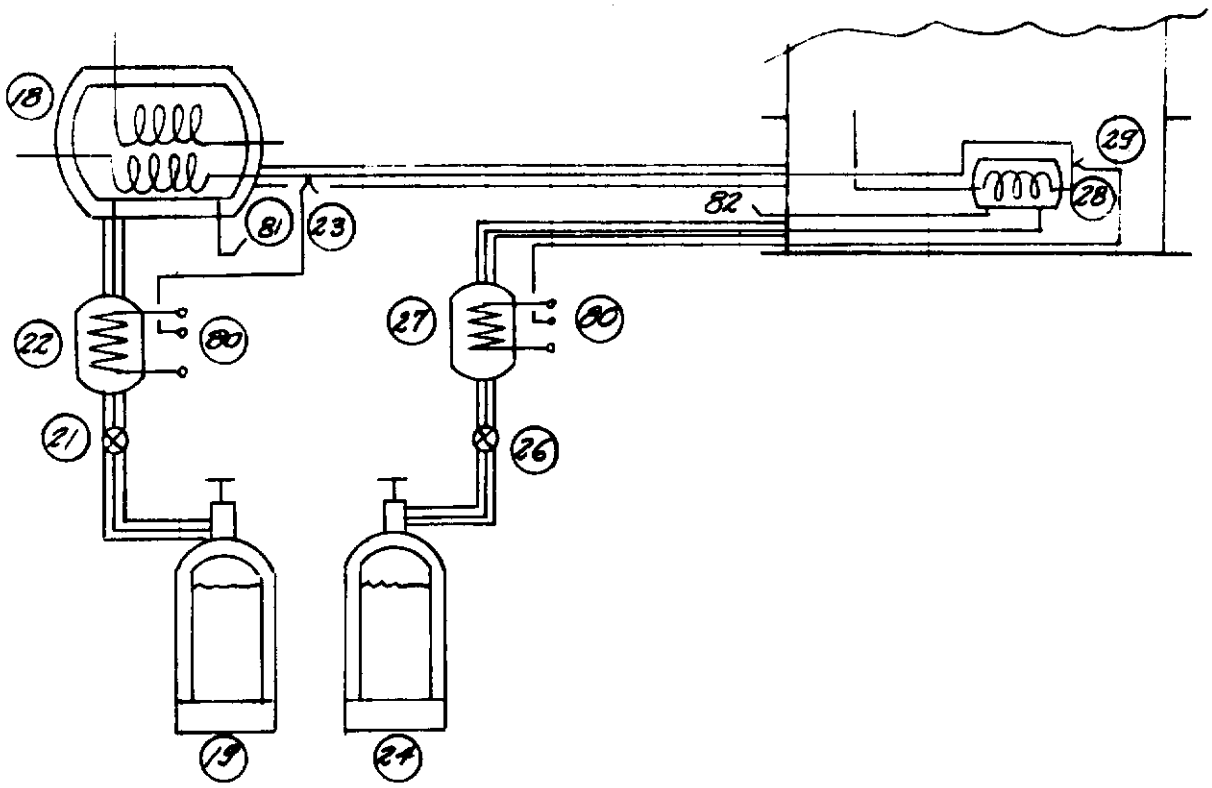

Figure 6

Liquid Nitrogen Cooling System

inside the environmental chamber as sketched in figure 7. This sketch shows approximately the relative locations of the cold walls, windows, and P-S-R plate inside the vacuum space. The vacuum feedthrough collar (47) sits on the base plate (48) and is provided with two diametrically opposed ports covered with flange-mounted windows (65, 66) of which one is used for illumination and the other for observation and photographic documentation. The vacuum bell jar (46) sits on top of the vacuum extension collar. Inside the vacuum space are the 3 segments of the LN_2-wall (52): a vertical shroud (52a) and a top cover (52b) surround the P-S-R plate so that the P-S-R plate's radiator surface (83) is exposed to a full 180° view of the cryogenic wall. Underneath the radiator plate the precipitator and sublimator open channels are located, covered with a transparent window (84) oriented in such a way as to permit a full view of the channels from an observation port. At the bottom, an LN_2-shield (52c) had been added to eliminate radiant heat loads from the warm base plate.

The prototype P-S-R plate assembly is sketched in figure 8. It consists of a radiator brass plate (83), black coated on the top surface, into which parallel channels had been milled from the bottom side, one for precipitation and one for sublimation; the channel 1 (33) and channel 2 (34) are separated by a thin brass wall. To this integral plate a low-temperature plastic window plate (84) is bolted; sealing between channels and between interior and the vacuum space is accomplished by means of a flexible gasket (85) squeezed between the plastic window and the brass plate. The inlets and outlets of both channels are connected to three solenoid three-way valves (30, 31, 32) that control the selection of channels (switch-over of the cycle). The two alternate possibilities are shown schematically in figure 9. In the first position, the passing air is processed in channel 1 while channel 2 is dumping the sublimated CO_2 to vacuum; in the second position the functions of the channels are reversed.

Extensive instrumentation for temperature and pressure drop measurements is attached to the P-S-R plate and enclosed in the vacuum. The systematic organization of various functional and instrumentation feedthroughs is sketched in detail in figure 10. The more significant components are shown: the vacuum feedthrough collar (47), the circulation feedthrough (85), the final cooler (28), the cooling nitrogen feedthrough (82), the final air (control temperature pickup (29) with its feedthrough (80), the channel selection valve (30), channel 1 (acting as precipitator in this case), (33), attached to the

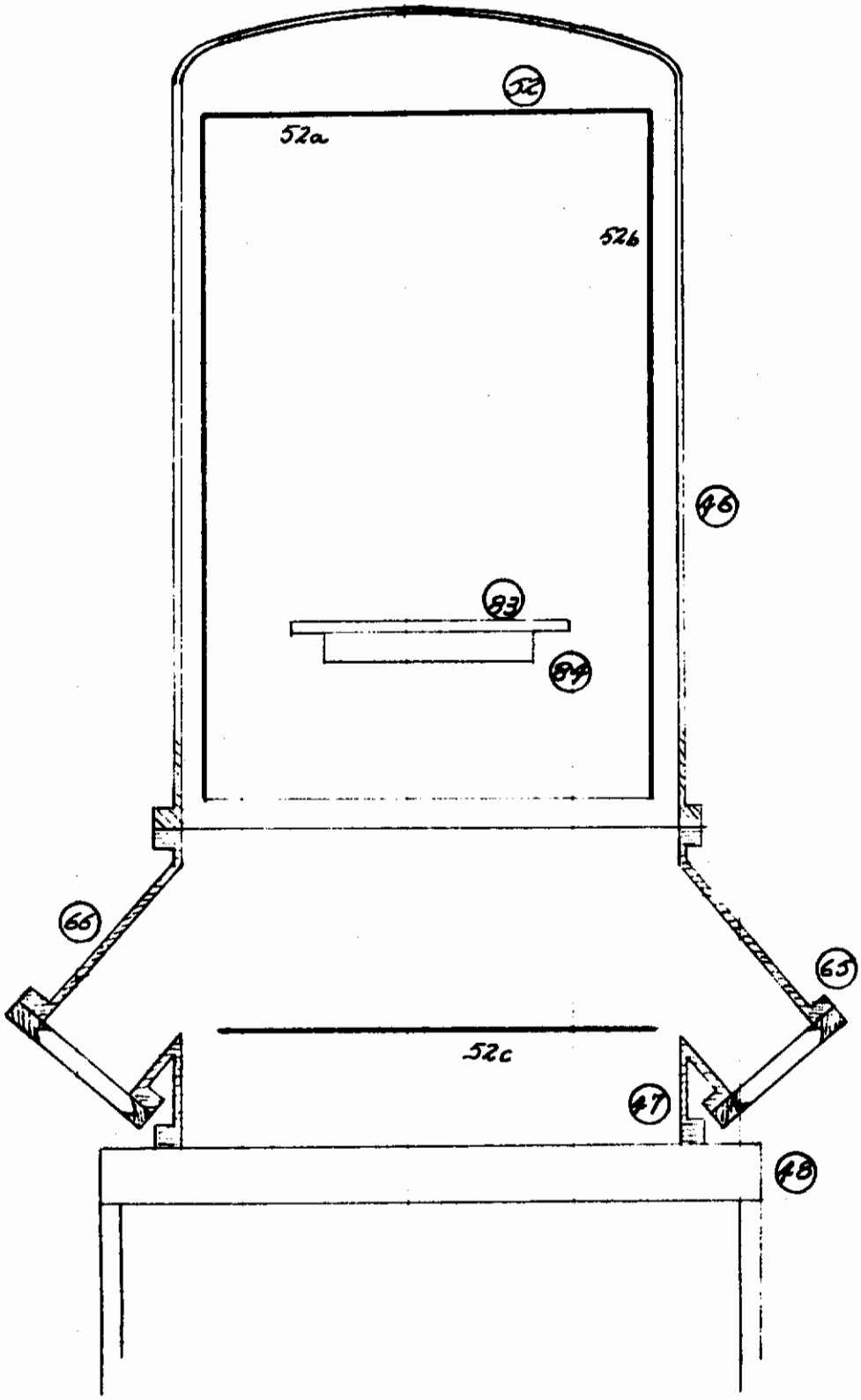

Figure 7

Observation Port Arrangement - Environments Chamber

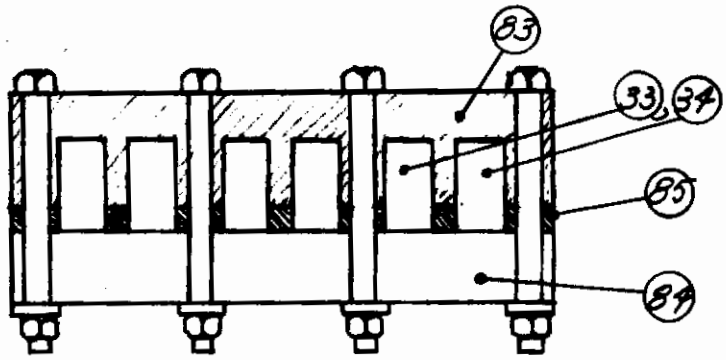

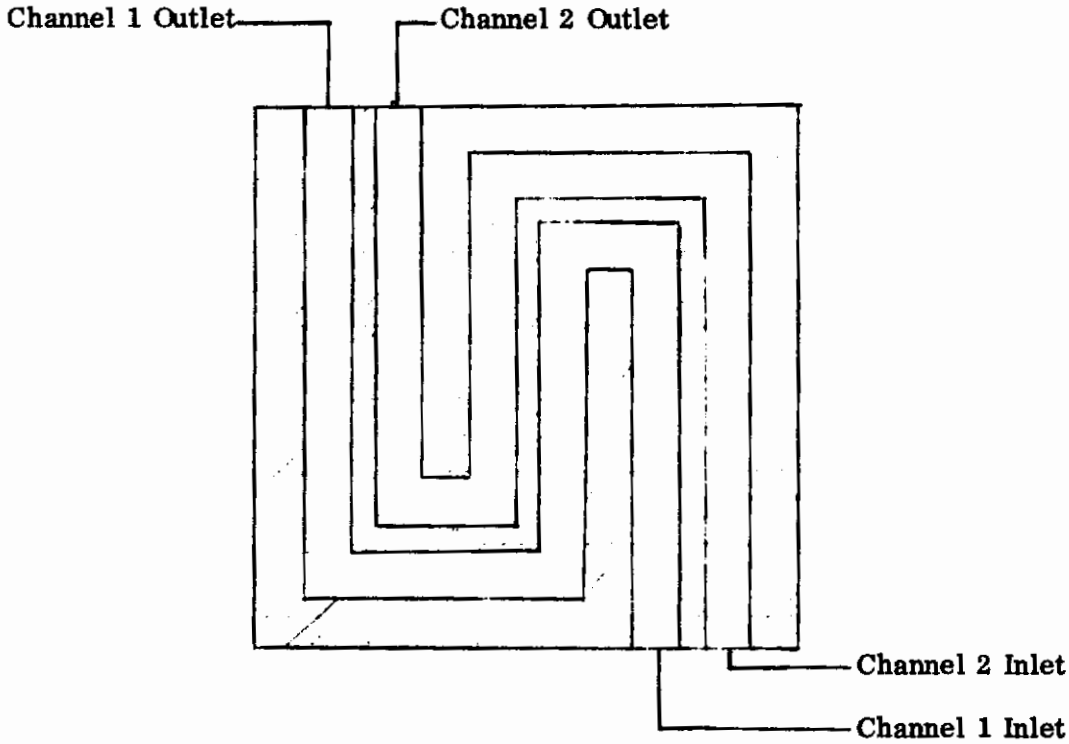

Figure 8

P-S-R Plate Asembly

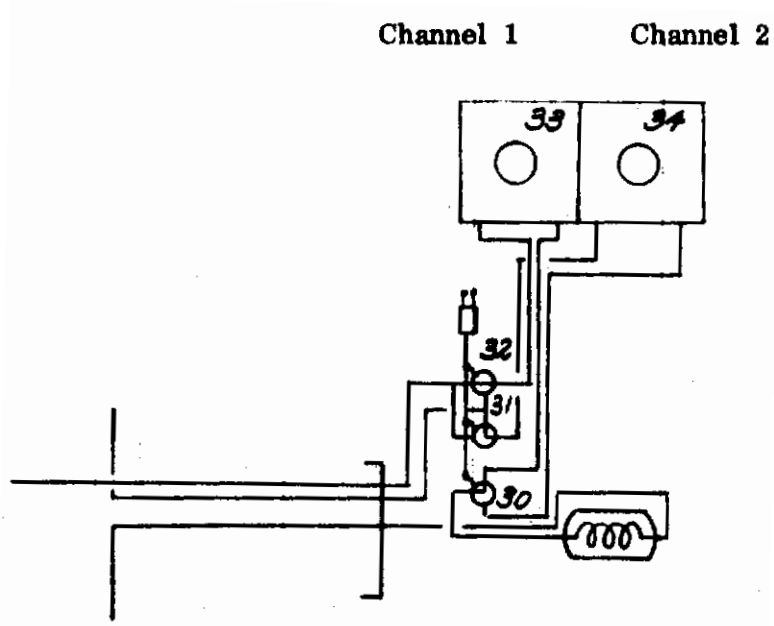

9a - P-S-R System In Channel 1 Position

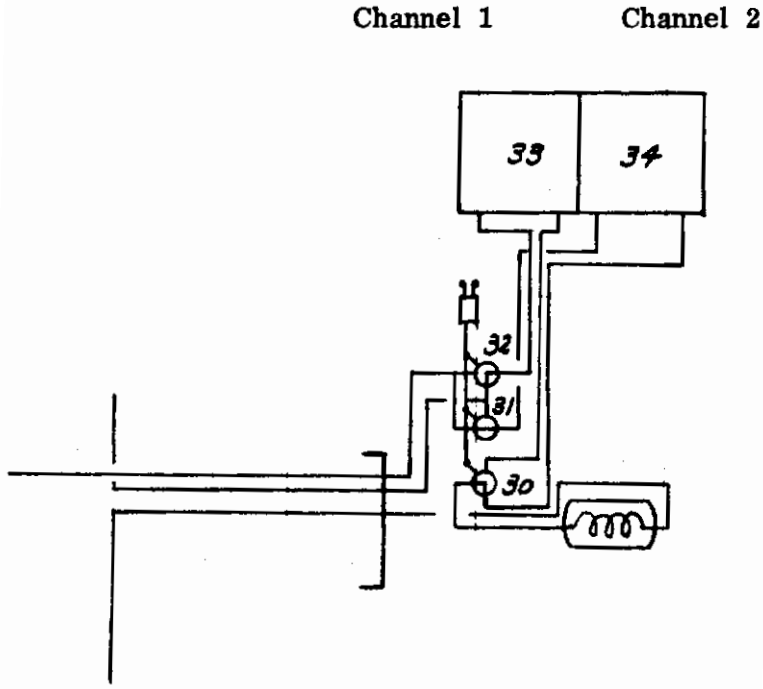

9b - System In Channel 2 Position

Figure 9

Alternate P-S-R Channel Position

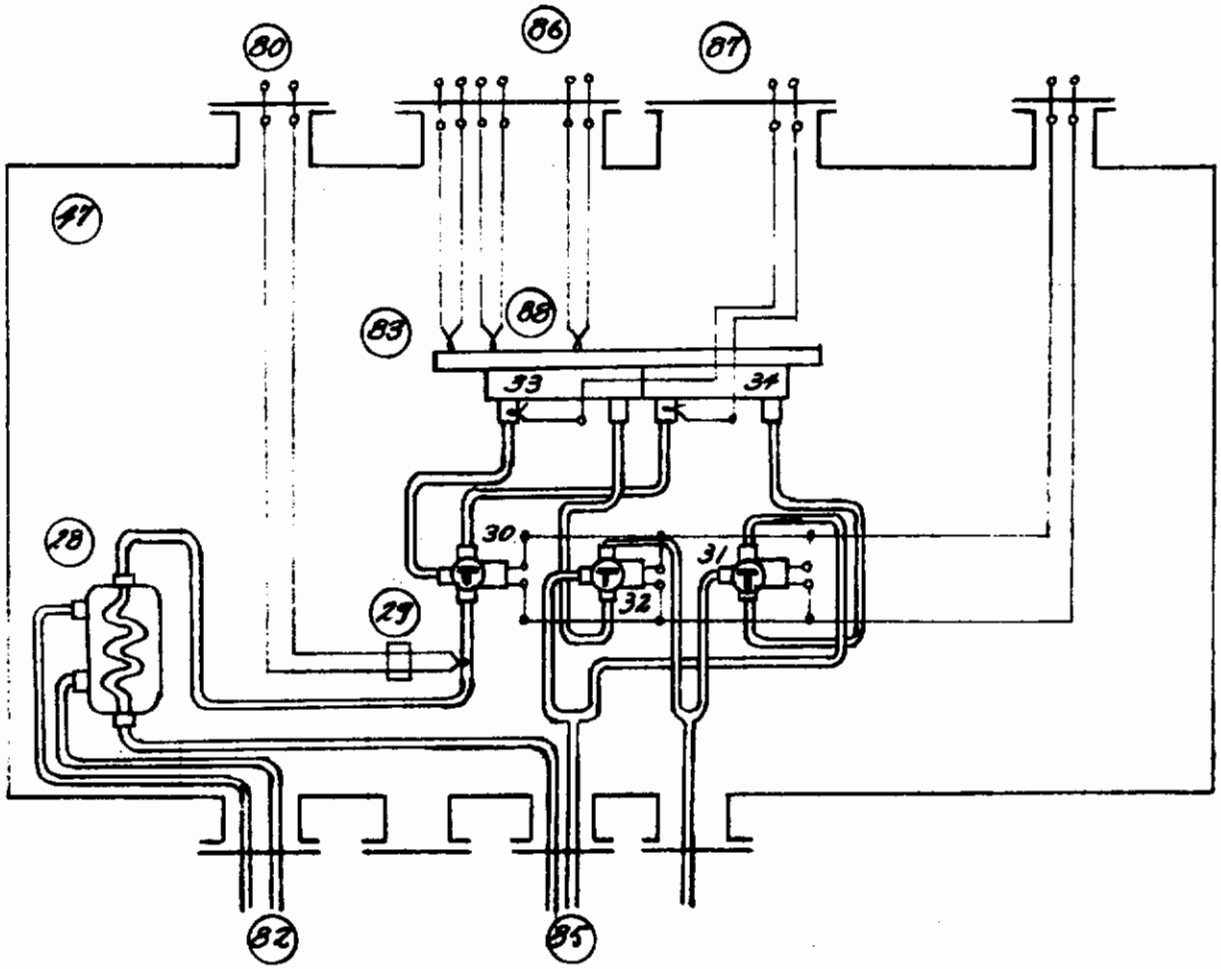

Figure 10

P-S-R System Valving, Piping, and Wiring

radiator plate (83), the channel 2 (34), the air return valve (32) and the dump valve (31). The power to the valve solenoids comes via feedthrough (79). A feedthrough (89) passes the dump gas to external vacuum (not shown). Feedthroughs (86) and (87) pass thermocouple leads of the surface thermocouples (88) and of the channel thermocouples.

System Controls

The following is a listing of the major controlled variables of the main test loop:

Flow Rates:	Air circulation rate
	CO_2 injection rate
	Sublimation rate
	Make-up air rate
Pressures:	Cabin pressure
	P-S-R precipitation channel pressure
	Sublimation channel pressure
	Pressure drop across precipitator
Temperatures:	Air leaving precooler
	Air leaving final cooler
	Air entering the P-S-R
	Return air
CO_2 Concentration:	At intake
Channel Selection:	Channel 1/2 switch

Instrumentation

Provision was made for recording the following quantities.

p_p - precipitation pressure

p_s - sublimator pressure

p_{vac} - environmental pressure (vacuum)

$\Delta p_{P\text{-}S\text{-}R}$ - pressure drop across precipitator

$\dot{w}_a$ - circulation air rate

$\dot{w}_c$ - CO_2 generation rate

$\dot{w}_L$ - air leakage and make-up rate

$\dot{w}_s$ - sublimate dump rate

$C_{c_{in}}$ - CO_2-concentration into P-S-R

$C_{c_{out}}$ - CO_2-concentration out of P-S-R

T_S - simulated (environmental) space temperature

T_P - radiator plate temperature

T_{PL_1} - channel wall temperature

T_{a_1} - entering air temperature

T_{a_2} - leaving air temperature

T_{FC} - temperature of air leaving final cooler

T_r - return air temperature

T_{subl} - sublimate leaving temperature

The listed quantities are measured and recorded. The pressures are indicated by bourdon gauges, except the environmental vacuum which is detected by a precision alphatron vacuum gauge; the flow rates are measured by precision through-flow rotameters; the CO_2 concentration is measured by a LIRA infrared gas analyzer with a special 0 - 1% scale; the temperatures are picked up by copper-constantan thermocouples and read by precision potentiometers.

The CO_2 analyzer requires numerous accessories and calibration devices; the connection of the instrument and accessories into the analyzer circulation loop is apparent from the schematic of figure 11. (75) and (76) are the air circulation and return connections with shut-off valves. The gas sample (air with CO_2 trace) is drawn into a diaphragm air pump (89), filtered at (90), controlled by restrictors (91) and by-pass (95), metered at (92) for an optimum sensitivity required by the instrument; the gas sample then passes through the analyzer itself (93) and is either rejected through the vent valve (94) or is returned into the cabin through a return valve (73) and line.

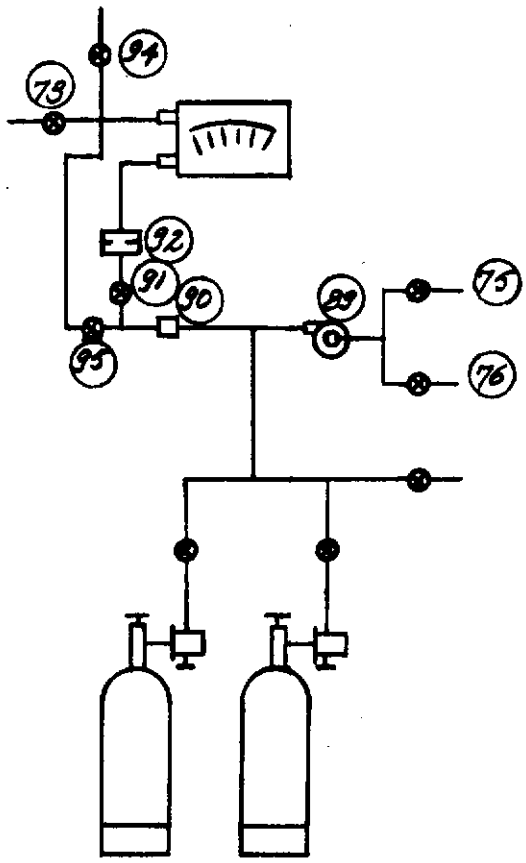

Figure 11

Analyzer Loop and Calibrated System

OVERALL SYSTEM CAPABILITY

Cabin

The cabin tank is the nearest size available to the desired 0.283 cu. meter volume and is 0.320 cu. meter.

P-S-R

The prototype P-S-R plate has an internal surface area in excess of 290 sq. cm. per channel and has nearly 200 linear centimeters of vacuum-tight seal necessitated by the observation window design requirement. The radiator plate black surface is 845 sq. cm.

Circulation Loop

The circulation line is of 0.635 cm. I.D. copper tube. A diaphragm type air pump provides a maximum air flow of 550 cc/sec at nominal cabin pressure. A 200-watt heater has enough power to reheat the return air to normal (near-room) temperatures.

Environmental Chamber

The cryogenic wall is maintained near -196 C by boiling liquid nitrogen. The vacuum system can be pumped down to 1×10^{-4} millimeters of mercury.

CO_2 Control

Up to 100 cc's per minute of gaseous CO_2 can be added to the cabin system. A maximum CO_2 concentration within the cabin and the air loop is limited to 1% by volume by the range of the LIRA analyzer, especially modified for this experiment. This is well above the bio-medical maximum CO_2 concentration, however.

SECTION III

TEST PROCEDURE

This section provides a brief description of a typical test.

PREPARATION OF TEST FACILITY

1. Leak test circulation loop and P-S-R.
2. Set up LN_2 supply bottles.
3. Calibration check of LIRA analyzer and other instrumentation.
4. Circulate cabin air through drier.

PUMP-DOWN AND COOL-DOWN

1. Close up vacuum system and start roughing pumps.
2. Circulate air through pre-cooler and P-S-R.
3. Start nitrogen flow to pre-coolers.
4. Turn on diffusion pump (Vacuum at $\approx 10\mu$)
5. Fill cryogenic shrouds with LN_2 and activate level controllers.
6. Admit nitrogen flow to auxiliary P-S-R plate cooling loop (used only during cooldown).
7. Stabilize pre-cooler exit temperatures close to actual operating levels ($\sim$ 160 K for first cooler; $\sim$ 150 K for final cooler).
8. Monitor P-S-R plate temperature.

When the P-S-R plate temperature approaches its probable operating range ($\sim$ 145 K), the auxiliary cooling loop is turned off and the establishment of an operating point commences.

ESTABLISHMENT OF STEADY-STATE OPERATION

1. Start CO_2 injection to cabin; set rate.
2. Set desired circulation rate.
3. Set desired inlet temperature to P-S-R.
4. Wait for steady state (CO_2 concentration in cabin).
5. Read and record measured variables. (See table 1.)
6. Observe and/or photograph first formation.
7. Switch channels:
   a. when first channel plugs up, or
   b. when exit concentration rises appreciably with operating conditions held steady.
8. Set new operating point by resetting:
   a. CO_2 injection rate, or
   b. circulation rate, or
   c. inlet temperature to P-S-R.

Table 1

DATA RECORDING

The tabulated data are recorded during a test run.

Quantity	Location
Cabin:	
Pressure	Top, cabin tank
Temperature	Immersed in cabin
CO_2 concentration	Sampling at outlet from cabin
CO_2 injection rate	At entrance to cabin
Air make-up rate	At entrance to cabin
Circulation Loop:	
Air rate leaving cabin	At exit from cabin
Return air rate	At re-entry to cabin
CO_2 concentration leaving cabin	At exit from cabin
CO_2 concentration of return air	At re-entry to cabin
Pressure entering P-S-R	After final cooler, inside vacuum
Pressure drop across P-S-R	Between final cooler and common return line inside vacuum
Air temperature leaving precooler	After precooler
Air temperature leaving final cooler	Before admission valve
Air temperature before P-S-R	After admission valve
Return air temperature	After reheater
Dump Line:	
CO_2 sublimate flow rate, dual range	Before admission valve (to vacuum)
CO_2 sublimation pressure	In line

Table 1 (cont'd)

Quantity	Location
P-S-R Plate:	
Channel 1 inlet air temperature	Inside channel 1
Channel 1 outlet air temperature	Inside channel 1
Channel 2 inlet air temperature	Inside channel 2
Channel 2 outlet air temperature	Inside channel 2
Auxiliary temperatures	Various locations, channels and accessories
Plate (radiator) temperatures	Several locations
Environmental Chamber:	
Vacuum	Through base plate
Shroud surface	Side shroud
Mean radiant temperature	Above P-S-R plate

SECTION IV

DISCUSSION OF RESULTS

The results of the Phase I experimental program indicate that no unforeseen difficulties or drawbacks arise in the design and construction of a CO_2 precipitator-sublimator configuration. A significant portion of the experimental information derived from these tests is in the form of qualitative understanding of the precipitation and sublimation phenomena. This understanding, leading to the selection of an appropriate geometric configuration, will be presented in relation to the questions raised in Section I

QUALITATIVE OBSERVATIONS

The following comments concerning the qualitative behavior of the frost layer formation apply equally well to all the test conditions and geometric configurations covered in the experimental program.

Frost Layer Characteristics

The CO_2 layer always took the form of a snowy frost at reasonable CO_2 concentrations. The only case of a clear slab of ice forming occurred in a preliminary test where pure CO_2 was run through a cold channel. Attempts to force a different type of freeze-out, by introducing a CO_2-laden stream (~ 1.0% or $p_{CO_2} \simeq 9$ mm Hg) into a very cold channel (120 K or less) through the use of extended precooling with liquid nitrogen, were not successful.

Initial frost nucleation did not present any difficulty. Although the channel surfaces were quite smooth, frost deposition would begin as soon as the channel surface temperature dropped below the dew point. Even before a frost layer was clearly visible (noticeable only as a faint sparkly quality at the channel inlet), the exit stream concentration would show a definite decrease. Figure 12 shows some transient results. With the cabin atmosphere passing through the channel at constant flow rate, CO_2 inlet concentration, and inlet temperature, the plate temperature was decreasing toward its equilibrium condition. At the dew point corresponding to the inlet stream concentration, the exit concentration began to fall. Hence, any consideration of surface treatment to enhance nucleation is unnecessary.

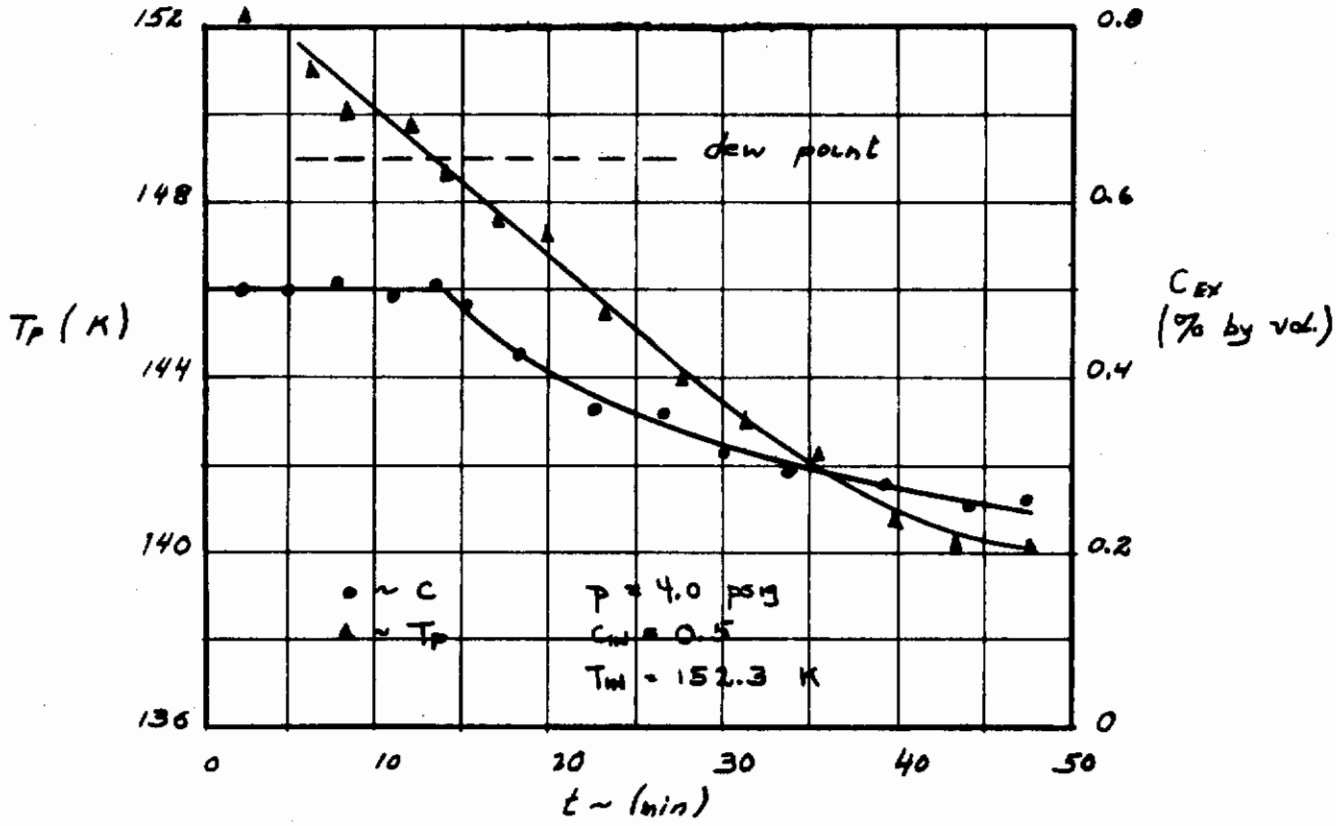

Figure 12

Transient Behavior
(Nucleation)

One characteristic of the frost layer which will have to be considered in the final configuration is its fragility. Once the layer builds up to a significant thickness (greater than ~1mm) it is not very firmly attached to the lower layer. Although there was no evidence that the air stream passing over the layer was sufficient to dislodge it under steady conditions, the layer could be partially dislodged by rapid switching of the channels. That is, the rapid rush of air out of the precipitating channel as it was exposed to vacuum for sublimation or the rush of air into a subliming channel which had some frost left on the walls was sufficient to carry along some solid CO_2 particles. In the gravitational environment, these particles would fall out of the stream down onto the transparent viewing window before being carried out of the channels. In zero-g, however, these particles could either be carried along with the air stream back to the cabin, or, in the case of the subliming channel, be dumped overboard before being sublimated. Both occurrences are undesirable, and some particle separator or trap must be devised to ensure that only gas leaves the precipitator-sublimator unit.

Mode of Layer Build-up (See figure 13.)

The way in which the frost layer builds up along the channel can be described as a progressive growth from inlet to exit. Initial frost formation takes place at the inlet end of the channel. The presence of this layer acts as an insulating layer and succeeding frost is mostly deposited further downstream on fresh channel surfaces. This is consistent with the observation that the channel wall provides excellent nucleation characteristics so there is no tendency toward preferential nucleation on the existing frost layer. Some deposition would continue on the frost layer until the layer reached sufficient thickness that the sensible heat load alone was enough to maintain the frost-air interface at or above the dew point. At this point, all deposition would move downstream tending to even out the frost layer thickness. As this process continued, a point would be reached at which the total freeze-out rate (or mass transfer effectiveness) was insufficient to handle the rate of CO_2 injection to the cabin. The inlet concentration would then rise, permitting freeze-out at a higher temperature and further thickening of the layer. Simultaneously, the heat load on the radiator would be reduced with a resultant drop in plate temperature, and still more frost deposition. All of this implies that a true "steady state" is never obtained. Experimentally, however, it was clearly established that these compensating factors resulted in good CO_2 level control until a relatively uniform frost layer of approximately 2.5 to 3 mm existed throughout the channel. At this point, freeze-out virtually ceased and the CO_2

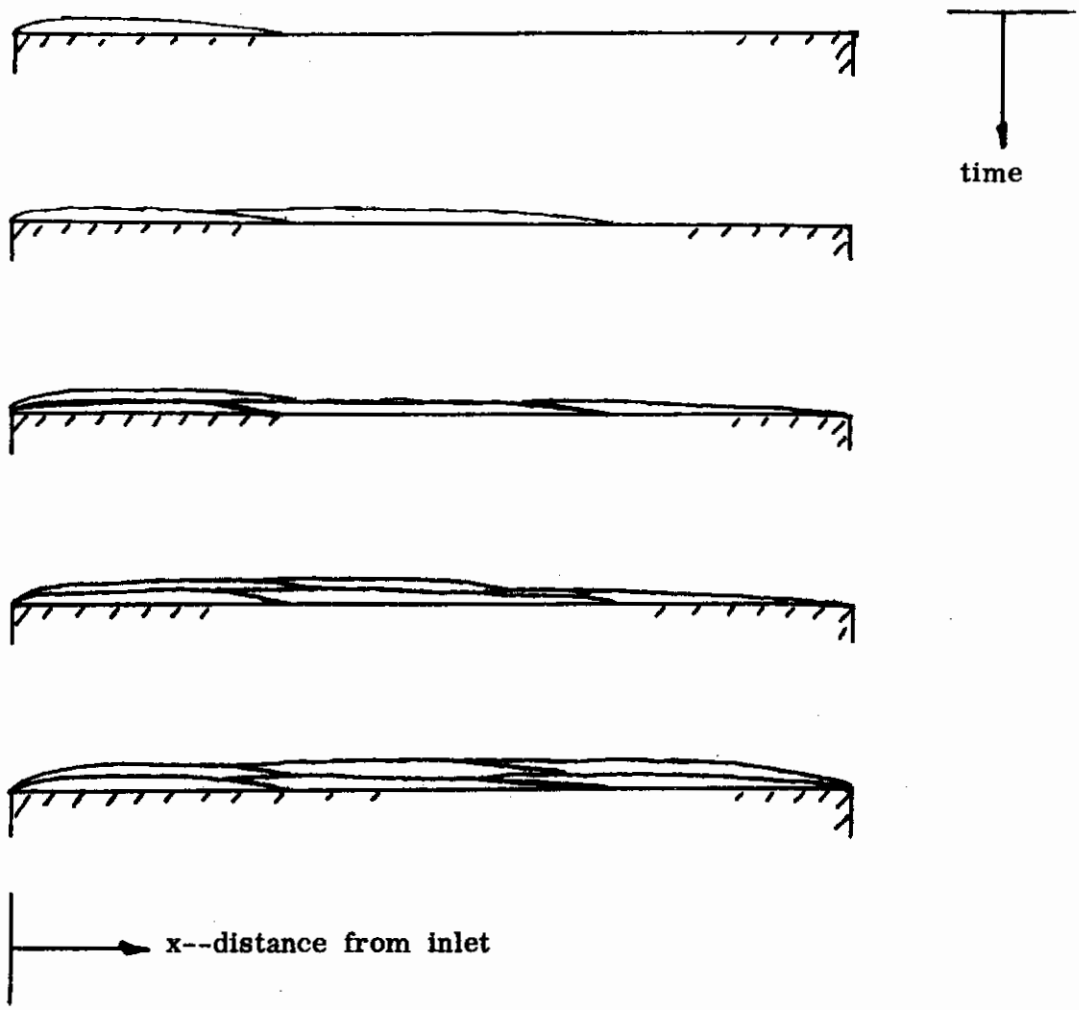

Figure 13

Mode of Frost Layer Buildup

concentration in the cabin began to rise. This critical layer thickness was virtually independent of channel size. The quantitative evidence for this behavior is presented in a later section.

The details of this transient behavior were very difficult to monitor and interpret accurately since they took place very slowly. This very slowness of response, however, is a great help in control of the system in that changes in the CO_2 concentration in the exit stream from the precipitator can be measured very closely, used as an indication of system performance, and cause corrective action to be taken well in advance of any detectable effect on cabin concentration.

Effect of Channel Geometry

Considerations of channel geometry did not present any difficulty in obtaining a uniform frost buildup. Disturbances in the boundary layer caused by corners or bends in the channel did not appear to affect the local freeze-out rate with the exception of the region close to the entrance. The inlet fittings and transition region although enlarged and insulated to forestall premature plugging of the channel, were constructed in such a way as to force a 90° turn of the flow as it entered the precipitator. (See figure 14). This produced a separated region on the frost surface of the channel which impeded frost buildup in a narrow, "finger-shaped" area just downstream of the inlet. In addition, wall surfaces normal to the flow (downstream of a right-angle bend - see figure 10) exhibited a slightly thinner frost layer due to the scrubbing action of the flow and, in all probability, some dislodgement of the frost that did form. These effects were, however, slight and never led to a premature plugging even in the smallest channel geometries. Whereas such local thinning of the layer will lead to a slightly greater expenditure of cabin atmosphere during the sublimation cycle, this is a very small effect. As Bonneville (ref 1) points out, even a relatively large volume of lost cabin air compared to the frost volume (x10) represents a very slight system penalty. The smaller channels could be run until they appeared to be at least two-thirds full of frost with no plugging.

QUANTITATIVE TEST RESULTS

With qualitative assurance that no fundamental difficulty or unexpected pitfalls exist in designing a workable precipitator configuration, it is possible to base a

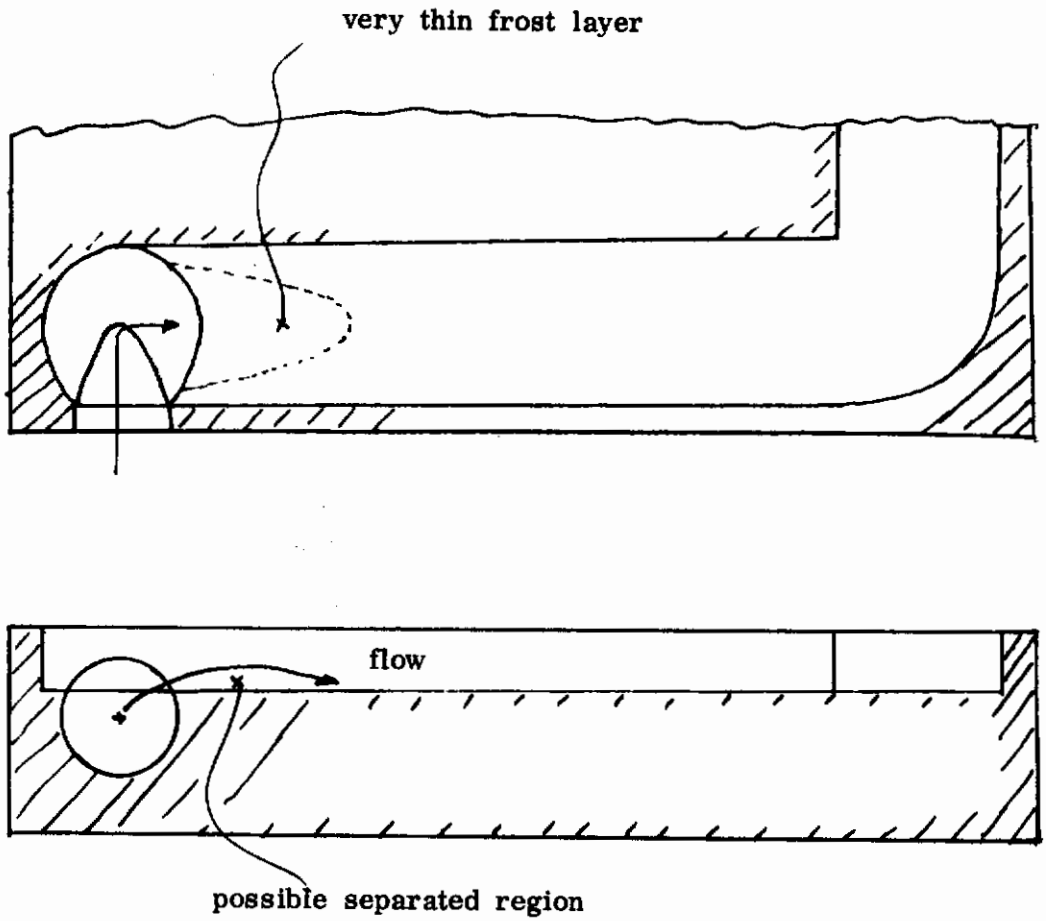

Figure 14

Effect of Inlet Configuration on Frost Layer

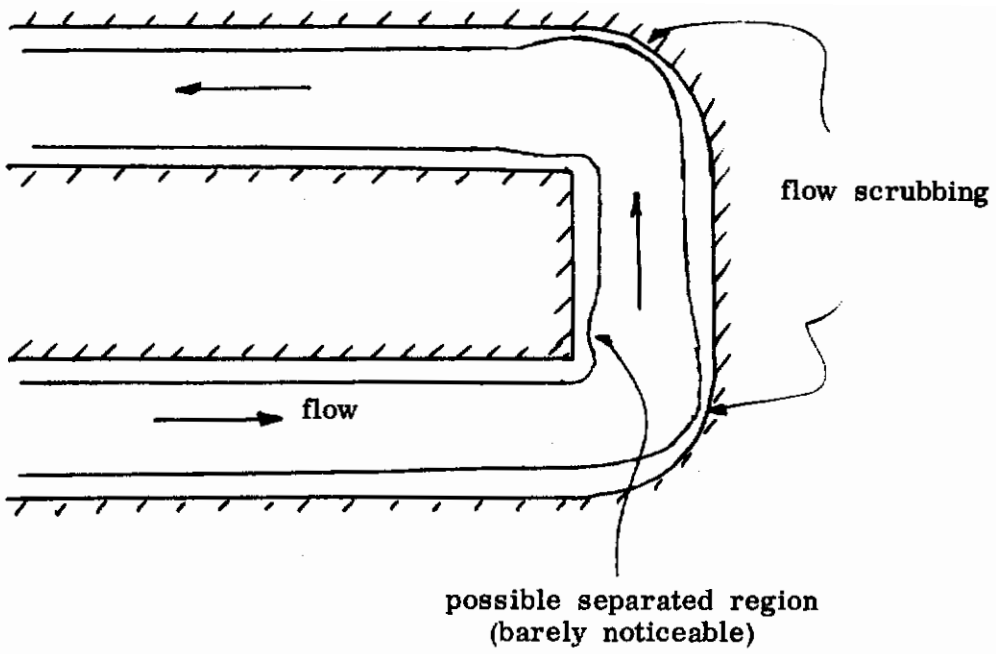

Figure 15

Effect of Right-Angle Bend on Layer

design on compactness, structural, and fabricational considerations. The required sizing information can be presented in the format of the usual heat exchanger design information. That is, heat transfer coefficients, heat transfer effectiveness, and pressure drop correlations are sufficient to design a precipitator with a high degree of confidence.

Heat and Mass Transfer Coefficients

The performance of the precipitator channel may be described in terms of the usual heat exchanger correlations with the addition of the mass transfer coefficients and the mass transfer effectiveness. The basic equations which characterize this performance are set out below. The terminology is defined in accordance with the accompanying sketch.

Consider a passage, with constant wall temperature, T_p, and a stream of dry cabin atmosphere entering at temperature, T_1, and CO_2 concentration, C_1.

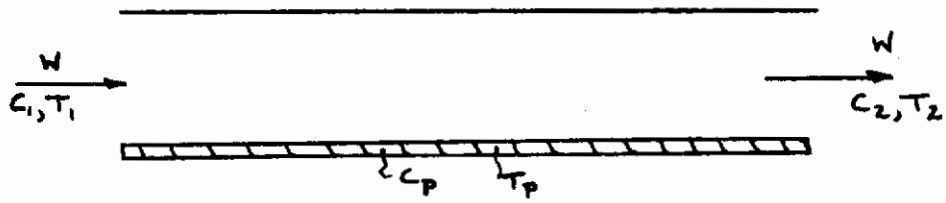

In the absence of any frost layer on the surface, the rate equations are simply of the form,

$$\frac{Q}{A} = h \Delta T_{\substack{ln \\ mean}}$$

where

$$\Delta T_{\substack{ln \\ mean}} \equiv \frac{T_1 - T_2}{ln\left\{\frac{T_1 - T_p}{T_2 - T_p}\right\}}$$

$$Q = (Wc_p)(T_1 - T_2)$$

and

$$\frac{W_{CO_2}}{A} = h_D \left\{ \frac{\rho_1 - \rho_2}{ln\left\{\frac{\rho_1 - \rho_p}{\rho_2 - \rho_p}\right\}} \right\}$$

The two transfer coefficients may be evaluated by test directly in the initial phases, before a significant depth of frost has formed. The heat transfer coefficients should also be predictable from standard correlations, such as those in London and Kays (ref 2). The mass transfer coefficient is related phenomenologically to the heat transfer and the commonly accepted analogy is of the form

$$h_D = \frac{h}{(\rho_A C_p)} (Le)^{2/3}$$

where

$$Le = \frac{\alpha}{D} \left(\frac{\text{thermal diffusivity}}{\text{mass diffusivity}}\right)$$

if $Le \approx 1.0$.

(For our case $Le \approx 0.85$ which is close enough to unity to justify the assumption.) Figure 16 shows a standard dimensionless plot of $(h/Gc_p)\, Pr^{2/3}$ versus Re for the geometry of the test precipitator channel. The data is, for the most part, slightly above the predicted value, presumably due to the disturbances induced in the flow by the right angle bends. Figure 17 shows the mass transfer coefficients along with a curve which represents the predicted values based on the analogy between heat and mass transfer. Again, the values are slightly higher than what would be expected, probably due to the mixing effect of the turns.

The data points, presented in dimensionless form, cover the full range of operating variables outlined in table 1.

The two basic channel geometries are shown in figure 21.

If a frost layer of any thickness exists, an additional resistance to heat transfer is presented and the governing equations must be re-examined. Consider again the sketch below, showing a plate at constant temperature, T_p, but covered with a frost layer of uniform thickness, δ, conductivity, k_f, and and interface temperature, T_i.

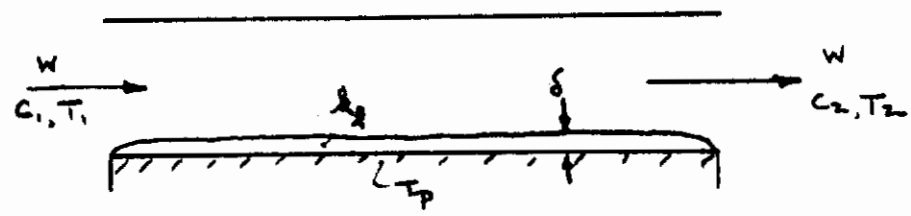

A complete solution of the combined heat and mass transfer problem would take the following form:

(i) heat transfer from the stream to the layer

$$\frac{Q}{A} = h_i (T(x) - T_i(x)) = - W c_p \frac{dT}{dx}$$

(ii) mass transfer from the stream to the layer

$$\frac{W_{CO_2}}{A} = h_D (\rho(x) - \rho_i(x)) = -\Phi \frac{d\rho}{dx}$$

(iii) heat transfer through the layer

$$\left(\frac{Q}{A}\right) + \left(\frac{W_{CO_2}}{A}\right) h_{sg} = \frac{k}{\delta(x)} (T_i(x) - T_P)$$

(iv) saturation conditions

$$\rho_i = \rho_i (T_i)$$

These relationships could, in theory, be solved exactly for a complete description of the channel separation and even integrated over time to predict the rate of layer buildup.

However, the use of three empirical observations results in a great simplification and simple means of presenting the data. First, it is noted that δ remains reasonably constant with distance down the channel. Second, for most of the cycle, the frost layer is a small resistance compared to the film resistance, so the interface temperature is close to the plate temperature and hence reasonably constant with distance. Finally, the heat load due to the latent heat of the CO_2 is usually much less (at least x 2) than the sensible heat from the air stream. Therefore, the interface temperature can be computed on the basis of the sensible heat transfer alone. These simplifications result in the following formulation:

$$Q = UA\left\{\frac{T_1 - T_2}{\ln\left(\frac{T_1 - T_P}{T_2 - T_P}\right)}\right\}$$

where

$$U = \frac{1}{\frac{1}{h_i} + \frac{\delta}{k}}$$

and

$$\frac{W_{CO_2}}{A} = h_{D_i}\left\{\frac{\rho_1 - \rho_2}{\ell n\ \frac{\rho_1 - \rho_i}{\rho_2 - \rho_i}}\right\}$$

$$T_i \approx \frac{\frac{(T_1 + T_2)}{2} + \frac{k}{h_i \delta}\ T_P}{1 + \frac{k}{h_i \delta}}$$

The effect of the frost layer on the overall heat transfer coefficient is presented in figure 22. These points are based on an observed layer thickness, constant value of thermal conductivity, and a value of h_i based on a best fit curve through the data on figure 16. Although this procedure tends to smooth the data somewhat, the general, agreement of the curves indicates that the assumptions listed above are, in general, correct. The fine structure scatter could be related to either variations in the thermal conductivity of the layer from run to run or inaccuracies in estimating the layer thickness.

On the basis of this information, the interface temperature can be computed and a new mass transfer coeffient can be computed as

$$h_{D_i} = \frac{\frac{W_{CO_2}}{A}}{\left\{\frac{\rho_1 - \rho_2}{\ell n\left[\frac{\rho_1 - \rho_i}{\rho_2 - \rho_i}\right]}\right\}}$$

These results are plotted in dimensionless form versus Reynolds Number (as in figure 17) in figure 23. As in the case of a nearly frost-free surface, the agreement with expected values based on the analogy to heat transfer is quite good.

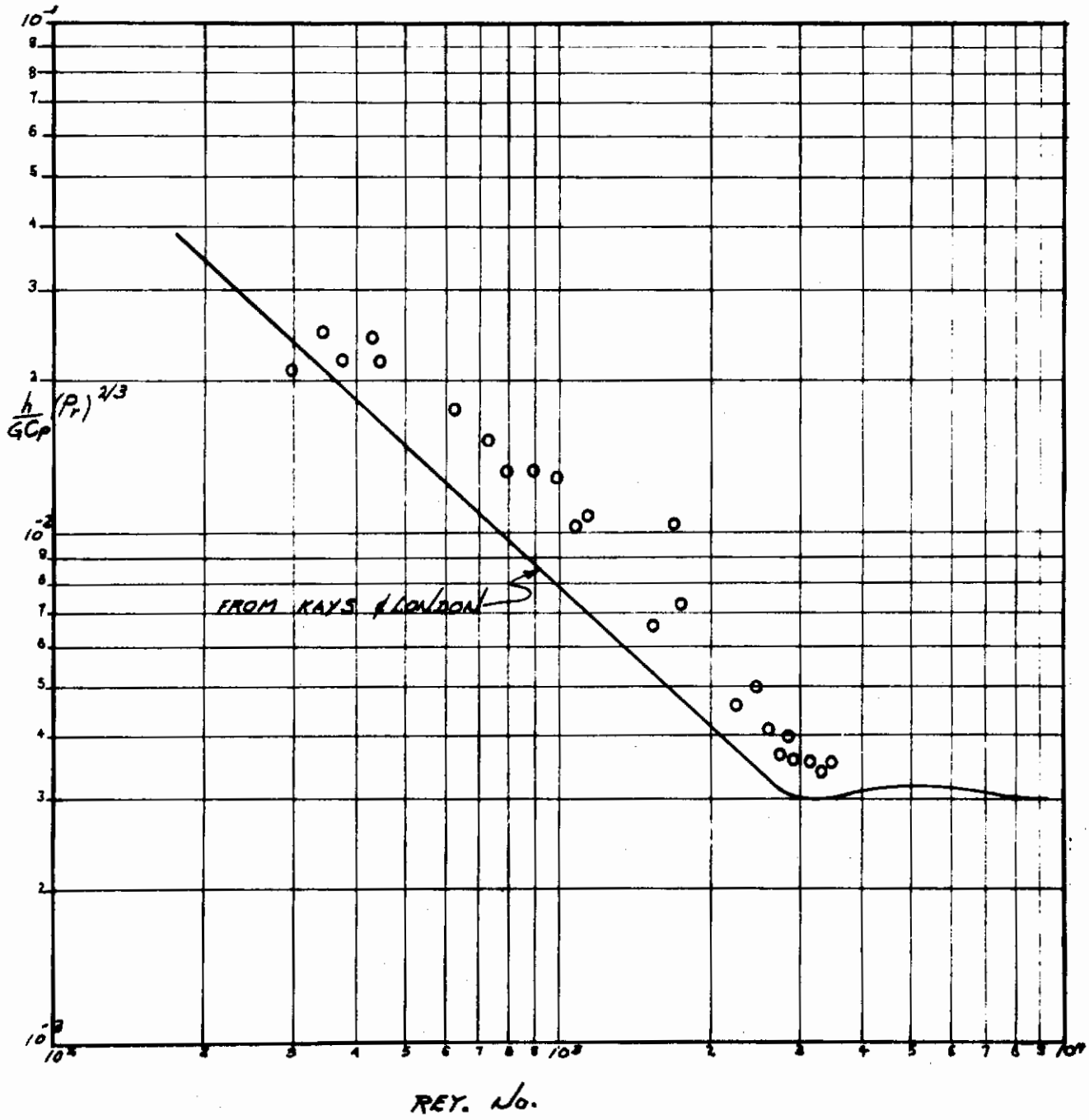

Figure 16
Heat Transfer Correlation

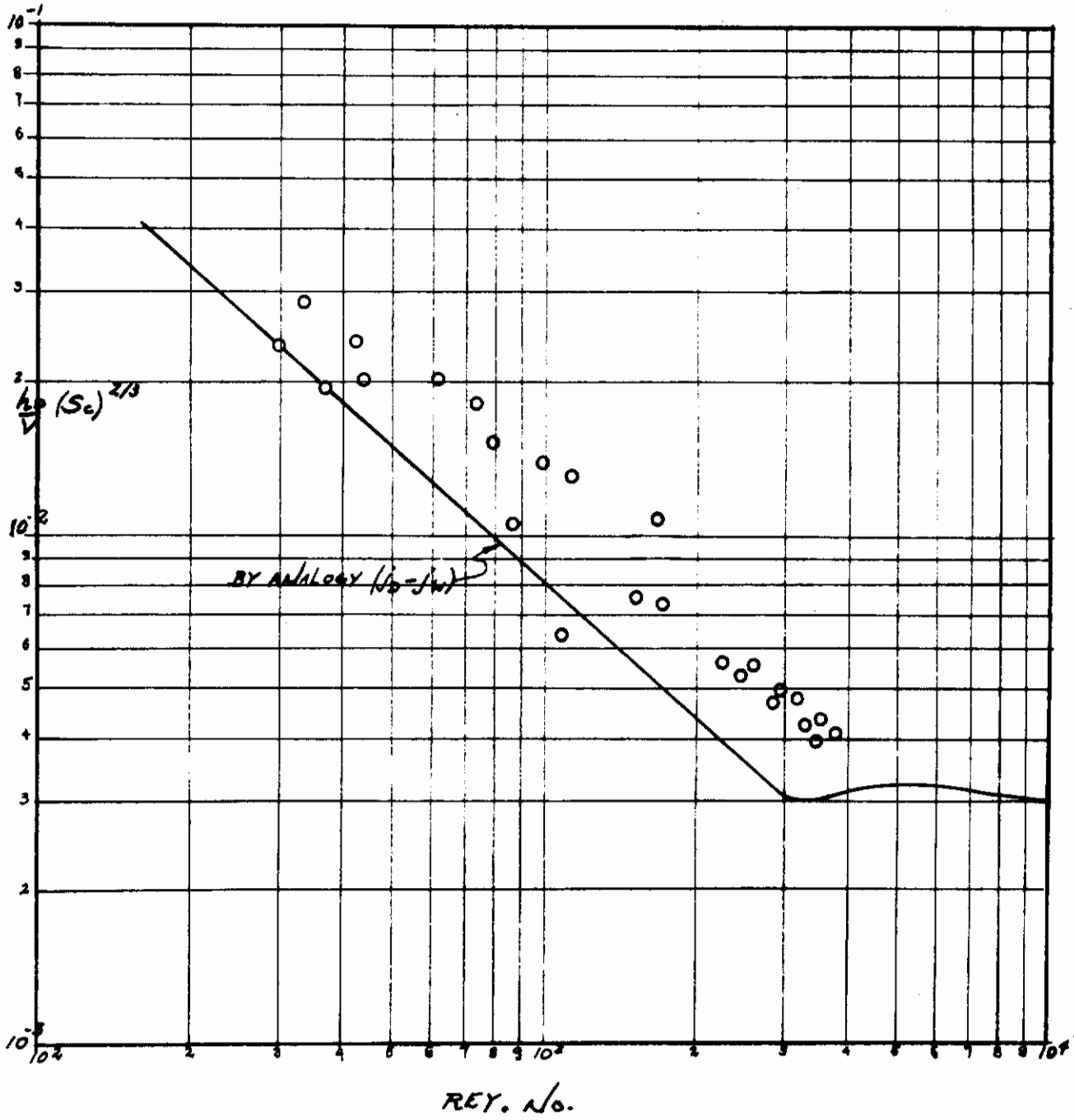

Figure 17

Mass Transfer Correlation

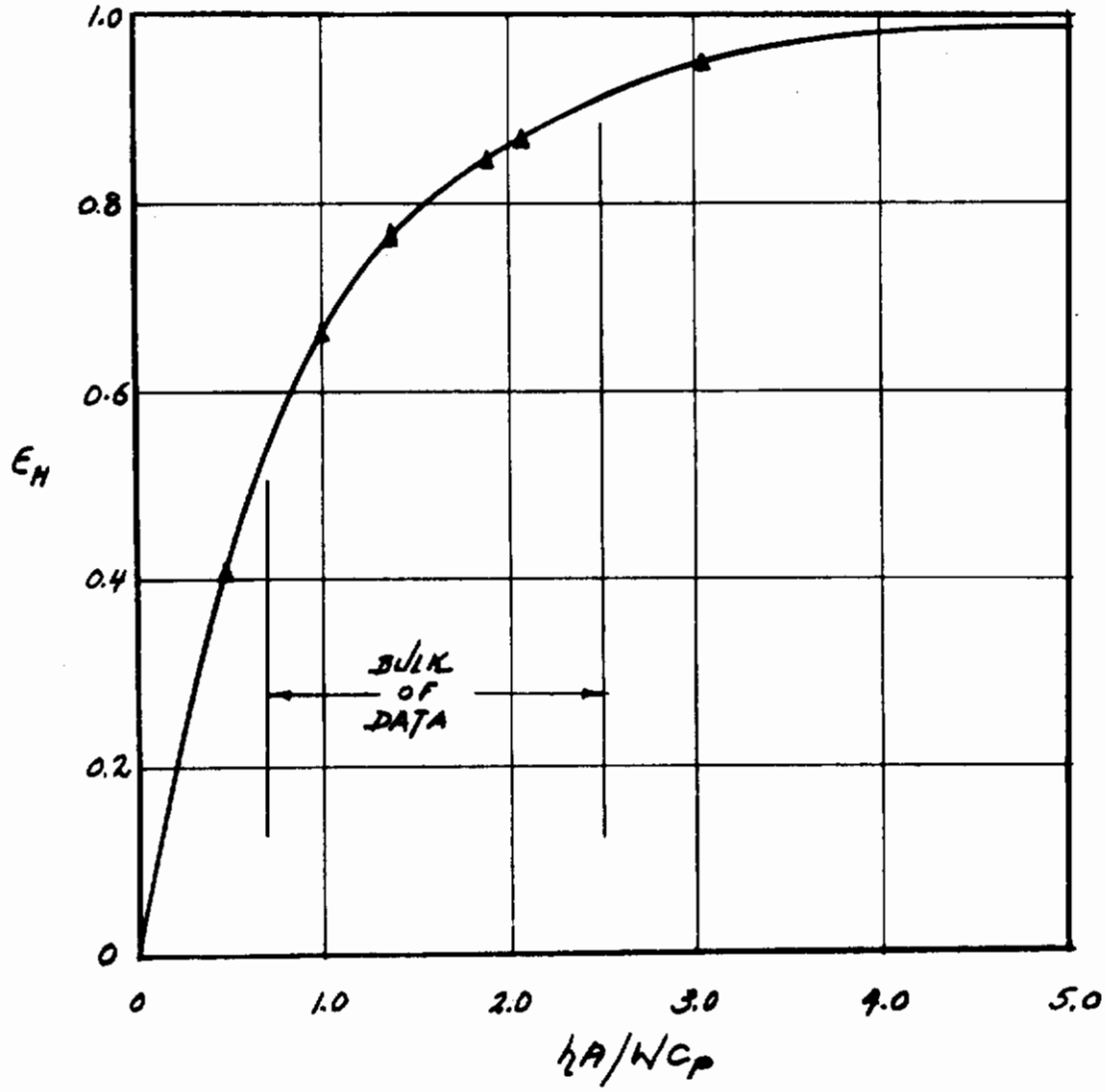

Figure 18
Heat Transfer Effectiveness

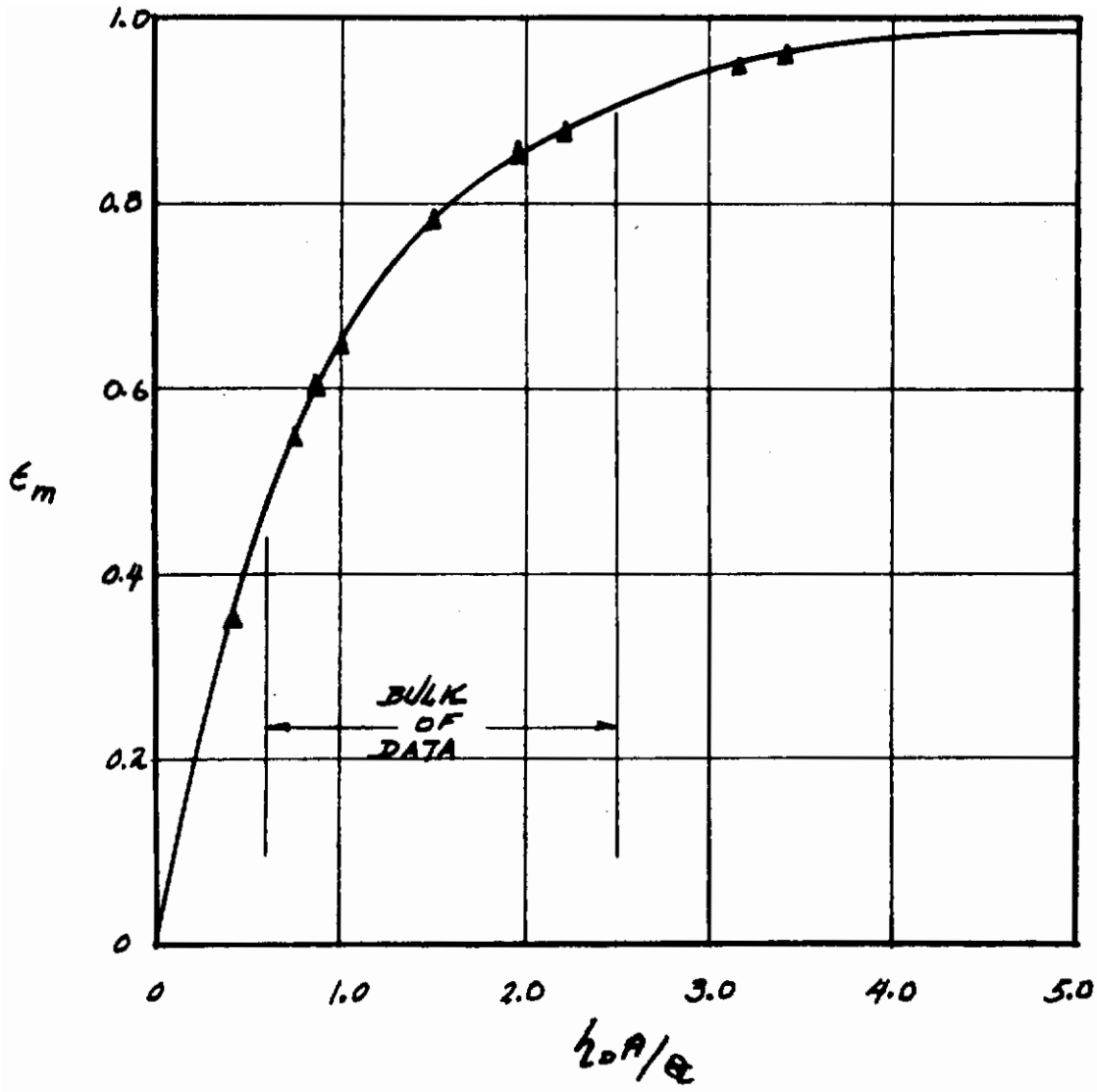

Figure 19

Mass Transfer Effectiveness

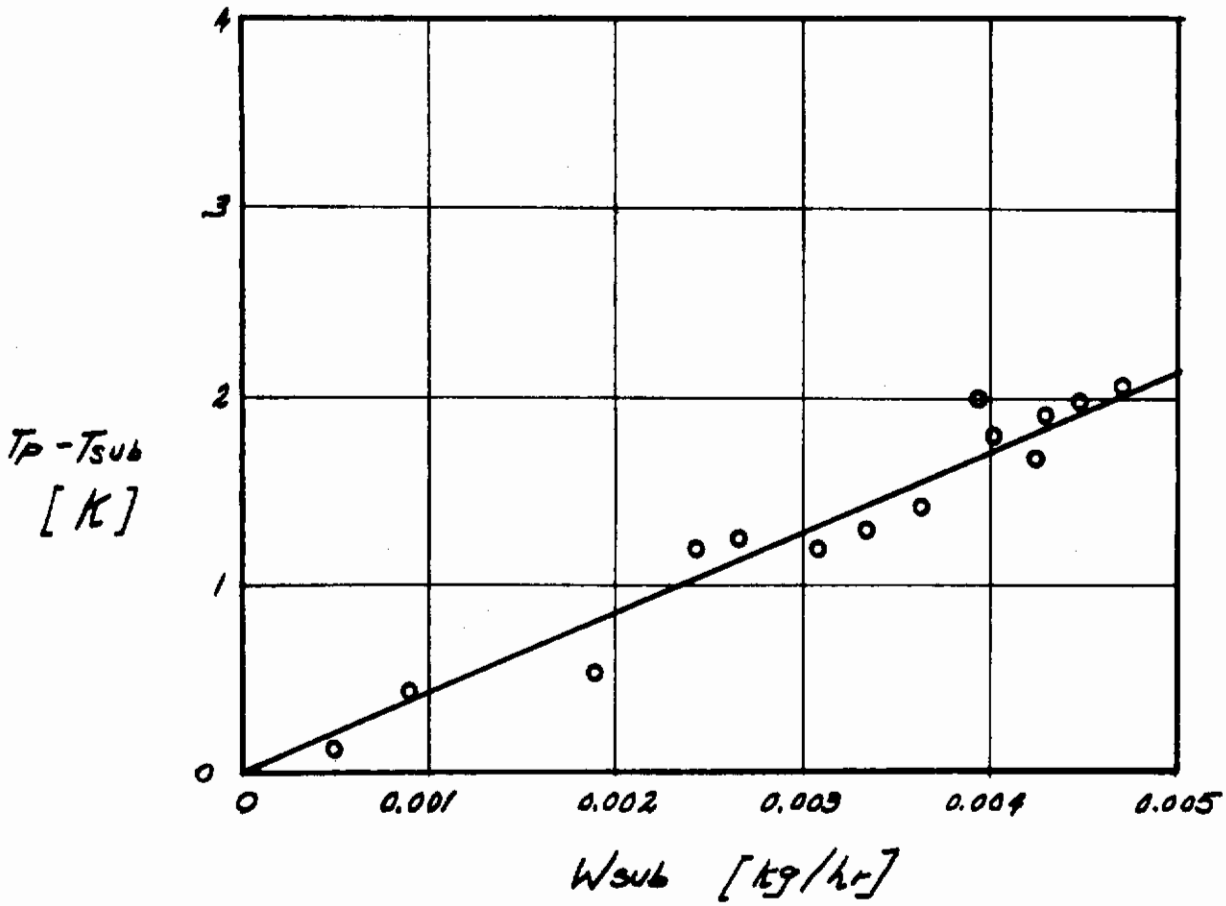

Figure 20
Sublimation Channel Temperature vs. Sublimation Flow Rate

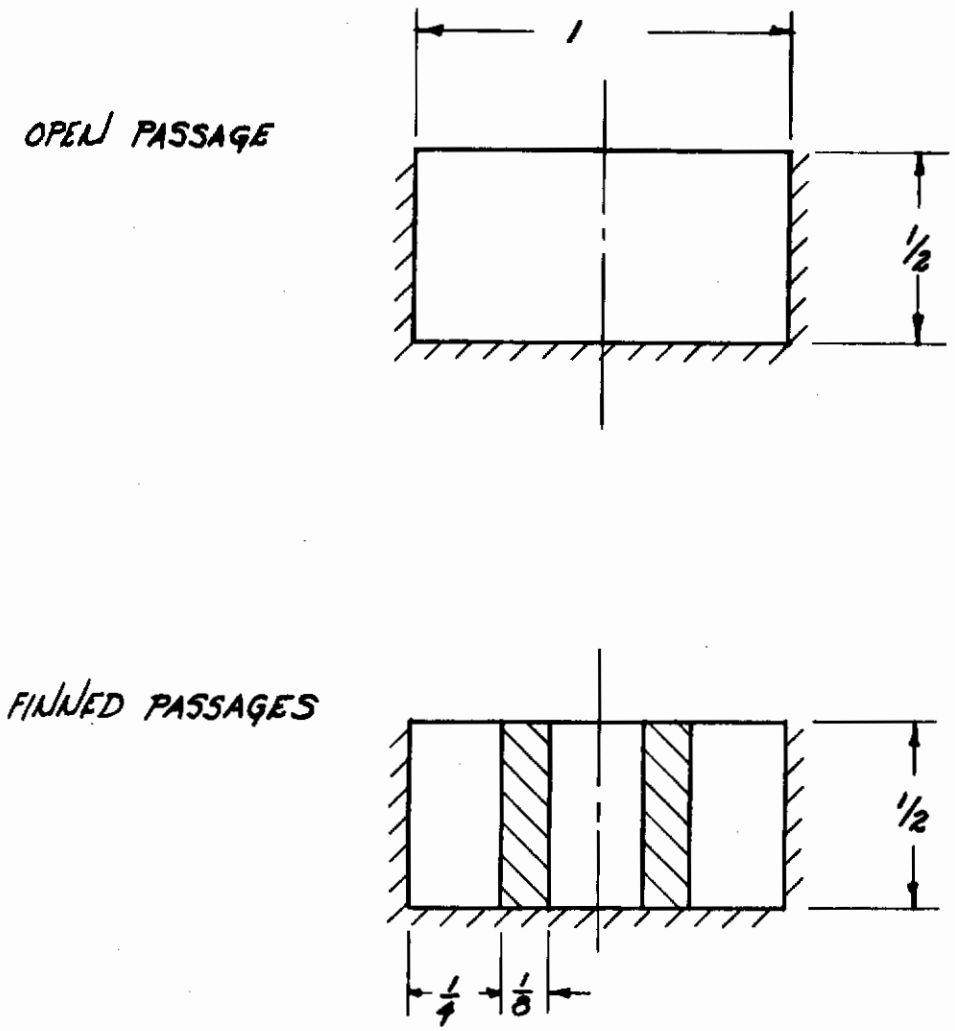

Figure 21

Channel Geometries

NOTE: 2 x SCALE
ALL DIMS. IN INCHES

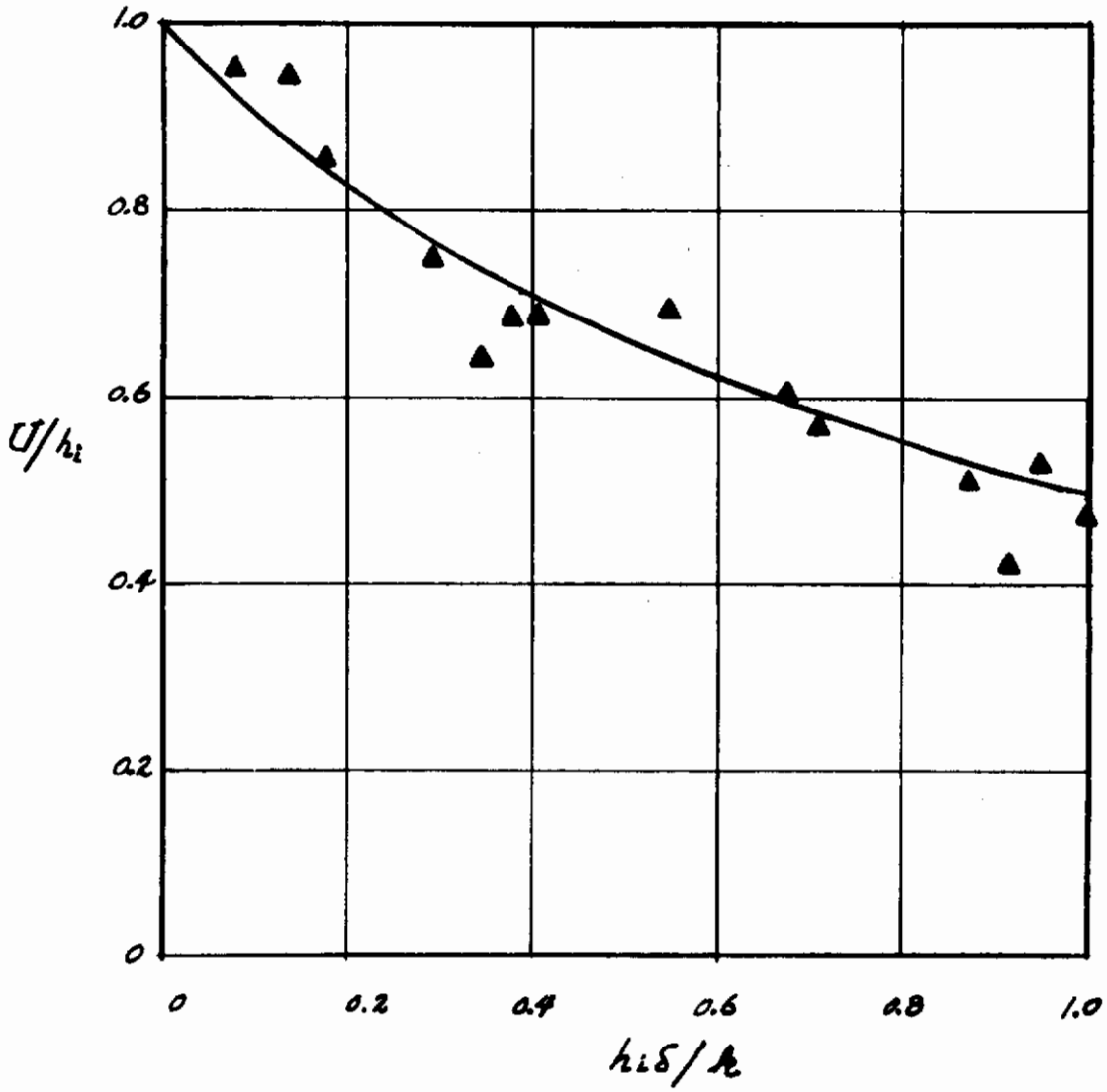

Figure 22

Effect of Frost Layer on Heat Transfer Coefficient

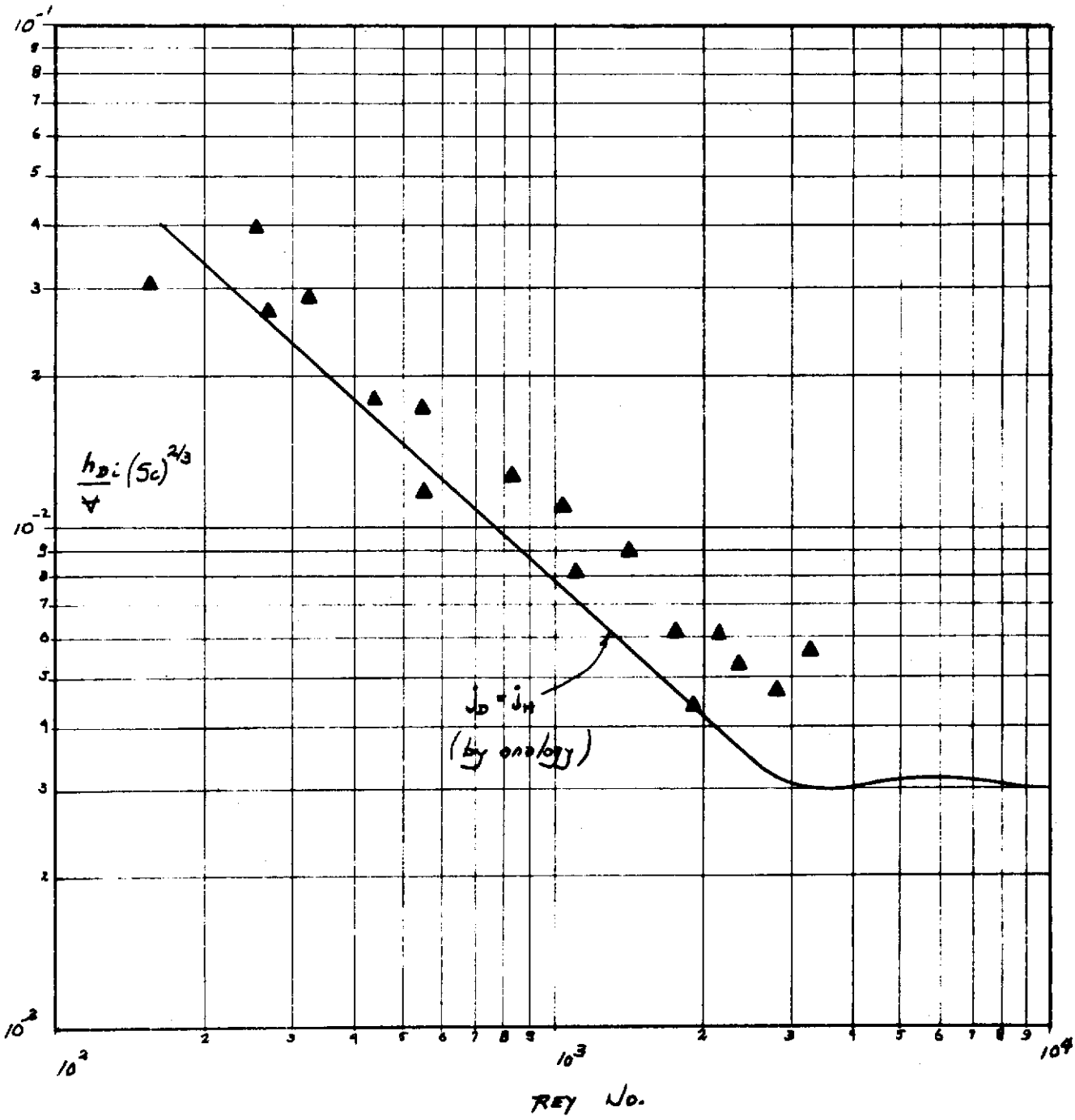

Figure 23

Mass Transfer Correlation to Frost Layer Surface

Effectiveness Concepts

The formulation of the heat exchanger design equations in terms of heat transfer effectiveness and NTU's has long been utilized as a concise and physically meaningful way of presenting heat transfer data. Heat transfer effectiveness is commonly defined as:

$$\epsilon_H \equiv \frac{T_{in} - T_{out}}{T_{in} - T_P}$$

and a corresponding mass transfer effectiveness may be written

$$\epsilon_H \equiv \frac{C_{in} - C_{out}}{C_{in} - C_P}$$

where C_p is the concentration corresponding to the plate temperature.

Although no new information is contained in this formulation, plots of heat and mass transfer effectiveness are presented in figures 18 and 19 in order to put the results in a convenient form.

The dimensionless grouping which corresponds to NTU ($\equiv hA/(Wc_p)_{min}$) for the case of mass transfer is $h_D A/Q$. It is seen that effectivenesses of the order of 0.75 to 0.85 are easily obtainable and may be designed to with confidence.

Pressure Drop Considerations

An attempt was made to measure the precipitator channel pressure drop. This would have provided friction factor data to complement the heat transfer results and was also considered as a means of activating the channel switching mechanism. It was found, however, as the following calculation will verify that the pressure drops, in any rational P-S-R design are extremely small. Thus, no meaningful friction factor information could be obtained, and the pressure drop was no longer considered.

$$\Delta p = 4f \frac{L}{D} \frac{\rho V^2}{2}$$

For the worst (highest pressure drop) case,

$$\frac{L}{D} \cong 150$$

$$V \approx 1.22 \text{ m/sec.}$$

and using Kays and London (ref 2) for the friction factor

$$f \approx 0.009$$

$$\Delta p = 0.076 \text{ mm Hg.}$$

Even increasing this by a factor of 100 to account for peculiar geometries results in a negligible pressure drop. If some estimate of the pressure drop is desired, the use of standard smooth channel correlations will clearly result in negligible error in relationship to any total circulation loop pressure drop.

Control of Sublimation Results

One of the crucial aspects of the test program was the verification of the contention that the sublimation rate could be controlled to match the precipitation rate. The act of dumping the sublimated CO_2 vapor to space was simulated by connecting the dump line to a mechanical vacuum pump through a fine control valve and a flow meter. At the flow rates involved, the pump operated at nearly its blank-off pressure of 20 microns (4×10^{-5} atm). At this pressure the equilibrium temperature of a solid-vapor interface is approximately 120 K. Hence if the dump line were not throttled the following sequence of events would take place.

1. Since the frost layer is quite porous, the vapor pressure would be essentially constant through the layer.

2. Evaporation would take place at all the solid-vapor interfaces with a corresponding reduction in the frost layer temperature.

3. Since the P-S-R plate has very high thermal inertia and high conductance, the plate temperature at the surface of the

sublimating channel would remain essentially constant, and large heat transfer rates to the subliming layer would be set up.

4. This would lead to rapid exhaustion of the subliming channel.

In this test case, where the large mass and high conductance of the P-S-R essentially decouple the phase change rates in the two channels, this is in fact an acceptable situation. This must be true since the heat of precipitation is removed as heat of sublimation although in a much shorter time. However, if weight penalties were to dictate the use of a low thermal inertia P-S-R in flight, such a rapid sublimation rate would take place at the expense of reduced plate temperature. This lower temperature would be felt at the precipitating channel with the result that an excessive amount of sensible heat would be removed rom the air stream.

Therefore, it was desired to match the rates rather than take advantage of characteristics which might be peculiar to the test setup. It was found that a simple adjustment of the throttle valve, setting the sublimation rate equal to the steady-state injection rate, resulted in a very stable situation. The temperature in the subliming channel measured in the middle of the channel would typically settle out at 1 to 2 K below the plate temperature. This was sufficient to maintain the necessary heat transfer rate for sublimation. Figure 20 presents data in the form of temperature depression in the sublimining channel ($T_P - T_{sub}$) versus sublimation rate. This temperature difference did not vary noticeably during a cycle, although it might have been expected that it would decrease as the layer became thinner. The fact that it did not would seem to indicate that sublimation occurs throughout the layer and that the primary resistance to heat transfer occurs at the surfaces rather than in a conductive path through the frost itself.

Properties of Frost Layer

The two important properties of the frost layer are density and thermal conductivity — the density because it relates channel volume to switching frequency for a given CO_2 removal rate, and thermal conductivity because it can be related to a maximum layer thickness at which precipitation can continue. Estimates of both of these properties were obtained from the experimental program.

Density

The density was estimated from visual observations of the frost depth after a given amount of CO_2 was removed. For example, a nearly uniform layer of about 2.5 mm builtup throughout the precipitator after about 1 hour at an injection rate of 0.005 kg/hr. This corresponds to a density of about 60 kg/m^3. This estimate is quite crude due to the difficulties of estimating the volume of the layer accurately. Other runs yielded estimates as high as 85 kg/m^3. These are, however, an order of magnitude less than the estimate of 10^3 kg/m^3 used in ref 1. This affects the amount of cabin air lost during the dump cycle. This amount is still small, however, amounting to approximately 6×10^{-3} kg of air per hour or 52 kg per year.

Thermal Conductivity

Here again, the thermal conductivity could only be roughly estimated based on the layer's effect on the heat transfer rate as a function of its observed thickness. With an inlet concentration of CO_2 of 0.5% by volume ($T_{\text{dew point}} = 149$ K), an inlet temperature of 152 K, a circulation rate of 1.7 kg/hr, and a plate temperature of 141 K, precipitation essentially stopped at a frost layer thickness of about 3mm. This indicates that the interface temperature was at or slightly above 149 K. From the definition of the overall heat transfer coefficient given in Section IV.

$$U \cong 3.95 \times 10^{-4} \text{ watts/cm}^2\text{- K}$$

For $h_i \cong 7.9 \times 10^{-4}$ watts/cm^2- K, the conductivity of the frost layer may be estimated at

$$k_\ell \cong 2.6 \times 10^{-4} \text{ watts/cm- K.}$$

This also differs from the estimate given in ref 1 by approximately a factor of x 10. This is consistent with density, however, which also was lower than the estimate by about a factor of x 10. It is reasonable to expect in a porous media of this kind that the thermal conductivity will likely vary in direct proportion to the density if the gas is of much lower conductivity than the solid. Air, at these temperatures is of the order of 1.3×10^{-4} watts/cm^2- K or lower by a factor of x 2 than the layer.

SECTION V

CONCLUSIONS AND RECOMMENDATIONS

SUMMARY OF CONCLUSIONS

1. Carbon dioxide precipitation always occurs in the form of a snowy frost.
2. Frost nucleation occurs spontaneously on ordinary machined surfaces at the expected thermodynamic dew point.
3. The frost layer builds up in a progressive way from upstream to downstream in the precipitating channel.
4. Maximum practical frost-layer thickness for sustained freeze-out at design conditions is approximately 2.5 to 3mm.
5. The only geometric restraint of real significance is the surface area-to-volume ratio of the channel. This is determined by the maximum frost layer thickness and the requirement that the channel be relatively full prior to flow reversal.
6. Details of the channel path are not important (corners, bends, etc.)
7. The frost layer is not firmly held together. As a result, carryover can and does occur during switch over.
8. Mass transfer effectivenesses of 0.75 - 0.85 are easily attainable.
9. CO_2 sublimation rate can be controlled to match the precipitation rate by simple throttling of the dump line.
10. The most critical variable(and most difficult to control for the experimental system) is the temperature of the inlet stream to the precipitator channel. CO_2 freeze-out in the pre-coolers is a constant threat.
11. Good control on CO_2 concentration in the cabin can be obtained by monitoring the exit stream from the precipitator.

DESIGN RECOMMENDATIONS

The essential conclusion of this investigation is that CO_2 concentration level control can be achieved by freeze-out techniques. No unexpected difficulties were encountered in channel design, nucleation characteristics, frost layer behavior, or system control that would indicate that such a system is not feasible.

The following design recommendations can be made:

1. Parallel rectangular channels are adequate as precipitating regions.
2. A high thermal inertia of the P-S-R configuration is desirable for stability and control purposes. Satisfying this requirement will virtually insure sufficiently intimate thermal contact between the precipitator and sublimator channels and the radiating surface.
3. The existing curves of mass transfer coefficients and effectiveness can be used with confidence to size the P-S-R.
4. A solid CO_2 particle trapping scheme must be provided for both channels.

SECTION VI

DESIGN OF ONE-MAN SIZE SYSTEM

INTRODUCTION - PHASE II

GENERAL APPROACH - PHASE II

The following sections describe the work carried out under Phase II of Contract No. F33615-67-C-1587. The purpose of this phase of the program was to design a system for the control of carbon dioxide and water vapor level in a one-man, manned space enclosure utilizing thermal radiation to space as the sole means of ultimate heat rejection. The system is based on the simultaneous precipitation and sublimation technique investigated experimentally in Phase I. The assumed operating characteristics of the precipitator-sublimator-radiator (PSR) are based upon these results. The system includes provision for water reclamation and return from the carbon dioxide removal loop, a means of injecting the accumulated carbon dioxide to vacuum with a minimum of cabin air loss, and all necessary shielding, supports, surface coatings, and controls for proper and stable operation of the system over an extended period of time. The system is described in sufficient detail to permit construction of the essential system elements. Adaptation to a particular vehicle or ground test chamber has not been provided.

The general approach taken in Phase II may be described as follows. The system which has been designed is intended to be a full-scale humidity and carbon dioxide control system which may be tested under simulated flight conditions on the ground to verify the feasibility of the total system concept,operating as it would in flight. It is not, however, optimized, space-rated flight hardware. Optimization criteria of minimum weight, volume, and power have been given full consideration. However, a detailed optimization on these bases has not been carried out.

Fundamental requirements for operation in space have been observed. That is, the presence of a gravitational field is not required for the operation of any of the components; frequent operator invention to maintain system performance or stability is not required; and components of excessive weight, volume, or input power have not been used. System penalties have been computed on the basis of estimates given by D. C. Popma of the NASA - Langley Research Center in ref 4.

GENERAL SYSTEM DESCRIPTION

The basic system concept is centered on the two-loop configuration described by Bonneville in ref 1. The high temperature loop is used solely for humidity control. The low temperature loop which controls the cabin carbon dioxide level, does not participate in the water vapor removal function. This arrangement was chosen because of significant simplification in the control problem, enhanced stability of operation, and a reduction in the complexity of the water return system.

Humidity Control Loop

A schematic diagram of the complete system is illustrated in figure 24. The humidity control loop, labelled Loop No. I operates as follows. Air is drawn from the cabin, through a filter, into a regenerative pre-cooler where the stream temperature is reduced to a level just above the dew point. The flow then enters the condenser-radiator where it is further cooled by radiation to black space. In this component, the excess water vapor is condensed out. The unit is designed to operate at a temperature above the freezing point of water, so the condensate will remain in its liquid phase. The condensed liquid, entrained in the air stream is trapped in a wicking device as it leaves the condenser. The liquid is periodically removed from the wick and stored for final processing prior to reuse. This represents the total water reclamation capability of the system.

The dry, low temperature stream is then returned to the cabin, through the regenerator, where it recovers its sensible heat and, in so doing, cools the outgoing stream. Upon leaving the regenerator, it passes through the blower, cools the blower motor, and discharges back into the cabin.

The important design criteria and control considerations of this loop are the following:

1. Condensation in the Regenerator

   It is necessary to prevent premature condensation from the outgoing stream in the regenerator. Should this occur and the condensate be trapped in the channel, the pressure

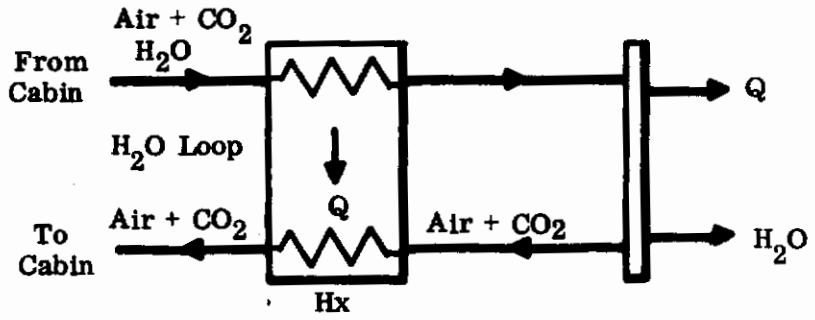

Note: Return air may contain some H_2O vapor.

Loop No. 1

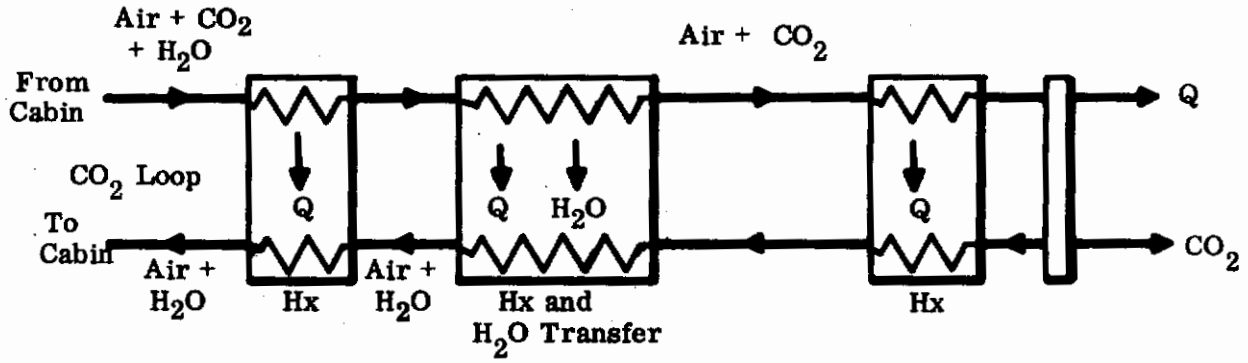

Note: Return air may contain some CO_2.

Loop No. 2

Figure 24

Double Loop Freeze-Out System

drop through the generator would increase and a reduction in flow would result. At the design point, this may be prevented through proper sizing of the heat transfer surfaces. At off-design operation, such as reduced water vapor production in the cabin, the possibility of over-cooling in the radiator occurs. This leads to increased regenerator capacity, and possible premature condensation in the regenerator. This is compensated for through the by-passing of some portion of the outgoing stream around the regenerator thereby increasing the sensible heat load on the radiator. Under these conditions, the return air stream will enter the regenerator at a higher temperature and premature condensation will be prevented.

2. Ice Formation in the Condenser-Radiator

A reduction in the water vapor generation load on the system could lead to over-cooling in the condenser - radiator and the unwanted formation of solid ice. The resultant blockage and increased pressure drop would lead to a reduced flow, further over-cooling, and eventual total stoppage of the system. As in the case of premature condensation in the regenerator, this possibility is prevented through the by-passing of a portion of the outgoing stream directly to the condenser-radiator.

3. Location of the Blower

The placement of the fan in the return line as opposed to the withdrawal line serves two purposes. First, the total heat loss from the cabin is reduced through the returning of fan work to the cabin as heat. Second, the size of the regenerator is minimized if fan work does not have to be removed from the outgoing stream prior to condensation.

The details of the thermodynamic operating conditions, individual component design, and the control functions are given in Sections VI, VII and VIII respectively.

Carbon Dioxide Level Control Loop

The carbon dioxide level control loop, labelled loop No. 2 in figure 24, operates in the following way. Cabin atmosphere is drawn from the cabin, through an intake filter, through a series of three regenerative heat exchangers, and into the precipitator-sublimator-radiator. In the precipitating channel, the carbon dioxide is condensed out as frost. The clean, low temperature air is then returned through the three regenerators where it is rewarmed, passed through the blower, and discharged back into the the cabin. Each of the three regenerative heat exchangers performs a separate function. In the first unit, the outgoing stream temperature is reduced to a level just above the dewpoint of the water vapor. In the second heat exchanger, the temperature is lowered further with an accompanying condensation and/or freeze-out of the water vapor. The atmosphere leaves the second heat exchanger with 99% of the water vapor removed and enters the third regenerator for final pre-cooling, prior to entering the carbon-dioxide precipitator.

In returning to the cabin, the clean, low-temperature, return stream regains its sensible heat and recovers all but a small fraction of the water vapor that was condensed and frozen out from the outgoing stream. This is accomplished by means of an alternate channel switching arrangement, similar to that described in the experimental program of Phase I. That is, in the first two heat exchangers a valving arrangement enables the outgoing and return channels to be interchanged. Therefore, the water vapor removed from the outgoing flow during one portion of the cycle will be picked up by the return flow during the other portion. During that time, the water vapor in the outgoing flow is being collected in the channel which was previously cleaned by the return flow.

In this loop, as well as in the humidity control loop, the placement of the blower in the return line reduces not only the ultimate heat loss from the cabin but also the required capacity of the regenerators. Here again, the primary design considerations in the loop are that of premature carbon dioxide freeze-out in the final pre-cooler and the

possible blockage of the PSR channels. Furthermore, provision must be made for occasional auxiliary removal of water vapor from heat exchangers I and II. The details of the individual components as well as the control functions are described in Sections VII and VIII.

SPECIFICATION OF SYSTEM REQUIREMENTS

The system must be capable of maintaining control of carbon dioxide and water vapor concentration levels in a one-man, manned space enclosure. The design parameters are:

Orbit: 300 nautical miles, circular, polar and equatorial
(23° inclination of the earth is ignored)

Cabin Volume: 2.83 cu. meters.

CO_2 Generation Rate: 4.5 - 45.0 gm/hr
(0.01 - 0.1 lbm/hr)

Cabin conditions at the design point are:

Atmospheric Composition: Sea-level air

Cabin Pressure: 760 mm Hg

Cabin Temperature: 21 C ($\pm$ 5 C)
[70 F ($\pm$ 10 F)]

Relative Humidity: 50% ($\pm$ 10%)

Carbon Dioxide Concentration: 0.5% by volume
P_{CO_2} = 3.8 mm Hg

Max. Allowable Concentration: 1.0% by volume
P_{CO_2} = 7.6 mm Hg

DESCRIPTION OF DESIGN POINT OPERATION

In the following paragraphs, the conditions of the two loops, operating at their design points, are described.

Humidity Control Loop - Design Point

In figure 25, a schematic representation of the humidity control loop is given, and the notation necessary to define the design point is indicated. At the design point, the cabin is assumed to be at a temperature of 21 C a relative humidity of 50%

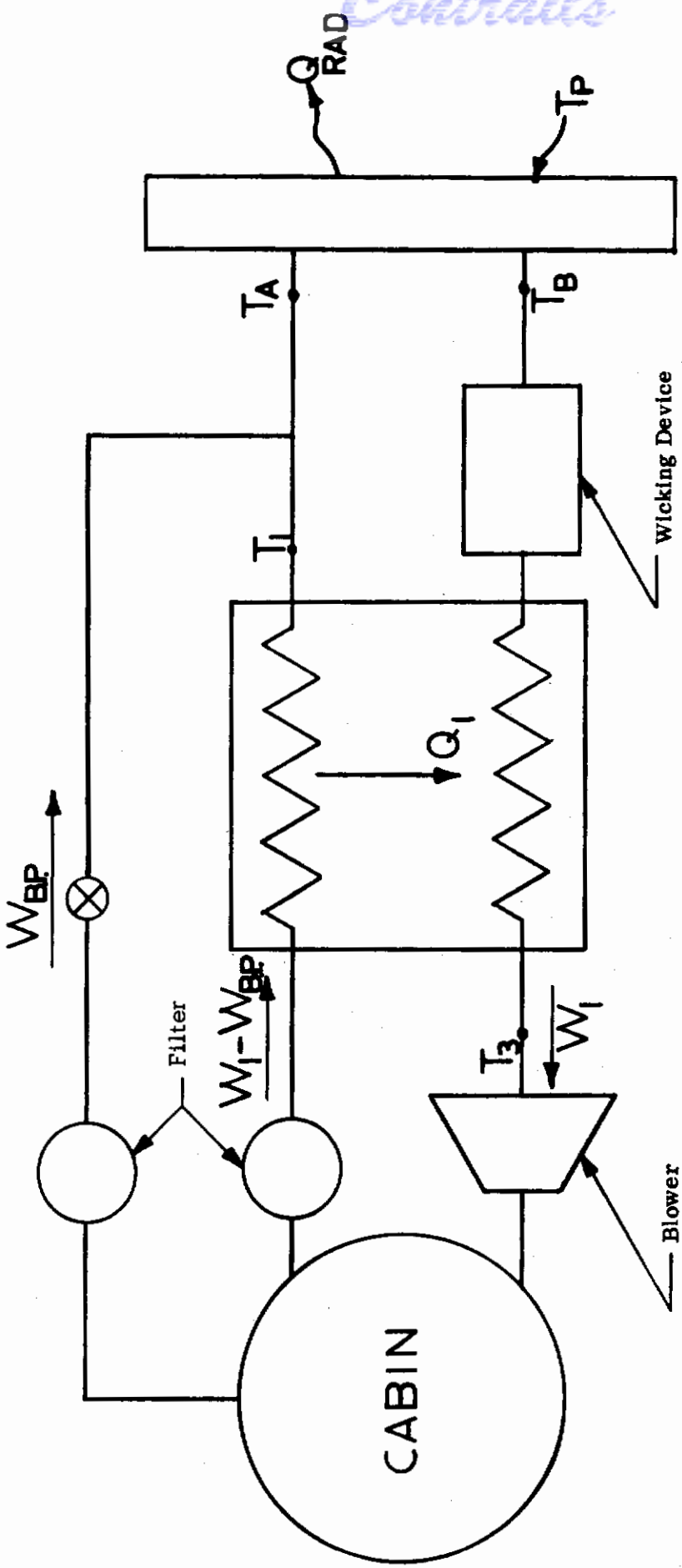

Figure 25

Humidity Loop Schematic

(corresponding to a dewpoint of 10 C), and subject to a water vapor generation load 45 gm/hr. The operating point represents a compromise between pumping power, radiator size, heat exchanger weight, and sensible heat loss from the cabin. The system-describing equations leading to the design point determination, are detailed in Section VII.

In table 2 below, the design point values of the critical flow rates, temperatures, component heat loads, and component capacities are given.

Table 2

Design Point Conditions for Humidity Control Loop

	Quantity	Design Point Value
1.	W_1, Circulation Flow Rate	18.2 kg/hr (39 lbm/hr)
2.	$W_{b.p.}$ By-pass Flow Rate	0
3.	T_1 (Outgoing Stream Leaving Regenerator)	285 K (52.6 F)
4.	T_b, (Stream Leaving Condenser-Radiator)	278 K (40.4 F)
5.	T_3, (Return Stream Leaving Regenerator)	287 K (57.8 F)
6.	T_p, (Radiator Plate)	275 K
7.	Q_{RAD} (Heat Load on Radiator) (Net Heat Loss from Cabin)	55.4 kcal/hr (220 Btu/hr)
8.	Q,(Required Capacity of Regenerator)	42.8 kcal/hr (170 Btu/hr)
9.	(UA), req'd	6.1 kcal/hr- K (13.5 Btu/hr- F)
10.	$(\epsilon A)_{RAD}$ req'd	0.204 m^2 (2.2 ft^2)
11.	Δp_{loop} (total loop pressure drop)	1.12 mm Hg. (0.6 in H_2O)
12.	Blower Power	12 watts.

Carbon Dioxide Control Loop - Design Point

In figure 26, a schematic diagram of the carbon dioxide control loop is given and the notation for the thermodynamic variables describing the design point operation is indicated. Here again, the design point is chosen to represent a reasonable trade-off between pumping power, component size, and load on the cabin. The design cabin concentration of carbon dioxide is 0.5% by volume (P_{CO_2} = 3.8 mm Hg) and the design carbon dioxide generation rate is 45 gm/hr (0.1 lbm/hr). Table 3 below sets out the values of the critical flow rates, temperature, heat loads and required component capacities throughout the loop.

Table 3

Design Point Conditions for Carbon Dioxide Loop

	Quantity	Design Point Value
1.	W_1 Circulation Flow Rate	10 kg/hr (22 lbm/hr)
2.	T_1, Outgoing Stream Temperature Leaving HX I	285 K (57.6 F)
3.	T_2, Outgoing Stream Temperature Leaving HX II (after water removal)	225 K (-54 F)
4.	T_3, Outgoing Stream Temperature Leaving HX III	148 K (-193.3 F)
5.	T_4, Stream Temperature Leaving Precipitator	141 K (-205.9 F)
6.	T_5, Return Stream Leaving HX III	215 K (-73 F)
7.	T_6, Return Stream Leaving HX II	275 K (35 F)
8.	T_7, Return Stream Leaving HX I	284 K (52 F)
9.	Q_1, Capacity of HX I	23.4 kcal/hr (93 Btu/hr)
10.	$(U A)_{1\ req'd}$	2.34 kcal/hr- K (5.16 Btu/hr- F)
11.	Q_2, Capacity of HX II	175 kcal/hr (696 Btu/hr)
12.	$(U A)_{2\ req'd}$	17.5 kcal/hr- K (38.7 Btu/hr- F)

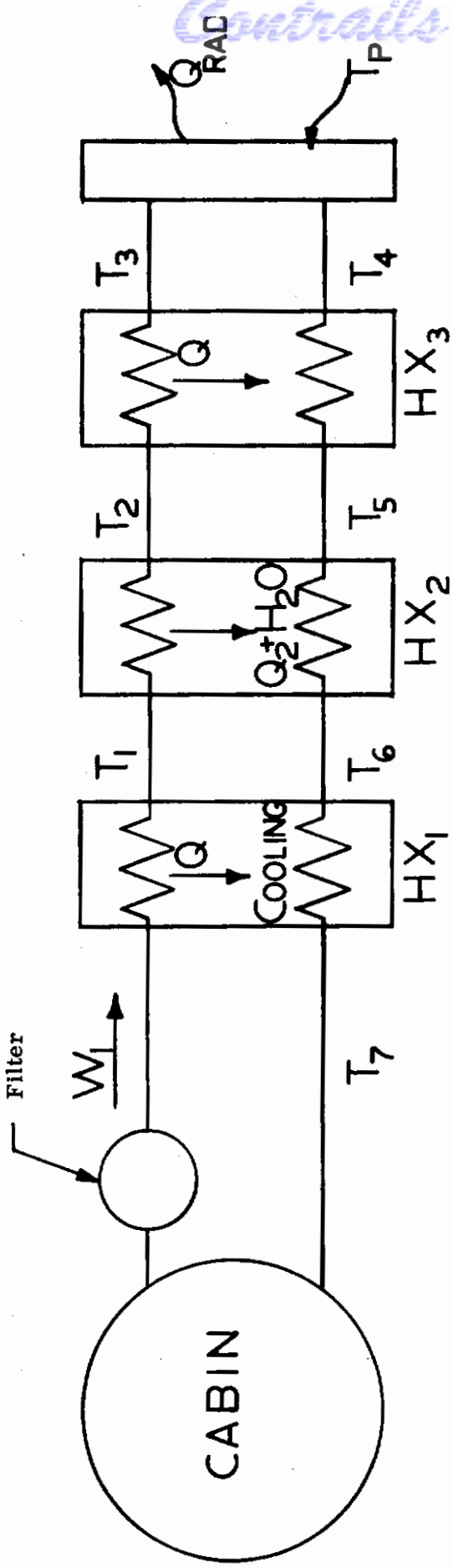

Figure 26

Carbon Dioxide Loop Schematic

Table 3 (continued)

	Quantity	Design Point Value
13.	Q_3, Capacity of HX III	187 kcal/hr (730 Btu/hr)
14.	$(U\ A)_{3\ req'd}$	18.7 kcal/hr- K (40.5 Btu/hr- F)
15.	Q_{RAD}, Heat Load on Radiator (Net Heat Loss from Cabin)	16.8 kcal/hr (66.5 Btu/hr)
16.	$(\epsilon\ A)_{RAD\ req'd}$	(1.07 m^2) (11.5 ft^2)
17.	T_p, Radiator Plate Temperature	134 K (-219 F)

SECTION VII

SYSTEM COMPONENT DESIGN

In this section, the design calculations and trade-off decisions are documented in detail. The off-design calculations, the control functions, and the system assembly and interfacing requirements are described in Section VIII.

SYSTEM-DESCRIBING EQUATIONS

The following relationships define the thermodynamic performance of the system. The notation is defined in figures 25 and 26.

Humidity Control Loop

The fundamental requirement of the humidity control loop is that 45 gm/hr (0.1 lbm/hr) of water vapor be condensed out in the condenser-radiator at a temperature above 273 K (32 F). In addition, the following constraints must be satisfied.

Water Vapor Generation Rate:

$$W_I (C_{wa} - C_{wb}) = W_{H_2O} \tag{1}$$

Heat Load on Radiator:

$$Q_{RAD.} = W_1 c_p (T_a - T_b) + W_{H_2O} h_{fg} \tag{2}$$

Radiator Performance:

$$Q_{RAD.} = \sigma (\epsilon A)_{rad.} T_p^4 \tag{3}$$

Condenser Effectiveness:

$$\epsilon_{cond} = \frac{T_a - T_b}{T_a - T_p} \tag{4}$$

Condenser Capacity:

$$(UA)_{\text{cond req'd}} = Q_{rad} \Big/ \frac{T_a - T_b}{\ell n \frac{(T_a - T_p)}{(T_b - T_p)}} \tag{4a}$$

Regenerator Heat Balance:

$$(W_1 - W_{b.p.})\ (T_{cab} - T_1) = W_1\ (T_b - T_3) \tag{5}$$

Regenerator Effectiveness:

$$\epsilon_{reg} = \frac{T_{cab} - T_1}{T_{cab} - T_b} \tag{6}$$

Regenerator Performance:

$$(UA)_{\text{reg. req'd}} = \frac{W_1\ (T_b - T_3)}{\ell n \frac{(T_{cab} - T_3) - (T_1 - T_b)}{(T_1 - T_b)}} \tag{7}$$

By-pass Mixing:

$$T_a = T_1 + \frac{W_{b.p.}}{W_1}\ (T_{cab} - T_1) \tag{8}$$

Constraint on T_1:

$$T_1 > T_{\text{dew point}} \tag{9}$$

arbitrary choice is

$$T_1 = T_{\text{dew point}} + 2\ K \tag{10}$$

For design point calculations, assume

$$W_{b.p.} = 0$$

$$W_{H_2O} = 45 \text{ gm/hr}$$

These assumptions, coupled with Equations (1) and (2), permit a calculation of the net heat load on the radiator versus condenser exit temperature. This is shown in figure 27. The design point was chosen slightly to left of the minimum heat load because of the considerable reduction in circulation flow rate and hence pumping power. Figure 28 indicates the variation in required flow rate with stream temperature leaving the condenser. A further reduction in stream temperature would have required condenser surface temperatures too close to the freezing point for safe operation.

The requirement that

$$T_{p_{min}} \geq 35 \text{ F} \tag{11}$$

sets the required value of (ϵ A) rad. From this point, all of the thermodynamic quantities and the required regenerator capacity may be computed directly from Equations (4) through (7) with the resultant values tabulated in Table 1.

Carbon Dioxide Control Loop

The fundamental requirement of the carbon dioxide control loop is that it precipitate out 45 gm/hr in the precipitator-sublimator-radiator at an inlet concentration of 0.50% by volume (p_{CO_2} = 3.8 mm Hg). The system describing equations are as follows using the notation defined in figure 26.

Carbon Dioxide Generation Rate:

$$W_1 (C_{c3} - C_{c4}) = W_{CO_2} \tag{12}$$

Heat Load on Radiator:

$$Q_{RAD.} = W_1 c_p (T_3 - T_4) + W_{CO_2} h_{sg} \tag{13}$$

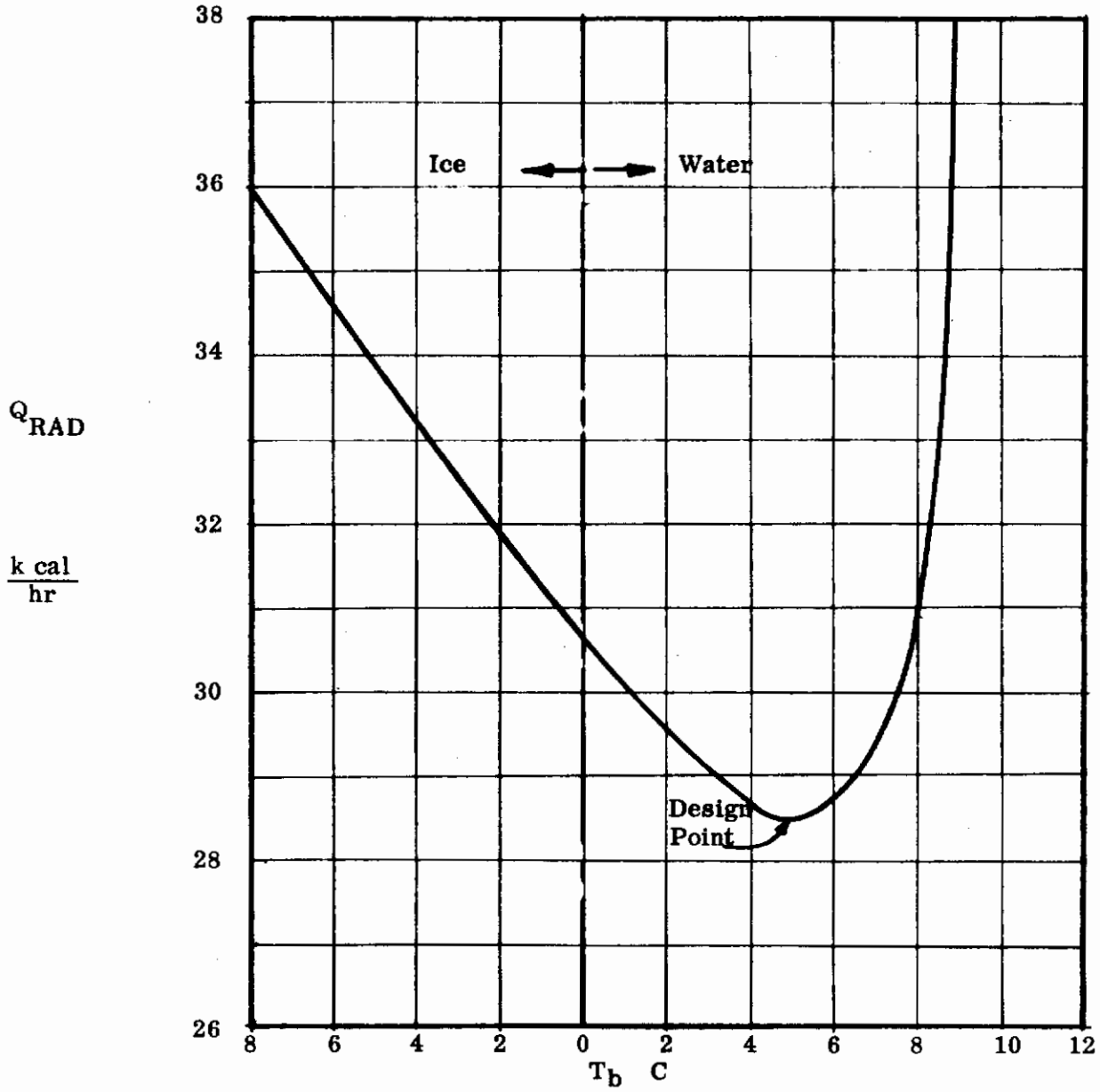

Radiator Heat Load vs. Condenser Exit Temperature

Figure 27

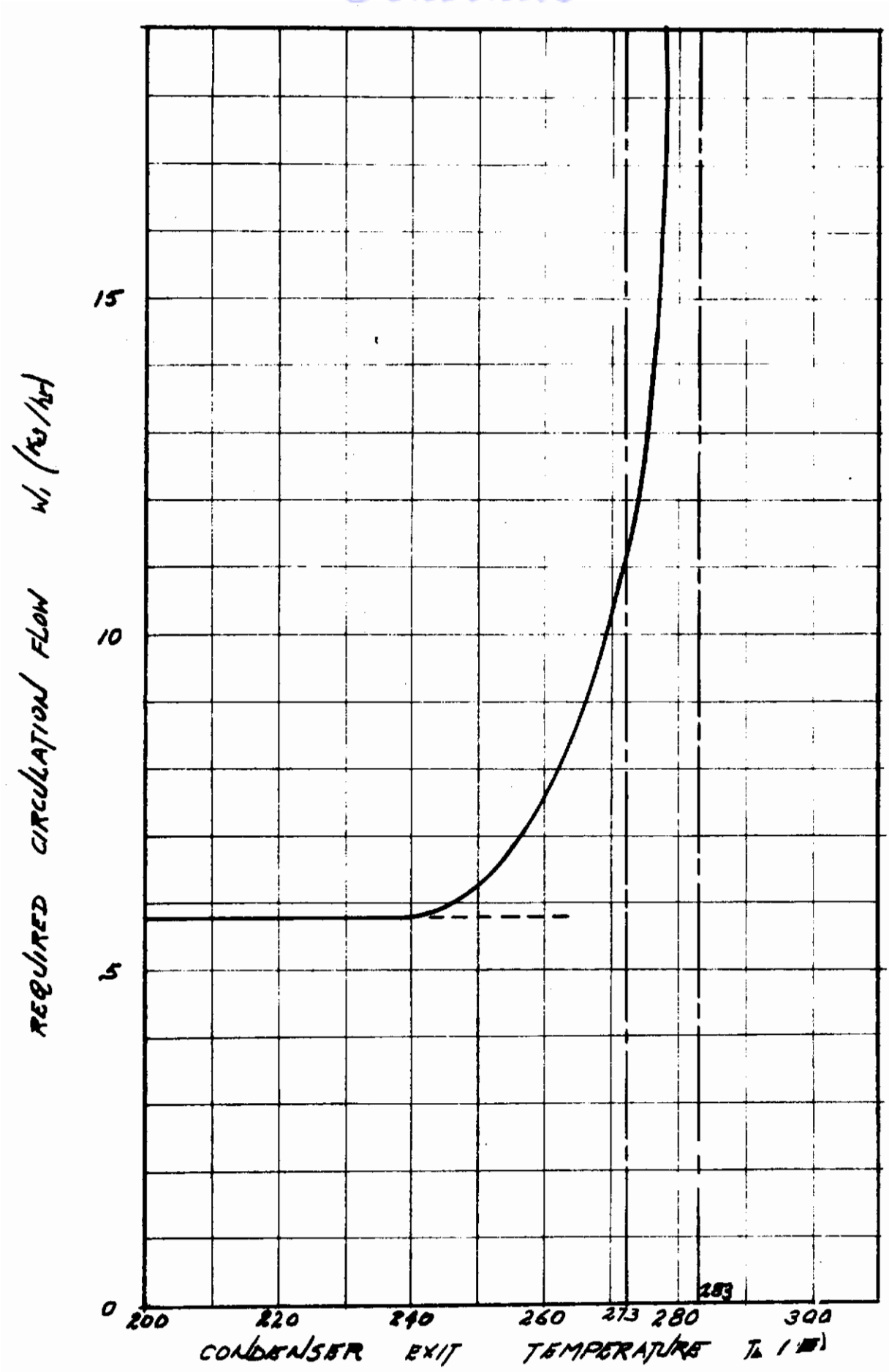

Figure 28
Required Circulation Flow vs. Condenser Exit Temperature

Radiator Performance:

$$Q_{RAD.} = \sigma \, (\epsilon A)_{RAD.} \quad T_p^{\,4} \tag{14}$$

Precipitator Effectiveness:

$$\epsilon_{prec.} = \frac{T_3 - T_4}{T_3 - T_p} \tag{15}$$

Precipitator Capacity:

$$(U A)_{prec.\ req'd.} = \frac{Q_{rad}}{\left(T_3 - T_4\right) \Big/ \ell n \left\{\frac{T_3 - T_p}{T_4 - T_p}\right\}} \tag{16}$$

Precooler Heat Balance:

$$T_2 - T_3 = T_5 - T_4 \tag{17}$$

Precooler Effectiveness:

$$\epsilon_{III} = \frac{T_2 - T_3}{T_2 - T_4} \tag{18}$$

Precooler Capacity:

$$(U A)_{III\ req'd} = \frac{Q_3}{\Delta T_3} = \frac{W_1 \, c_p \, (T_2 - T_3)}{T_3 - T_4} \tag{19}$$

Dehumidifier Heat Balance:

$$T_1 - T_2 = T_6 - T_5 \tag{20}$$

Dehumidifier Effectiveness:

$$\epsilon_{III} = \frac{T_1 - T_2}{T_1 - T_5} \tag{21}$$

Dehumidifier Capacity:

$$(UA)_{II\ req'd} = \frac{Q_2}{\Delta T_2} = \frac{W_1 c_1 (T_1 - T_2) + W_{H_2O} h_{sg}}{(T_2 - T_5)} \quad (22)$$

HX-I Heat Balance:

$$T_{cab} - T_1 = T_7 - T_6 \quad (23)$$

HX-I Effectiveness:

$$\epsilon_I = \frac{T_{cab} - T_1}{T_{cab} - T_6} \quad (24)$$

HX-I Capacity:

$$(UA)_{I\ req'd} = \frac{Q_1}{\Delta T_1} = \frac{W_1 c_p (T_{cab} - T_1)}{(T_1 - T_6)} \quad (25)$$

Constraints on Temperature:

$$T_1 > T_{dew\ point} \quad (26)$$

$$T_2 \simeq T \text{ (at which 99\% of water vapor is removed)} \quad (27)$$

$$T_3 > T_{precip.\ CO_2} \quad (28)$$

As in the case of the humidity control loop, the choice of a freeze-out temperature is determined by considering the circulation rate and radiator load as

related through Equations (12) and (13). In this case, the radiator heat load is the primary constraint because of the low emissive power at the low temperatures. Figures 29 and 30 show the required heat loads and circulation rates for various precipitator exit temperatures. The choice of a reasonable effectiveness for the precipitator channel chosen on the basis of figure 18, sets the radiator plate temperature and hence the required $(\epsilon A)_{RAD}$ and $(UA)_{prec.\ req'd.}$ From this point, the remaining thermodynamic quantities and the required regenerator capacities can be calculated directly from Equations (17) through (25) resulting in the values tabulated in Table 2.

INDIVIDUAL COMPONENT SPECIFICATIONS

In the following sections, the individual components of the two loops are specified.

Humidity Control Loop

The elements of the humidity control loop requiring further discussion are listed below, in order, proceeding around the loop.

- (a) Intake filter
- (b) Flow control valves
  - (b-i) Humidity sensor
  - (b-ii) Amplifier
  - (b-iii) Torque motor
- (c) Regenerator
- (d) Condenser - radiator
  - (d-i) Shield
- (e) Wicking device
- (f) Blower
- (g) Ducting
- (i) Insulation
- (j) Supports
- (h) Emergency shut-off

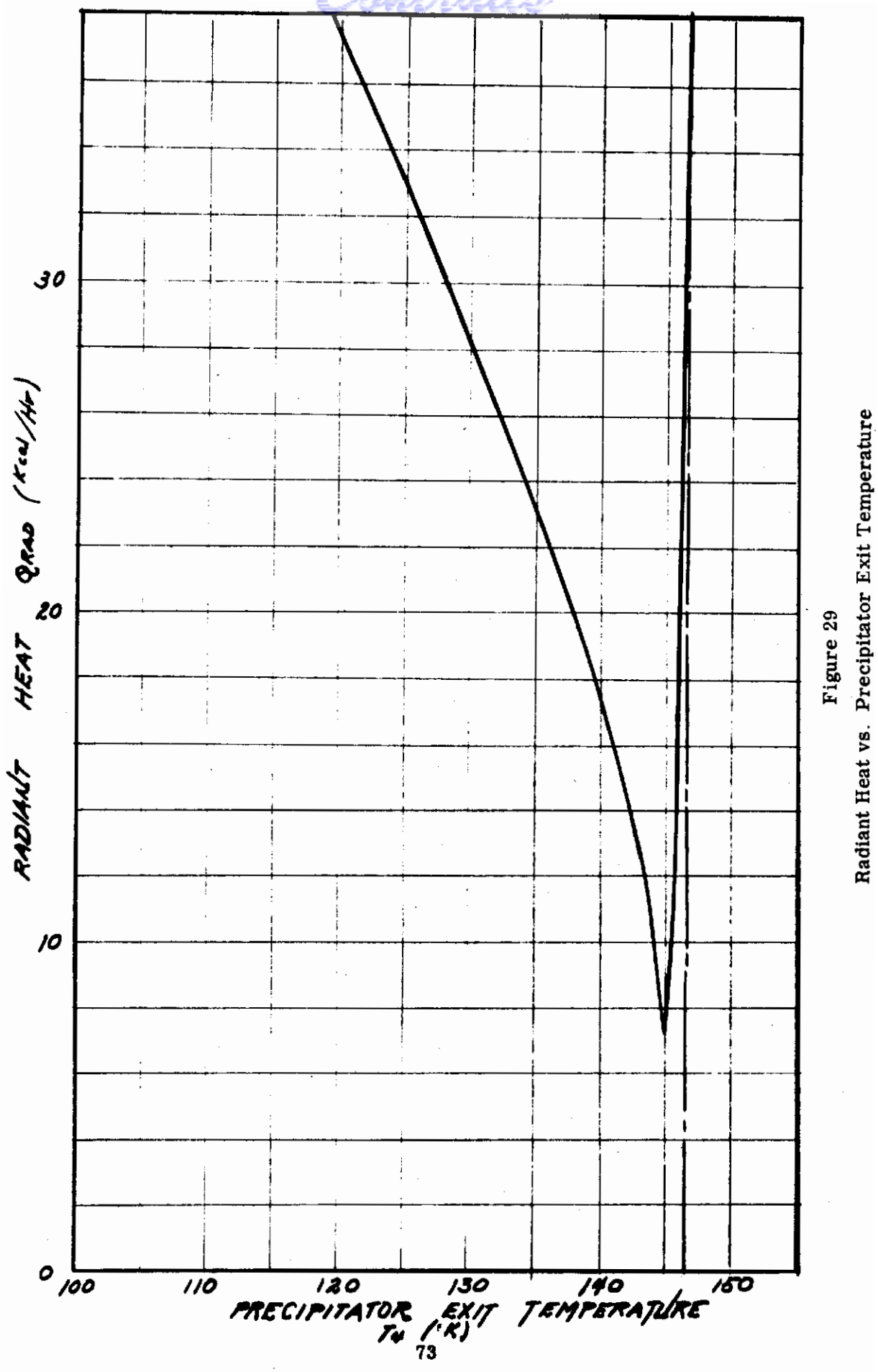

Figure 29
Radiant Heat vs. Precipitator Exit Temperature

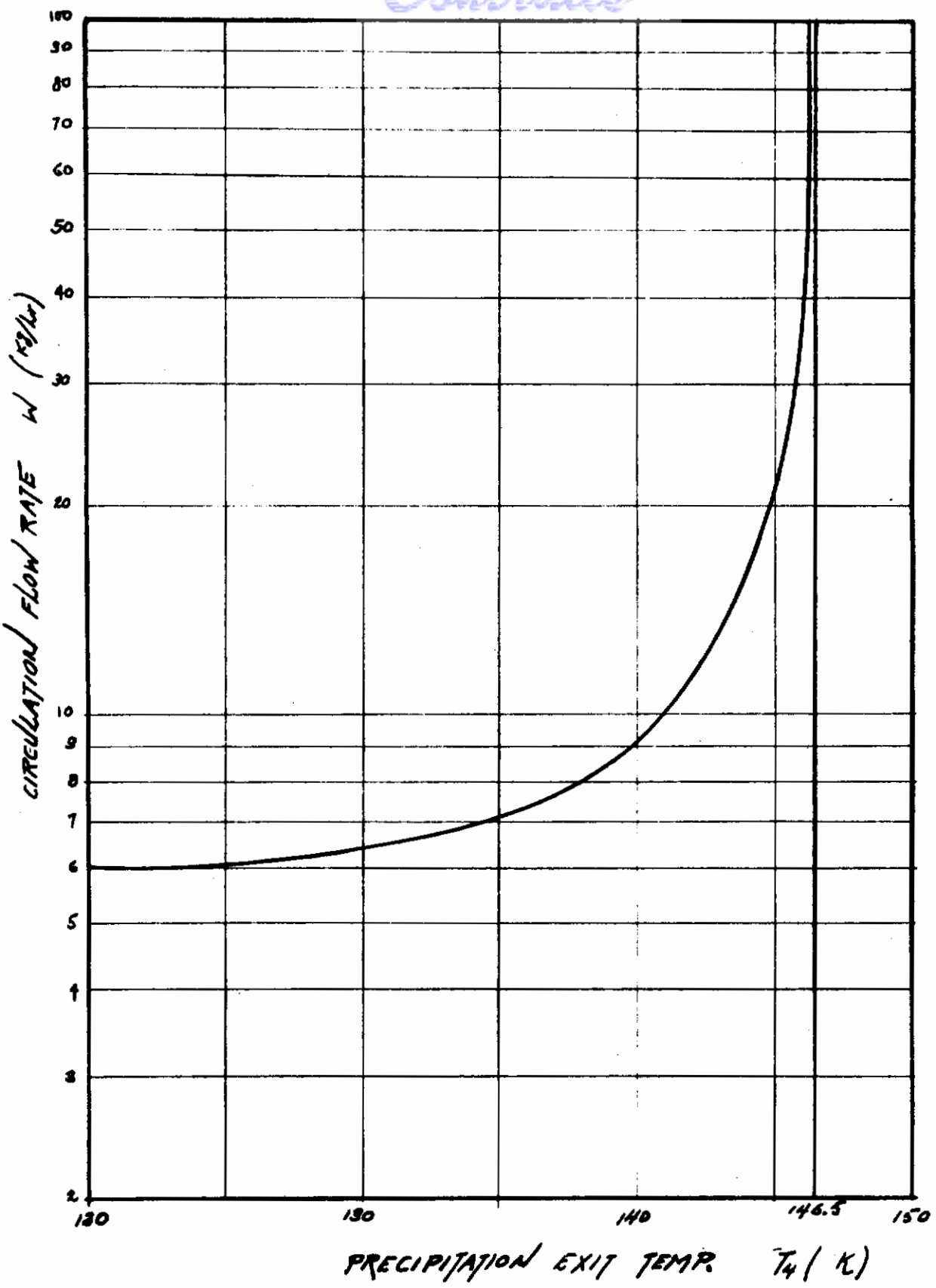

Figure 30

Required Circulation Flow vs. Precipitator Exit Temperature

The unit as a whole is modular and is mounted on a section of cabin wall which would be bolted in place as the final installation. The attachment to the cabin is indicated in figure 31.

Intake Filter

It is of particular concern in a zero-gravity environment to insure that no particulate matter or extraneous objects become entrained in circulation stream. Such an occurrence could block the passages or foul the heat transfer surface, leading to degradation of performance of some of the system elements, or at worst, total system failure. This contingency is avoided through the use of "Millipore" filter strips on both the main, and by-pass, flow intakes. Such filters have been shown to be 99.7% effective in removing particles above 0.3 microns with minimum pressure drop. In the carefully controlled atmosphere of a spacecraft, filter plugging should not be a problem. However, these filters are easily replaceable from inside the cabin should a mishap or spillage take place.

Flow Control Valves

As described in Section VI, the control function for the humidity control loop is realized by means of a by-pass line around the outgoing side of the regenerator. When control is required, a flapper valve is moved, opening the by-pass line, while simultaneously closing down on the main line. In the fully open position, all of the circulation flow is taken in through the by-pass line. Appropriate valves are not available commercially and have been designed for the system.

The control valve, held in its "NORMAL" position by means of a spring, is opened by a small torque motor (Aeroflex Labs, Inc., TQ 10 W-1) which receives its signal from a humidity sensor (RCA - Hygropake), mounted so as to sample intake air, through a torque amplifier (Aeroflex Labs, Inc., TA - 4DC). The control system characteristics are described in a later section.

Regenerator

The regenerator is a plate-fin heat exchanger with the following specifications. The fin configuration on the outgoing stream side is of the type specified in London and Kays (ref 5) as Type 10-58. The fin configuration for the return stream

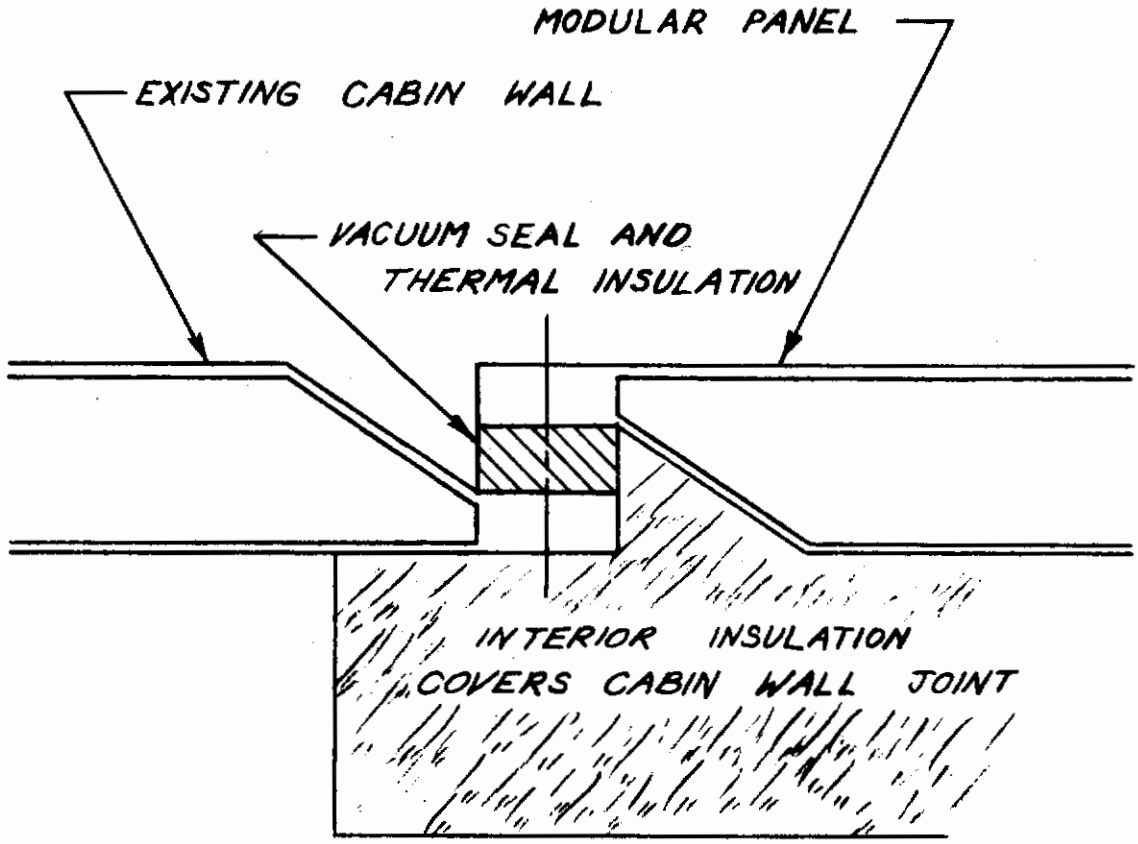

Figure 31

System Module Attachment to Cabin Wall

side is of the plain fin type specified as Type 10-23 (ref 5). This arrangement, with higher heat transfer coefficients on the outgoing side, insures that the exchanger surface temperatures will run close to the outgoing stream temperature and prevent local condensation.

Quantitatively the heat exchanger specifications are as follows:

Outgoing Stream (warm side) 10-58 Fin Configuration

Frosted Area: .056 sq. ft. (9.67 in x 0.839")
Heat Transfer Surface: 4.24 sq. ft.
Heat Transfer Capacity, $(UA)_1$ 16 Btu/hr- F
Flow Length: 8.59 in.
Pressure Drop (Design): 0.526 in H_2O.

Return Stream (cold side) 10-23 Fin Configuration

Frosted Area: 0.0325 sq. ft. (9.67 x .470)
Heat Transfer Surface: 7.16 sq. ft.
Heat Transfer Capacity: 85.2 Btu/hr- F
Flow Length: 8.59 in.
Pressure Drop (Design): 0.028 in. H_2O (includes heaters)

The flow areas were designed to maintain a flow velocity of 5 ft/sec. This will be sufficient to insure good mixing and to entrain any condensate should the control system experience any transient malfunction. The entire regenerator is encapsulated in a polyurethane foam insulation with a vapor barrier to prevent heat leakage from the warm cabin.

Condenser-Radiator

The condenser-radiator consists of a plate-fin heat exchanger module, where the back plate is extended to form the radiator. The fin configuration is Type 10-23, (ref 5), the same as used for the return side of the regenerator. The quantitative specifications are as follows:

Condenser: 10-23 Fin Configuration

Frontal Area: 0.0325 sq. ft. (9.67" x .420")

Heat Transfer Area: 8.33 sq. ft.

Heat Transfer Capacity: 27.5 Btu/hr- F

Flow Length: 1.4 ft.

Pressure Drop (design): 0.056 in H_2O
(includes heaters)

The radiator is an extension of the condenser back plate surrounded by tapered fins as illustrated in figure 32. The central portion of the radiator is covered by a meteorite shield which also serves as a finned radiator surface. The fin effectiveness (see fig. 32) is η_f = 0.97, and the shield accounts for nearly 40% of the total heat rejection. The shield and the tapered fins are copper with surface emmissivities of 0.9. This emissivity is assumed to be reasonable from ref 6. This provides the required (ϵ A) capacity of 2.2 ft^2.

The condensate will be removed from the condenser by entrainment in the air stream traveling at approximately 8.5 ft/sec. This will provide sufficient entrainment under zero-gravity conditions. While it should be sufficient for ground testing, it may prove necessary to provide a separate drain for water removal, whereas, this will by-pass the wicking device, this device is already proven space-worthy on Mercury flights (ref 6).

Wicking Device

The wicking device chosen for this application is sketched in figure 33. It is of the in-line type used successfully in Mercury flights. The U-bend just prior to entering the device will insure that the entrained liquid is on the wall for collection. A small pump for water removal and collection (not specified) is required.

Blower

The main circulating blower is of the vane-axial type with an integral motor. (Globe Industries, Type VAX-1.5-AC). This blower will permit 1.2 in H_2O head rise at the design flow of 10 CFM. The fan characteristics are sketched in figure 34. Approximately 12 watts of 400 cycle, 115 volt ac power is required.

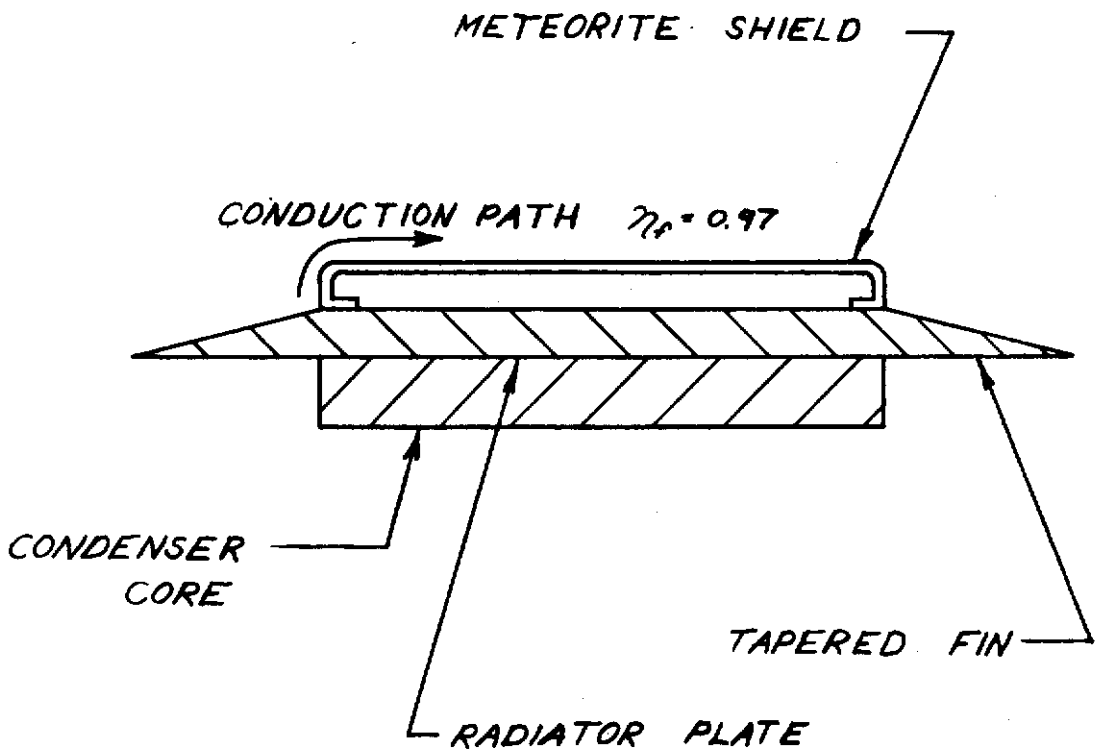

Figure 32

Condenser-Radiator Plate and Shield

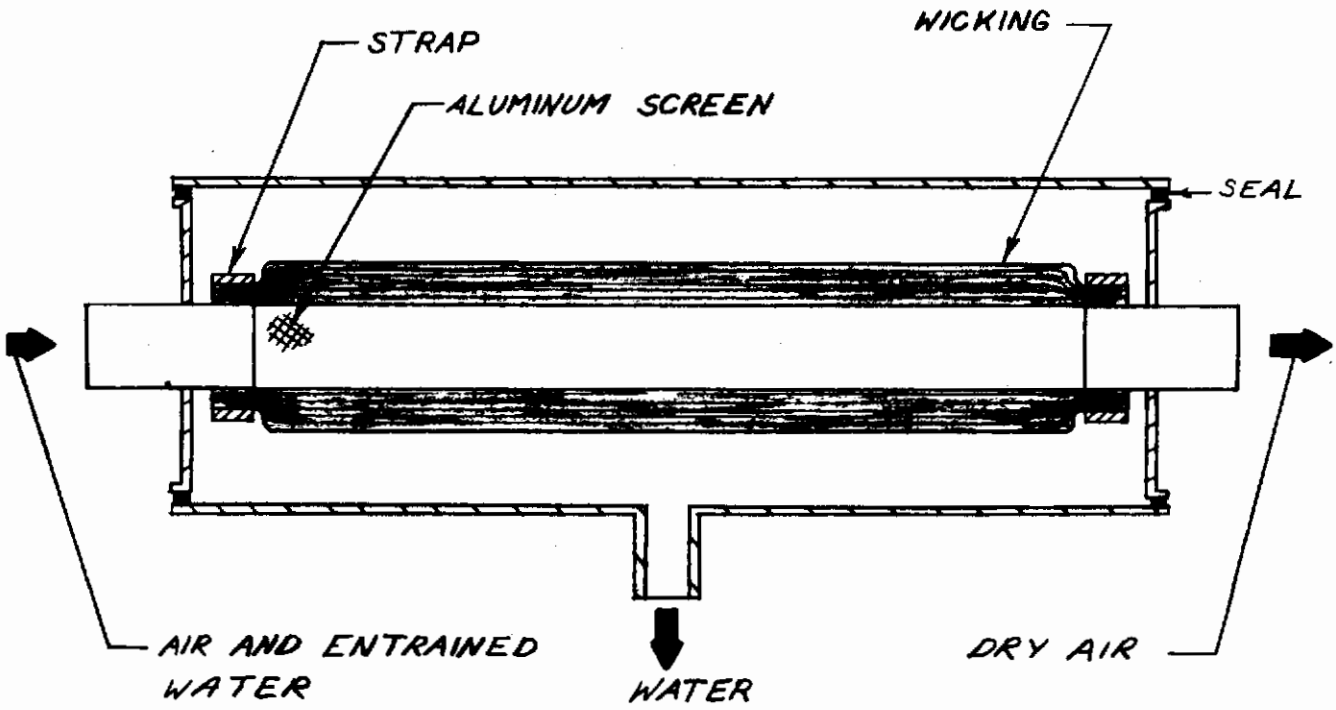

Figure 33

Water Separator - Wicking Device

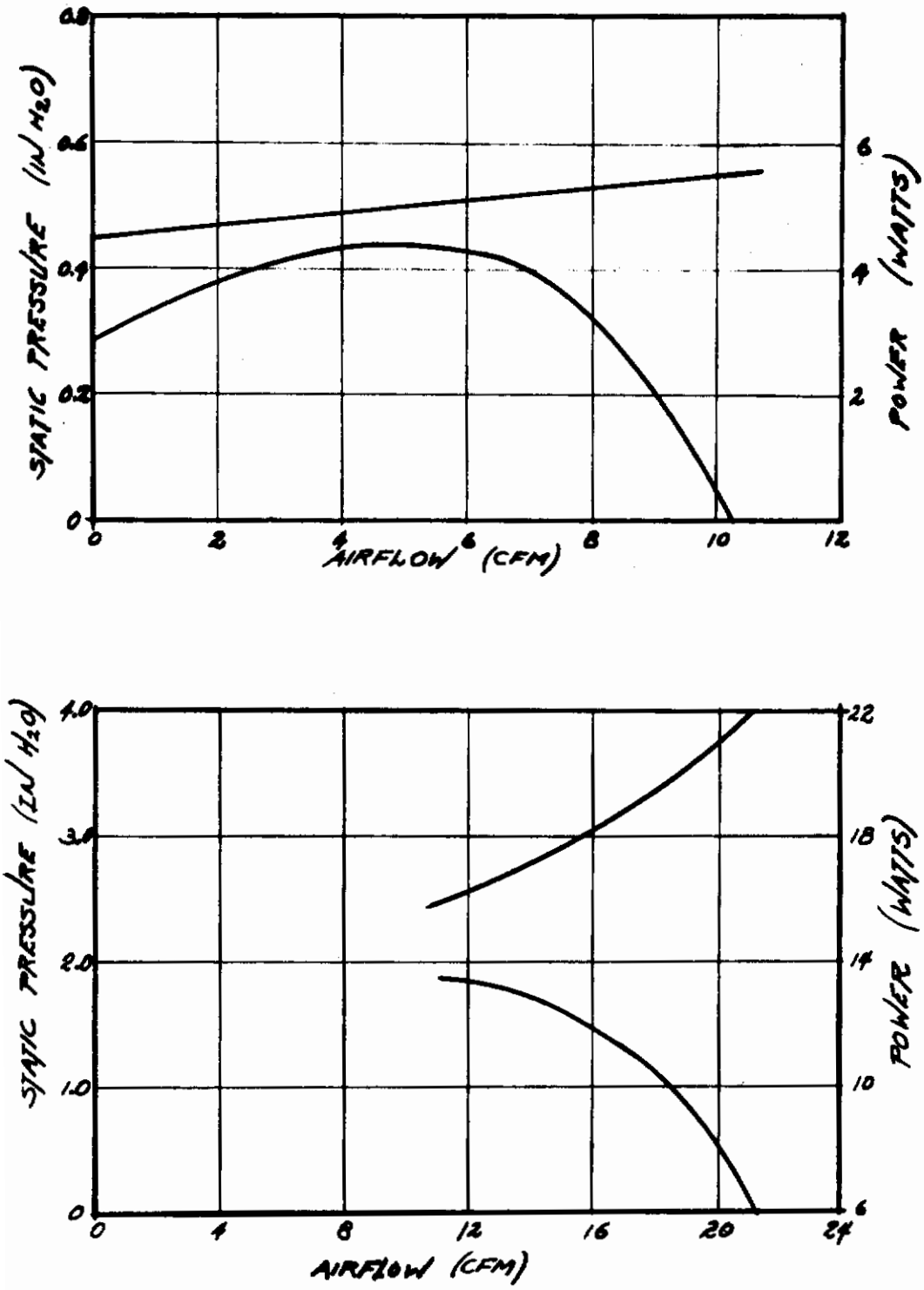

Figure 34
Blower Characteristics

Ducting

The duct work is all constructed from sheet aluminum, 0.020" thick. The passages are rectangular and present the same cross-sectional flow area as the heat exchangers. The duct work blends smoothly into the headers on the heat exchangers.

Insulation

Two types of insulation are provided to prevent heat leaks from the system. Around the components internal to the cabin, a 3/4" thick layer of polyurethane foam, with an external foil to serve as a vapor barrier is provided. This insulation permits a maximum heat leak to the regenerator and surrounding duct work of at most 5.0 Btu/hr which is quite negligible. ($k_{foam} \approx .01$ Btu/hr-ft^2- F)

The radiator itself is protected from radiant heat leaks from the cabin wall by a 1/4" thick layer of super-insulation (Norton Corporation; NRC-2) consisting of 15 layers of aluminum coated mylar. This will serve to reduce back losses to the radiator to less than 1 Btu/hr.

Emergency Shut-Off

In the unlikely event that the system should be penetrated and left open to space, provision has been made to prevent a loss of cabin atmosphere through the humidity control system. Two valves (see fig 35), held in the normal open position by springs, will be forced shut by the sudden pressure differential between the cabin (atmospheric pressure) and the condenser-radiator (zero pressure in case of accident) These valves are provided with guide rails to prevent jamming and to insure a good seat. Of course, under these conditions, the humidity control system will not function.

Tabular Summary

The following table summarizes the components of the humidity control loop. The individual component pressure drops, volumes and weights are given. The total system weight is 16.7 lb.

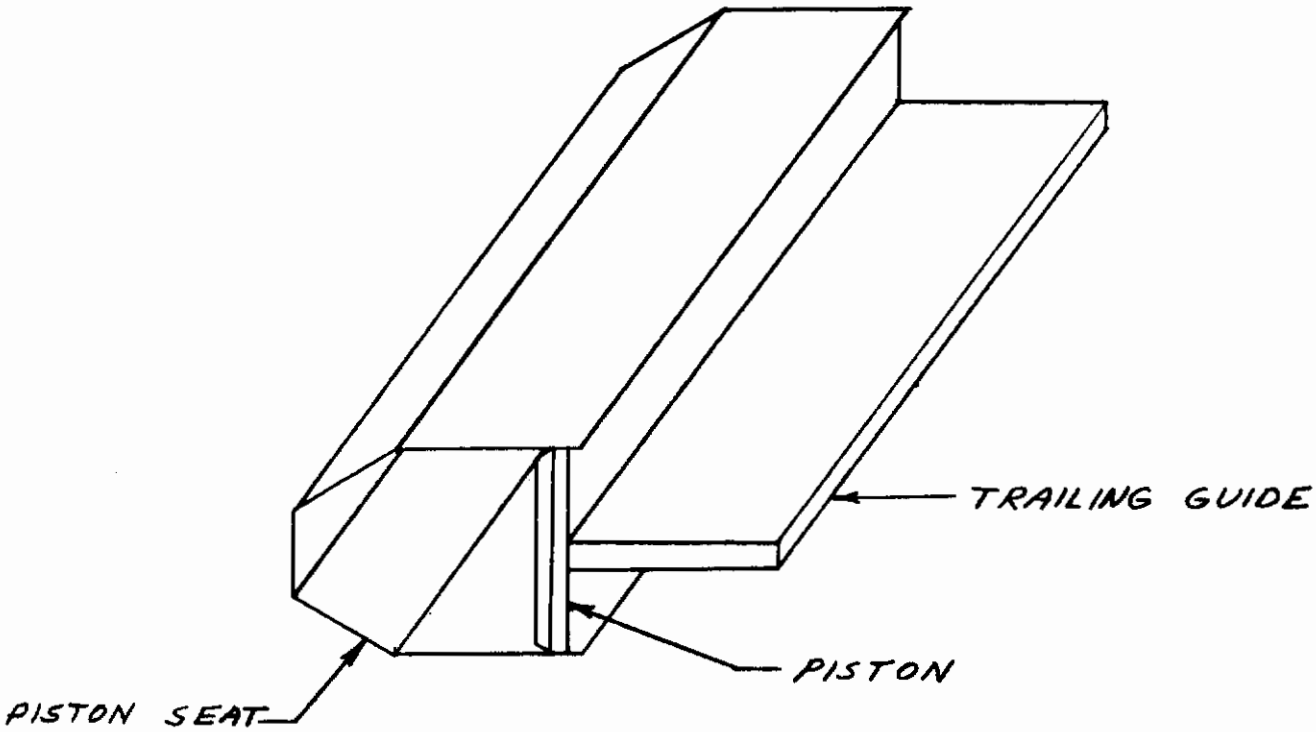

Figure 35

Shut-Off Valve

Table 4

	Description of Components	ΔP I. W. C.	Vol. in^3	Weight #
1.	Regenerative compact heat exchanger Hot side - London & Kays Fig. 10-58 Cold side - London & Kays Fig. 10-23	.36	70	.7
2.	Condenser London & Kays Fig. 10-23	.06	70	1.0
3.	Radiator The radiator is a trapezoidal cross-section extended fin, which for a part acts as a meteorite shield. Area 4.8 ft^2			1.2
4.	Wick device with large surface area wick	.02	100	
5.	Fan van axial blower Make: Globe Industries Type: VAX - 1.5 - AC Weight Delivery required: 10 CFM at 1.2 I.W. C. Estimated power: 12 watt Power/weight penalty		4	.25 4.00
6.	Servomotor for by-pass valve Make: Aeroflex Labs, Inc. Torque motor product div. Type: TQ 10 W-1 Weight: Power: 3 watt		.5	.13 1.00
7.	Humidity Controller Make: Honeywell Type: H93A modified to reduce weight Description: Hair element type with set point and potentiometer		20	.5
8.	Torque amplifier Make: Aeroflex Labs, Inc. Type: TA-4DC Weight: Power: 6 watt est. Power penalty:			.4 2.00
9.	Manifolds			4.00
10.	Insulation polyurethane foam- vapor seal			1.00
	TOTAL ESTIMATED WEIGHT			16.7

Carbon Dioxide Loop

The component elements of the carbon dioxide level control loop to be described in this section are listed below. They will be discussed in order proceeding around the loop.

a. Intake filter
b. Regenerators
   - b-i pre-cooler
   - b-ii de-humidifier
   - b-iii final pre-cooler
c. Precipitator-Sublimator-Radiator
   - c-i switching valves
d. Blowers
e. Valving
f. Insulation
g. Supports
h. Emergency Shut-off

As in the case of the humidity control loop, the system is mounted on a section of cabin wall as a modular insert. The mounting details are identical to these of the humidity control loop and are shown in figure 31.

Intake Filter

The use and choice of intake filters on this loop are dictated by the same considerations as were the case in the humidity control loop. The details are discussed in Section VII.

Regenerative Heat Exchangers

The loop contains three separate regenerative heat exchangers as outlined in Section VI. Each of these is a plate-fin compact heat exchanger with the same configuration on both the outgoing (warm) and return (cold) stream sides.

The purpose of the first heat exchanger is to reduce the temperature of the cabin air prior to dehumidification. At the design point, no condensation will occur. However, if through some transient condition, some water vapor does condensate in the passages, it is of no consequence. The water will be returned to the cabin on a following cycle just as from Heat Exchanger II. The quantitative specifications, applying to both the warm and cold side of the unit are as follows:

HX - I Fin Configuration (10-58)

Frontal Area: 0.027 sq. ft. (5.3" x .72")

Heat Transfer Surface: 2.89 sq. ft.

Heat Transfer Capacity: 30.2 Btu/hr- F (per side)

Flow Length: 7.2 in.

Pressure Drop: 0.25 in H_2O (including headers)

HX - II Fin Configuration (10-58)

Frontal Area: 0.055 sq. ft. (10.99 x .720)

Heat Transfer Surface: 9.13 sq. ft.

Heat Transfer Capacity: 87.0 Btu/hr- F (per side)

Flow Length: 9.6 in.

Pressure Drop: 0.28 in H_2O (including headers)

HX - III Fin Configuration (10-58)

Frontal Area: 0.055 sq. ft. (10.99" x .720")

Heat Transfer Surface: 11.31 sq. ft.

Heat Transfer Capacity: 10.78 Btu/hr- F (per side)

Flow Length: 11.9 in.

Pressure Drop: 0.35 in H_2O (including headers)

The flow areas were designed to maintain a stream velocity of 5 ft/sec. This is sufficient to provide good entrainment in the return stream and to insure that the water vapor is returned to the cabin. Axial conduction, often a source of degraded performance in compact heat exchangers has been checked and in each case, is less than 1% of the capacity.

Precipitator-Sublimator-Radiator

The PSR consists of two sets of long parallel channels spread out on either side of a large radiator plate. The channels in which the precipitation and sublimation occur are simply four parallel rectangular passages (3/16" x 9/32") arrayed opposite each other on the radiator. (See fig 36) The channels serve to provide some structural support to the radiator as well as spread the heat transfer surfaces out over the radiator plate.

The initial concept of a small, centrally located precipitator-sublimator unit led either to intolerable temperature gradients in the plane of the radiator or to excessively high radiator weight. Hence, the PSR was designed as a long duct, spread out over the radiator area, to permit the radiator fin to be both very thin (0.005 in) and highly effective (μ_{fin} = 0.9). The channel geometry was then optimized on the basis of minimum weight for a given pressure drop. The quantitative specifications for the precipitator channels are as follows:

Flow Area:	0.0013 sq. ft.
Heat Transfer Surface:	3.0 sq. ft.
Heat Transfer Capacity:	5.4 Btu/hr- F
Flow Length:	10 ft.
Pressure Drop: (including heaters)	0.20 in H_2O

The radiator plate is a copper sheet (5' x 5') with a uniform thickness of 0.005". An assumed emissivity of 0.9 provides the required $(\epsilon\ A)\ RAD_{req'd} = 22.5 ft^2$.

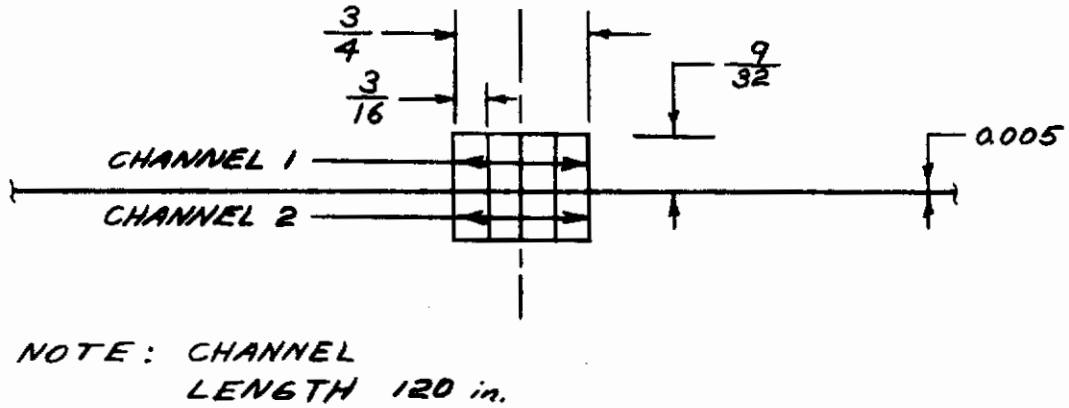

Figure 36

P-S-R Channels

The results of Phase I (Section I through V) indicated that geometrical considerations were not at all critical in the construction of the precipitator channels and that standard correlations were applicable in the absence of frost. Furthermore, figure 22, in which the effect of a frost layer on the overall heat transfer coefficient is presented, indicates that an overall coefficient of one-half (1/2) that predicted by standard correlations is a conservative estimate. Therefore, this value was used. As will be seen in Section VIII, the frost layer thickness will never become significant in the system, so the precipitator will have ample capacity.

Blowers

The system utilizes two blowers of the type specified under "Blowers". The use of two blowers results in considerable simplification of the valving arrangement which provides for water return to the cabin. When one blower is operating, the intake air is by-passed around the other, in order to eliminate the additional pressure drop of pulling the stream through a stationary fan.

Valving

Numerous valves are required for proper flow direction in the carbon dioxide loop. All of these valves are pressure-activated. The details of the control air loop are given in Section VIII. However, the valves themselves are of four types.

a. Main Flow Bypass Valves

In order to return condensed water to the cabin, the flow passages through the regenerators (H X I, II, and III) are reversed periodically. This switching frequency in pre-set and controlled by a timer. Whereas this results in a slightly greater loss of cabin atmosphere than a system which monitors pressure drop in the condensing lines, the difference is quite small. Therefore, this system, which seems inherently more reliable, was chosen.

At regular intervals, a double flapper valve opens one inlet line and closes the other. Similtaneously, one blower is shut off, while the other is started. These valves serve no throttling function, but are simply of the "OPEN-CLOSE" type. The system is entirely symmetrical, except for ducting details, so that the pressure drop-flow rate characteristics are the same in each half of the cycle.

b. Precipitator-Sublimator Valves

The precipitator-sublimator channels are switched, on a timed basis, at the same time as the regenerators. This is accomplished through two, double-acting, air-activated valves, mounted directly on the PSR. There are bellows - type valves which have been especially designed for the system in the interest of minimum weight. They are shown in figure 37.

c. Sublimation Valves

It is also necessary to alternately open and close the two sublimating channels The sublimating flow has been routed through the warm cabin in order to prevent any jamming up of the passages by solid carbon dioxide particles. The flow could be either redirected out to space or attached to an over-board vaccum pump for carbon dioxide reclamation. These dump valves, also air-operated are commercially available. (Hoke, 4251F2Y and 0477A4G air operated; aluminum).

d. Pressure Regulation Valve

In order to maintain a controlled sublimation rate, a pressure regulator must be installed in the dump line to maintain the necessary pressure in the sublimating channel. No commercially available regulators were found which operated reliably at these pressures. Therefore, a suggested regulator with a vacuum reference is sketched on assembly drawing WRI-18-3.

Insulation

The system is insulated in the same manner as the humidity control loop described earlier. In this case, however, the radiator plate is backed with a one-inch (1") thickness of super-insulation, comprising 60 layers of aluminized mylar.

Tabular Summary

The following table summarizes the components of the carbon dioxide level control loop. The individual component pressure drops, volumes, and weights are indicated. The total system weight is 34.5 lb.

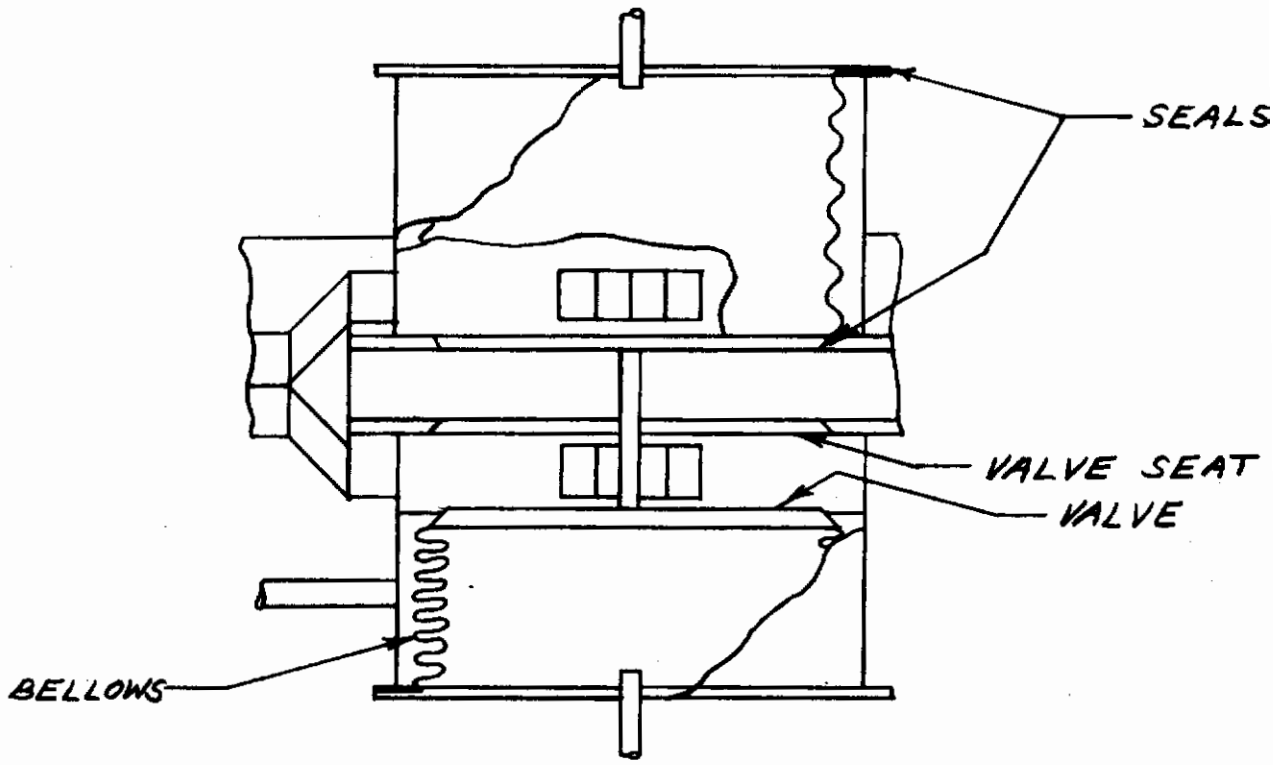

Figure 37

P-S-R Valve

Table 5

	Description of Components	ΔP I.W.C.	Vol. in^3	Weight lbs.
1.	Regenerative Compact Heat Exchanger No. I	.15	32	.32
	Hot side - London & Kays Fig. 10-58 Cold side - London & Kays Fig. 10-23			
2.	Regenerator No. II	.28	75	.98
	London & Kays Fig. 10-58			
3.	Regenerator No. III	.35	84	1.21
	London & Kays Fig. 10-58			
4.	PSR Channels	.2	51	.6
5.	Radiator, aluminum			1.8
	Polystyrene foam backing 1/4"			2.0
6.	Fan, Nonaxial Blower (2)			.25
	Make: Globe Industries, Inc. Type: VAX - 1.5 - AC Delivery required: 6 CFM at 1.0 I.W.C. Estimated power: 9 watt Power Weight Penalty: 9/3 = 3			3.0
7.	Three-way valve (2) (PSR valves)			4.0
8.	Solenoid Valve (to control PSR valves from timer			1.5
	Make: Automative Switch Co., N.J. Type: 8345-A Power: 11 watts, 50% duty cycle Power weight penalty			1.8
9.	Super insulation, 26 ft^2 of 60 layers, 1 inch			3.0
10.	Urethane Foam Insulation, 1 cu. ft.			2.0
11.	Manifolds, piping, wiring			4.0
12.	Shut-off HOKE valve (2 required) 4251 F2Y and 0477A4G air operated, aluminum (sublimation valves)			3.0
13.	Timer Control		21	4.0
	Make: Industrial Timer Corp. Type: CM-4 (40 sec. - 6 min) Power: .1 A at 28 V, 3 watt; power weight penalty, 3/3 = 1			1.0
		TOTAL		34.5 lbs.

SECTION VIII

SYSTEM CONTROL AND OPERATION

The following sections describe the functioning of the system control elements, discuss system stability, and define some of the auxiliary operating requirements.

SYSTEM CONTROL

The systems must operate at other than design conditions without extensive operator intervention in order to be useful in a space-flight mission. In the case of the humidity control loop, an active control element is required. However, in the case of the carbon dioxide control loop, the purely passive response of the system is sufficient to meet the varying load conditions.

System Control - Humidity Loop

The humidity control loop is controlled by means of a by-pass valve which diverts flow from the cabin, around the regenerator, directly to the condenser. The monitored variable which controls the by-pass flow is the cabin humidity. The sensor is placed near the main intake duct to insure a representative sampling. As the water vapor generation rate falls, the humidity in the cabin will decrease. This will result in a reduction of the latent heat load on the condenser. If unchecked, condenser exit temperature will fall with resultant freeze-up in the condenser and/or premature condensation in the regenerator.

Opening the by-pass valve has two effects. First, the temperature of the condenser inlet stream is raised, increasing the sensible heat load on the radiator and preventing freeze-up. Second, the condenser exit temperature will be raised, providing a higher temperature return stream in the regenerator and preventing premature condensation in the outgoing stream.

A computation of performance at two "off-design" operating points is made to document the validity of the control system.

Operation at Minimum Load

The minimum water vapor generation rate is 4.5 gm/hr. This implies a ten-fold reduction in the latent heat load on the system. Under these conditions, the cabin is intended to operate at 40% relative humidity with the by-pass value fully opened. The total system flow resistance is reduced by the elimination of the warm-side regenerator pressure drop and the flow rate will increase, according to figure 38, to about 50 lbm/hr. Since the condenser operates in laminar flow, this results in approximately a 10% increase in the heat transfer capacity. This will result in a new set of operating conditions with the following specifications. The component capacities at the new flow rate are:

$$(U\,A)_{cond.} = 4.3 \text{ kcal/hr- K}$$

$$\epsilon_{cond.} = 0.62$$

Therefore, the new temperature levels and heat loads are

$$Q_{RAD} = 63.5 \text{ kcal/hr (248.6 Btu/hr)}$$

$$T_p = 276^\circ\text{K (38 F)}$$

$$T_b = 280.5^\circ\text{K (48 F)}$$

which are consistent and satisfy the overall system requirements.

Off-Design Operation--An Example

Intermediate conditions, in which the outgoing flow is split between the regenerator and the by-pass, are associated with intermediate water vapor generation rates. For example, the following operating point is reached for a water vapor generation rate of 20 gm/hr.

$$W_1 = 20.5 \text{ kg/hr}$$

$$W_{b,p} = 11.5 \text{ kg/hr}$$

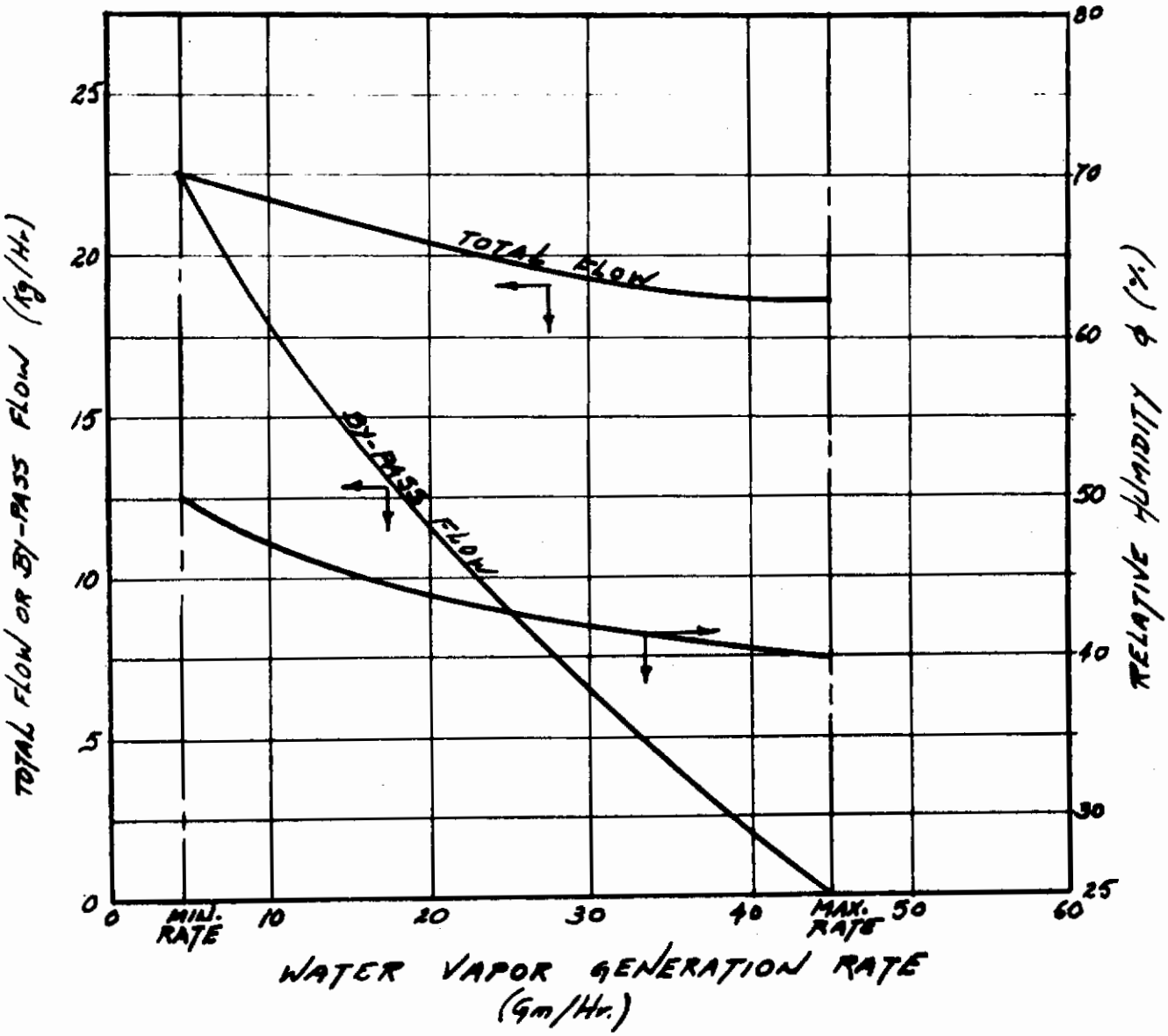

Figure 38

Off-Design Operation

$(U A)_{reg}$ = 5.2 kcal/hr- K

ϵ_{reg} = .67

$(U A)_{cond.}$ = 8.2 kcal/hr- K

$\epsilon_{cond.}$ = .68

T_1 = 290.3 K

T_a = 287.3 K

T_b = 283.5 K

T_p = 278.5 K

Q_{RAD} = 57.9 kcal/hr

Figure 38 gives the cabin humidity, total flow rate and required by-pass flow rate as functions of water vapor generation rates.

System Control - Carbon Dioxide Loop

It can quickly be shown that no active control is required on the carbon dioxide loop. The simultaneous sublimation and precipitation of the CO_2 frost removes the heat of precipitation from the ultimate heat load on the radiator. Therefore, variations in the carbon dioxide generation rate have no effect on the heat loads or temperature levels around the loop. Furthermore, since the system is sized to maintain a cabin concentration of 0.5%, (P_{CO_2} = 3.8 mm Hg) at the maximum carbon dioxide generation rate, there is no possibility of higher partial pressures existing in the outgoing flow and leading to premature precipitation in the final precooler.

Two secondary effects may be considered. These are

1. a reduction in cabin temperature to 16 C (60 F)
2. a reduction in cabin relative humidity to 40%.

These,even if occuring simultaneously, will result in only a slight shift in the operating points. This is due to slightly reduced sensible and latent heat loads on

the three regenerators. The new temperature levels, in the notation of figure 26, are as follows:

T_1 = 283 K

T_2 = 222.3 K

T_3 = 147 K

T_4 = 140.7 K

T_5 = 216 K

T_6 = 276.7 K

T_7 = 287.7 K

T_p = 16.2 kcal/hr.

Q_{RAD} = 135 K

These conditions are perfectly acceptable for carbon dioxide level control. Hence, the system will operate over the entire tolerance range of cabin conditions in a purely passive mode.

COMMENTS ON GENERAL SYSTEM OPERATION

Humidity Control Loop

The only component of the humidity control loop requiring further clarification is the water reclamation system or wicking device. The particular design chosen has been successfully used on the Mercury flights. It is necessary, however, to insure that the liquid to be collected is on the walls. This is provided for by a 180° bend just upstream of the wicking device which will deposit any entrained liquid on the outer wall. Furthermore, the length-to-diameter ratio of the wicked passage itself is sufficiently high to provide a very high collection of any droplets which have been re-entrained from the liquid film near the entrance of the wicking device. It is estimated that the overall collection efficiency will be of the order of 97%. Therefore, at most, 3% of the condensed water will be returned to the cabin as water vapor. The condenser has been over designed by approximately 5% to account for this eventuality.

Carbon Dioxide Control Loop

There are three aspects of the carbon dioxide control loop requiring further discussion. The first of these is the valve arrangement and control system which activates the valves for flow reversal. This system is sketched schematically in figure 39. As indicated previously, the system is cycled at pre-set time intervals in the interests of system simplicity and reliability. (An alternate method would be the monitoring of the regenerator pressure drops. These pressure drops, however, are quite small and difficult to measure accurately.)

Switching Frequency

The required system switching frequency is computed as follows. The freeze-out rate of water vapor in HX - II is given by

$$W_{H_2O} = W_1 (C_{W_1} - C_{W_2})$$

which, for the design temperature is

$$W_{H_2O} = .08 \text{ kg/hr}$$

or, for an assumed frost density of 60 kg/m^3 will fill up the passages in approximately 8 minutes. Therefore, a switching frequency of one flow reversal every 4 minutes was chosen somewhat arbitrarily as a safe operating condition. This corresponds to a calculable loss of cabin atmosphere from the sublimator channels. At switch over, the precipitating channel would be expected to be approximately 1/3 full. This is based on

CO_2 frost build-up per cycle: 3 gm/cycle

Volume of frost: 50 cc

Cabin air lost per cycle: .54 gm/cycle

This corresponds to a total atmosphere loss of about 0.2 kg/day or 73.0 kg/yr. Whereas this is somewhat in excess of the estimates made in Phase I, a significant reduction in this quantity would require a considerably more complex and presumably less reliable system.

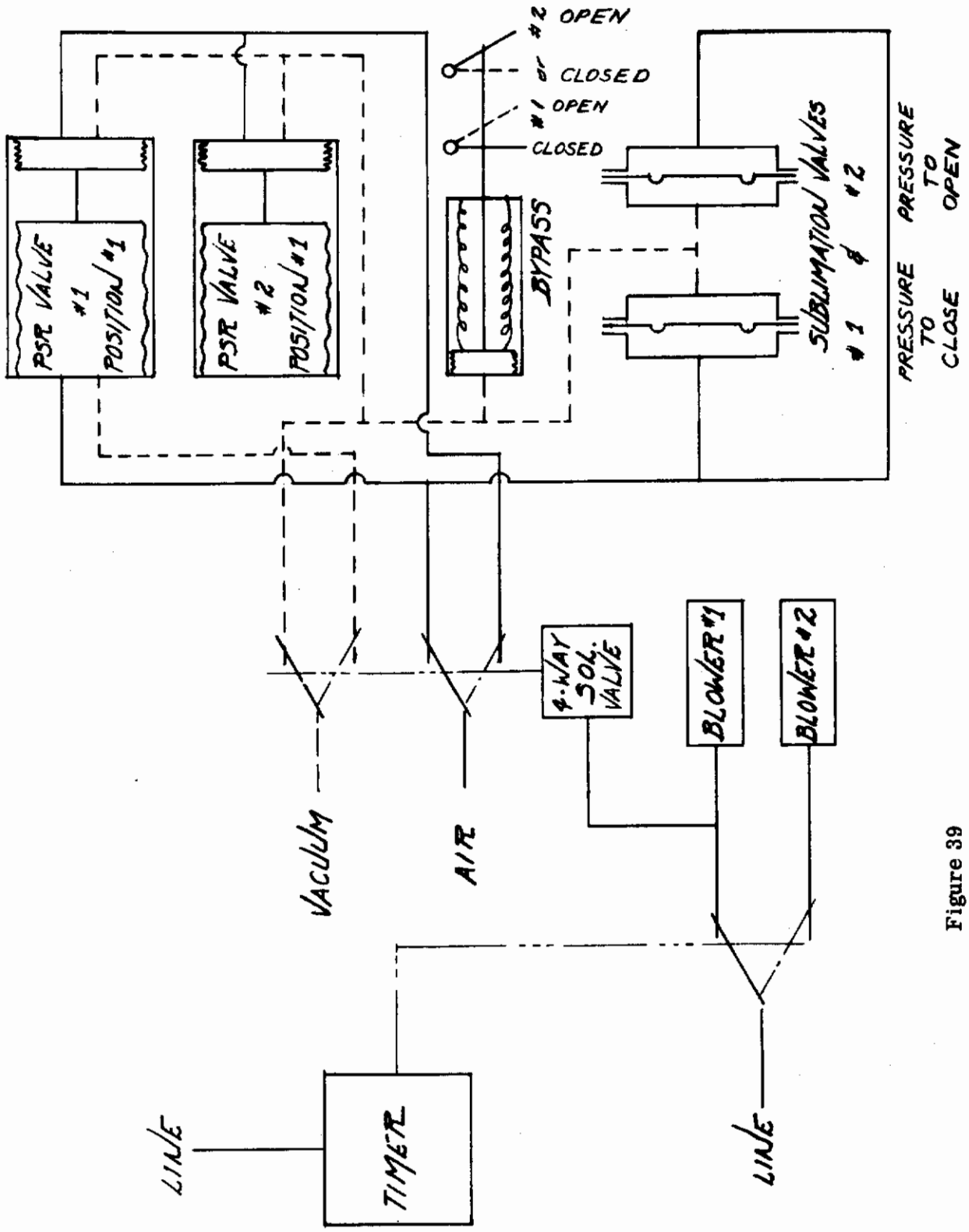

Figure 39

Electric-Pneumatic Control System

Sublimation Rate Control

As demonstrated in Phase I, the sublimation rate can be set by a simple adjustment of the sublimation channel pressure. At the design point, the sublimation rates must equal 45 gm/hr. This corresponds to the mass flux of .05 gm/hr. This corresponds to a mass flux of .05 gm/hr-cm^2, which is attainable at a pressure of 0.12mm Hg. At lower carbon dioxide generation rates, the sublimation channel will experience a slight temperature cycling. This results from a too rapid exhaustion of the sublimator followed by a period of precipitation with no simultaneous sublimation. However, in the worst case of a generation rate of 4.5 gm/hr, this temperature deviation of the metal walls of the channels is limited to 1.5 K. This has a negligible effect on radiator performance. In this light, the additional complexity of precise sublimation water control was considered unnecessary.

COOLDOWN STARTING TRANSIENT

There is one remaining sub-system which is required to make the total system operate in a practical situation. This sub-system makes provision for rapid cooldown. The regenerative features of the two control loops operate well once the operating conditions have been established. However, the starting transient presents a particular problem. If the system is simply started from an initial isothermal condition at ambient temperature, it will eventually reach the design conditions. In fact, in the case of the humidity control loop, this is the recommended procedure. Because of the relatively high radiator temperatures in the water loop, steady state is reached in approximately 34 minutes. Presumably, in this short time after launch, the astronauts would still be suited,and the cabin humidity would not be effected by the delay time. However, in the case of the carbon dioxide loop, because of the extremely low temperatures of the radiator and the correspondingly low radiative power, the attainment of steady-state conditions would require several days. Therefore, auxiliary cooling coils (shown in the assembly drawing, WRI-18-3) must be used to provide for quick-cooldown. This will require the expenditure of on-board cryogenics. The precise quantity required depends somewhat on the details of the particular installation but a preliminary estimate indicates that a 1/2 hour cooling period with a coolant flow rate of about 10 lb/hr (total coolant expenditure of is 5.0 lb) will suffice.

REFERENCES

1. Bonneville, Jacques M., A Study of Water and Carbon Dioxide Precipitation Techniques Using Thermal Radiation Principles, AMRL-TR-66-188 (AD 673 000), Aerospace Medical Research Laboratories, Wright-Patterson Air Force Base, Ohio, August 1966.

2. Kays, W.M., and A.L. London, Compact Heat Exchangers, McGraw-Hill Book Company, Inc., New York, 1958.

3. Rohsenow, W.M., and H. Choi, Heat, Mass, and Momentum Transfer, Prentice-Hall, Inc., New Jersey, 1961.

4. Popma, D.C., "Oxygen Reclamation for Manned Spacecraft," Presented at 37th Annual Meeting, Aerospace Medical Association, Las Vegas, Nevada, April 1966.

5. Kays, W.M., and A.L. London, Compact Heat Exchangers, 2nd Edition, McGraw-Hill Book Company, 1964.

6. Purser, P.E., M.A. Faget, and N.F. Smith, Manned Spacecraft: Engineering Design and Operation, Fairchild Publications, Inc., 1964.

Security Classification

DOCUMENT CONTROL DATA - R & D

(Security classification of title, body of abstract and indexing annotation must be entered when the overall report is classified)

1. ORIGINATING ACTIVITY *(Corporate author)*
Dynatech R/D Company, Division of Dynatech Corp.
17 Tudor Street
Cambridge, Massachusetts 02139

2a. REPORT SECURITY CLASSIFICATION
UNCLASSIFIED

2b. GROUP
N/A

3. REPORT TITLE
AN EXPERIMENTAL INVESTIGATION AND SYSTEM DESIGN FOR HUMIDITY AND CARBON DIOXIDE LEVEL CONTROL USING THERMAL RADIATION

4. DESCRIPTIVE NOTES *(Type of report and inclusive dates)*
Final Report, 1 March 1967-1 October 1968

5. AUTHOR(S) *(First name, middle initial, last name)*
John S. Maulbetsch

6. REPORT DATE
April 1969

7a. TOTAL NO. OF PAGES
101

7b. NO. OF REFS
6

8a. CONTRACT OR GRANT NO. F33615-67-C-1587

b. PROJECT NO. 6373

c. Task No. 637302

d. Work Unit No. 637302042

9a. ORIGINATOR'S REPORT NUMBER(S)
Dynatech Report No. 803

9b. OTHER REPORT NO(S) *(Any other numbers that may be assigned this report)*
AMRL-TR-68-174

10. DISTRIBUTION STATEMENT
This document has been approved for public release and sale; its distribution is unlimited.

11. SUPPLEMENTARY NOTES

12. SPONSORING MILITARY ACTIVITY
Aerospace Medical Research Laboratory, Aerospace Medical Div., Air Force Systems Command, Wright-Patterson AFB, OH 45433

13. ABSTRACT

An experimental investigation was carried out to verify the feasibility of controlling carbon dioxide levels in space cabin atmospheres by freeze-out techniques using therma radiation as the only mode of heat rejection. A one-tenth scale system was constructed with the primary aim of gaining understanding of the CO2 precipitation mechanism and determining the operating characteristics of a precipitator plate. Both quantitative measurements and visual observation of the frost formation were made. The geometric characteristics of the precipitator channel were found to be not critical. Uniform frost layer formation could be obtained and premature channel plugging was not a problem. Typical precipitator plate effectivenesses of 0.75 - 0.85 were easily obtainable. Simultaneous CO2 sublimation was achievable at a controllable rate. System stability was easily achieved. Solid CO2 carryover in both the precipitating and sublimating streams is a real possibility and preventive measures must be taken in the final design of the system. Based on these results, a complete test system was designed to handle the water vapor and carbon dioxide loads in a one-man, manned space enclosure. The system, with a total weight of 51.2 lb, is a two-loop configuration where one loop maintains humidity control and the other removes the generated carbon dioxide and returns all of the accompanying water vapor to the cabin. The system will operate indefinitely with no operator intervention, is operable in zero-gravity, and is of low weight, volume, and power.

DD FORM 1 NOV 65 1473

Security Classification

Security Classification

14. KEY WORDS	LINK A		LINK B		LINK C	
	ROLE	WT	ROLE	WT	ROLE	WT
Air regeneration						
Freezeout						
Thermal radiation						
Carbon dioxide removal						
Water removal						

Security Classification